



FTG Working Paper Series

The Tokenomics of Staking

by

Lin William Cong (??)

Zhiheng He

Ke Tang

Working Paper No. 00134-00

Finance Theory Group

www.financetheory.com

*FTG working papers are circulated for the purpose of stimulating discussions and generating comments. They have not been peer reviewed by the Finance Theory Group, its members, or its board. Any comments about these papers should be sent directly to the author(s).

The Tokenomics of Staking*

Lin William Cong[†]

Zhiheng He[§]

Ke Tang[¶]

First draft: Dec. 2020; this draft: Oct. 2023.

Abstract

Blockchain-based platforms and decentralized finance prominently features “staking”: Besides offering a convenience yield for transactions as digital media of exchange, tokens are frequently staked for base-layer consensus generation or for incentivizing economic activities and network development, and consequently earn stakers rewards. To understand the economics of staking, token pricing, and network evolution, we build a continuous-time model of a token-based economy where agents heterogeneous in wealth and preference for a digital platform dynamically allocate their wealth among consumption, onchain transaction, and staking. We cast the interactions as a mean-field game with individual stochastic control and systematic shocks, which underscores aggregate staking ratio as a key variable linking staking to equilibrium reward rate and token pricing. We further characterize using a master equation the expected steady state of wealth distribution, the drivers for tradeoff between welfare and inequality, and redistribution due to staking and aggregate shocks. From a comprehensive dataset covering all major stable tokens, we derive empirical findings corroborating the model predictions. In particular, staking ratio is positively correlated with reward rates in the cross-section and negatively correlated in the time series. Higher reward rates and wealth concentration attract greater future staking, increasing the aggregate staking ratio, which in turn positively predicts token excess returns. Finally, consumption and transaction conveniences help rationalize violations of the uncovered interest rate parity and crypto carry premia (e.g., a long-short portfolio with OOS Sharpe ratio of 1.6) in the data.

Keywords: Carry, Cryptocurrencies, DeFi, Heterogeneity, Inequality, PoS, Redistribution, UIP.

*We thank Bruno Biais, Philip Bond, Jonathan Chiu, Rod Garratt, Niklas Haeusle, Shiyang Huang, Huisu Jang, Stephen Karolyi, Leonid Kogan, Tao Li, Evgeny Lyandres, Urban Jermann, Julien Prat, Daniel Rabetti, Qihong Ruan, Fahad Saleh, Ville Savolainen, Donghwa Shin, Jingjie Zhang, Shunming Zhang, and conference and seminar participants at the Asian Bureau of Finance and Economic Research (ABFER) 10th Annual Conference, the 36th Australasian Finance and Banking Conference (AFBC), the 18th Annual Conference of the Asia-Pacific Association of Derivatives (APAD), the 19th Chinese Finance Annual Meeting (CFAM 2022), University of Cincinnati, Columbia Business School and School of Engineering and Applied Science (Digital Finance Seminar), Crypto and Blockchain Research Economics (CBER), the Department of the Treasury Office of Financial Research, the Economic Club of Memphis, Luohan Academy Webinar Series, Rizzo Center Decentralized Finance (DeFi) Conference at UNC Chapel Hill, the Fields-CFI Workshop on Mathematical Finance and Cryptocurrencies, FinTech Conference at the Fubon Center for Technology, Business and Innovation (NYU Stern), Halle Institute for Economic Research (IWH), HEC Paris, 2022 Hong Kong Conference for Fintech, AI, and Big Data in Business, Office of the Comptroller of the Currency (OCC) Novel Charters Working Group, The Pennsylvania State University Smeal College of Business, 4th Shanghai Financial Forefront Symposium, Tsinghua University PBC School of Finance, University of International Business and Economics School of Banking and Finance, the China Meeting of Econometric Society (CMES 2021, Shanghai), 7th PHBS Workshop in Macroeconomics and Finance, Ripple Labs London Onsite (Markets Team), Wolfe QES Virtual Global Innovation Conference, and Zhejiang University QingYuan Academy Digital Social Science Public Lecture Series for helpful comments and discussions. We are also grateful to the stakingrewards.com team for generously sharing the updated data that cover Sept 2020 - Feb 2022 for academic research and to the Fintech Dauphine Chair in partnership with Mazars and Crédit Agricole CIB, the Hoge Blockchain Research Institute, as well as Ripple’s University Blockchain Research Initiative (UBRI) for financial support. The paper subsumes key results from the working paper titled “Staking, Token Pricing, and Crypto Carry.” Send correspondence to will.cong@cornell.edu.

[†]Cornell University and NBER. E-mail: will.cong@cornell.edu.

[§]Tsinghua University. E-mail: hezh19@mails.tsinghua.edu.cn.

[¶]Tsinghua University. E-mail: ketang@tsinghua.edu.cn.

1 Introduction

The past decade witnessed an explosive growth in blockchain-based platforms and cryptocurrencies, which totaled 2.5 trillion USD in market capitalization by the end of 2021, and a rising interest in Decentralized Finance (Harvey et al., 2021), which entails over 130 billion USD worth of assets as of Feb 2022. Platform tokens derive value by enabling users to complete economic transactions and hold stakes in the ecosystem, making them a hybrid of money and investible assets. The recent prevalence of token staking (value locking and yield farming, see, e.g., Augustin et al., 2022) for higher-layer DeFi innovations as well as for base layer consensus formation (e.g., through Proof-of-Stake, PoS, as discussed in John et al., 2022) further calls for a unified framework to understand the use of tokens as transaction media, investment assets, and deposit/collateral-like instruments.

To this end, we offer the first study relating various functions tokens provide to users (e.g., transaction convenience and financial rewards through holding and staking) to token prices, both theoretically and empirically, with endogenous adoption and agent heterogeneity. We start by building a continuous-time model of an economy with a tokenized digital network, where agents optimally conduct transactions on a platform subject to endogenous productivity shocks, stake tokens to earn rewards from both newly minted tokens and fees, and consume offline (off-chain or off-network). We cast the interactions as a mean-field game (MFG) with stochastic control and systematic shocks and apply the master equation approach, which marks a novel application of the methodology beyond macroeconomics and idiosyncratic shocks. The aggregate staking ratio is a key determinant for the equilibrium reward rate and token prices. The agents' onchain and overall wealth distributions in an expected steady state follow Pareto-like distributions, and staking facilitates redistribution from poorer or more usage-focused adopters to the richer or investment-focused adopters, as in an inflation tax. The wedge between usage convenience and financial returns explains the violation of uncovered interest rate parity (UIP) and predicts profitable carry trades.

Staking involves two broad categories of activities: those related to pan-PoS consensus protocols and those in higher-layer (decentralized) applications.¹ Fundamentally,

¹The two are not mutually exclusive. Solana, for example, uses both PoS and DeFi staking. The classification we use follows mainstream cryptocurrency data aggregators such as CoinMarketCap. Even on non-blockchain-based or centralized platforms, various programs that involve escrows or crowd funds can be analyzed as a form of business layer staking through the lens of our framework.

1 blockchain functions to generate a relatively decentralized consensus record of system
2 states to enable economic interactions such as value or information exchanges (e.g., [Cong
3 and He, 2019](#)). PoS consensus protocols have gained popularity with major market play-
4 ers such as Ethereum adopting them. Under PoS, agents stake native tokens to compete
5 for the opportunity to record transactions, execute smart contracts, append blocks, etc.,
6 to earn block rewards and fees (e.g., [Saleh, 2021](#); [Kogan et al., 2021](#); [Jermann, 2023](#)). Mean-
7 while, various staking programs have become popular means for incentivizing desirable
8 behavior in higher layer applications, escrowing a balance of tokens under custody in a
9 smart contract or deploying them to enable network economic functionalities with stakers
10 earning staking rewards (e.g., [Augustin et al., 2022](#)).

11 Our model applies to both categories and captures several distinguishing features of
12 PoS protocols and stakable projects. First, such tokens are used on platforms that support
13 specific economic transactions or broader use in onchain-based projects. This generates
14 utility flows in, e.g., transaction convenience discussed in ([Cong et al., 2021b](#); [Biais et al.,
15 2020](#)). Second, the rate of staking rewards that an agent earns is influenced by other
16 agents' behavior in aggregate, but individuals take it as given when making decisions.²
17 Third, staking participation can influence the platform's development, e.g. by improv-
18 ing the efficiency and security of services, which enriches the agents' roles within the
19 platform, although it is not a necessary feature in all the projects.

20 Specifically, agents potentially heterogeneous in wealth and preference for accessing
21 the digital network allocate and adjust their holdings of staked tokens, transaction tokens,
22 and consumption numéraire under budget constraints, trading off staking rewards, token
23 transaction convenience, and numéraire convenience for offline (off-chain or off-platform)
24 consumption. Transaction convenience endogenously increases in platform productivity,
25 which evolves over time and is potentially influenced by staking activities while the stak-
26 ing reward rate is jointly determined by aggregate reward and tokens staked.

27 In equilibrium, the staking reward rate solves a fixed point problem. Token price dy-
28 namics are fully endogenous and are described by a partial differential equation akin to
29 the Black-Merton-Scholes formula. We simplify the equation to an ordinary differential
30 equation concerning the total token valuation, subject to an intuitive boundary condition
31 that tokens are worthless for unproductive platforms. We show that the staking ratio,

²Polkadot (DOT) constitutes an example: the reward rate for validators is determined by the current aggregate staking ratio. The fewer DOTs are staked, the higher the yield is for a planned amount of reward.

1 defined as the ratio of aggregate tokens staked in the economy to the total quantity of
2 tokens in supply, proves crucial for token pricing and reward rate determination in equi-
3 librium. Related to the TVL (total value locked) metric that practitioners emphasize, it
4 constitutes a new predictor for token price dynamics. UIP is naturally violated because
5 of agents' usage utility which is generally divergent and not reflected in wealth or token
6 price returns, leading to staking-ratio-based trading strategies.

7 When agents are heterogeneous in wealth and types, the cross-sectional equilibrium
8 reward rate is then determined by the whole distribution of agents, each solving an op-
9 timal dynamic control problem taking the market states as given. Under the endogenous
10 evolution of the wealth distribution, the system is captured by coupled stochastic partial
11 differential equations. The staking ratio then involves the weighted average of individual
12 staking choices, which in turn is shaped by the agents' wealth distribution. The resulting
13 reward rate further enters agents' onchain wealth dynamics. Therefore, agents' individ-
14 ual dynamic optimizations interact and co-evolve with the wealth distribution in such an
15 MFG. The resulting equilibrium is characterized by a so-called master equation, which
16 relates the value function to individual states and also captures influence from the system
17 states with common shocks.

18 We show that our findings from the baseline model remain robust, and further discuss
19 the impact and evolution of wealth heterogeneity. In particular, we derive analytically the
20 expected stationary wealth distribution, which is Pareto-like. Higher platform productiv-
21 ity provides greater usage benefits for all users while exacerbating their wealth inequality.
22 In general, the tradeoff between aggregate welfare and inequality also depends on staking
23 design, user-type distribution, and the platform development stage. We further numeri-
24 cally examine the impulse responses of wealth distribution and staking ratio to aggregate
25 shocks, e.g., in platform productivity. We observe over-responses in the staking ratio due
26 to the intricate interplay among agents within a dynamically evolving distribution, along
27 with the cascading consequences of the platform's post-shock development.

28 We derive three main sets of model predictions concerning the economics of staking
29 and its asset pricing implications. First, the staking reward is positively related to the
30 staking ratio in the cross-section. While more staking reduces the reward rate for any
31 given reward quantity, more rewards induce more staking, creating a higher staking ratio
32 for individual agents and in aggregate (which is exacerbated by wealth concentration).

1 Second, expected price appreciation increases with the aggregate staking ratio. Note that
2 both the price drift and staking ratio are functions of platform productivity. In equilibrium,
3 agents stake more when the platform productivity is low, yet that is exactly the time
4 that more wealth can be potentially allocated onto the platform in the future. A higher
5 staking ratio also feeds back to the productivity growth, which increases future demands
6 for tokens and their prices. Third, there are generally predictable excess returns to staking
7 over holding the numéraire, which arise as compensation for the losses in transaction and
8 consumption convenience, in a similar spirit as [Valchev \(2020\)](#). The model thus implies
9 that UIP fails for stakable tokens. We derive the expression for crypto carry and find that
10 higher carry attracts greater staking, generating greater price appreciation and excess
11 return. Because the reward rate mechanically decreases with a greater staking ratio, carry
12 predicts lower excess returns in the time series than in the cross-section.

13 We test these model implications empirically and find corroborating evidence in a
14 comprehensive dataset covering all major stakable tokens and DeFi projects. We obtain
15 information about 66 tokens from [stakingrewards.com](#) spanning July 2018 to November
16 2022. We first document that a higher reward ratio for staking significantly and positively
17 relates to a higher staking ratio. A 10-percentage-points increase in the aggregate reward
18 ratio (e.g., from 10% to 20%) is associated with a 7.79-percentage-point higher staking ratio
19 in average. Moreover, the reward rate has a predictable effect on changes in the staking
20 ratio in both cross-section and short-time windows. On average, a one percentage point
21 increase in reward rate in the previous week increases the staking ratio in the following
22 week by about 0.026 percentage points. This property is robust to adding both two-way
23 fixed effect and control variables including market cap and token return volatility. How-
24 ever, its significance decreases with longer time intervals, reflecting to some extent the
25 mechanical downward adjustment of the reward rate when more tokens are staked (be-
26 cause the same staking rewards have to be divided among more staked tokens).

27 We next verify that a larger staking ratio indeed predicts greater token price appre-
28 ciation in subsequent weeks. When the staking ratio increases by one percentage point,
29 the corresponding token price appreciates by 0.066% in the following week. Considering
30 that the variation of staking ratio is often large, especially in the cross-section, this effect
31 is relevant for investment decisions. Crypto market return and size factors do not ex-
32 plain the predictive power of the staking ratio, which is closely related to market liquidity

1 and depth, and reflects the fact that tokens can be commodity-like.³ Staking reduces the
2 supply of liquid cryptocurrencies, and hence pushes up the token’s prices and increases
3 the convenience yields of tokens. This resembles how using commodities as collateral
4 increases the spot price and the convenience yield of the underlying commodities (Tang
5 and Zhu, 2016).

6 Finally, we follow Fama (1984) to test if “interest rate” (i.e. reward rate) predicts “cur-
7 rency excess returns” (i.e., token excess return) and find that UIP is indeed violated. We
8 construct a carry trade strategy that goes long high-carry crypto assets and shorts low-
9 carry assets, yielding an annualized Sharpe ratio of 1.60 with weekly rebalancing. Crypto
10 carry predicts excess returns almost one-for-one in the cross-section, with a reduced al-
11 beit significant effect in the time series. Intuitively, a higher reward rate attracts more
12 staking, which persists over the locked period, reducing the reward rate going forward
13 and thus the total expected return, as our model implies.

14 **Literature.** Our study adds to the literature on blockchain economics and cryptocurrency
15 markets.⁴ In particular, we build on the tokenomics framework of Cong et al. (2021b) and
16 Cong et al. (2021d) to add to emerging studies on Proof-of-Stake protocols (e.g., Fanti et al.,
17 2021; Saleh, 2021; Benhaim et al., 2021) and debates on the environmental and scalability
18 issues associated with Proof-of-Work (PoW) protocols (e.g., Cong et al., 2021a; Hinzen
19 et al., 2019). We also add to the emerging literature on DeFi (e.g., Park, 2021; Cong et al.,
20 2022; Li et al., 2022).

21 The most closely related paper to ours is John et al. (2022) which theoretically ex-
22 amines native PoS crypto assets that serve primarily as investment vehicles, whereas we
23 focus on the platform tokens with a combination of utility flow and investment function
24 while endogenizing agents’ dynamic consumption off the network. While both studies
25 demonstrate that the equilibrium staking ratio increases in staking rewards, John et al.
26 (2022) find that staked asset value can exhibit a non-monotonic relationship with block

³Commodities Futures Trading Commission (CFTC) regards cryptocurrencies as commodi-
ties, see, e.g., https://www.cftc.gov/sites/default/files/2019-12/oceo_bitcoinbasics0218.pdf.

⁴Existing studies mostly examine issues related to consensus algorithms (Biais et al., 2019; Saleh, 2021),
cryptocurrency mining (e.g., Cong et al., 2021a; Lehar and Parlour, 2020), scalability (e.g., Abadi and Brun-
nermeier, 2018; John et al., 2020), fee designs Easley et al. (2019); Basu et al. (2019); Huberman et al. (2021),
DeFi (e.g., Harvey et al., 2021; Capponi and Jia, 2021), ICOs (e.g., Lyandres et al., 2019; Howell et al., 2020),
pricing of crypto assets (e.g., Liu et al., 2019; Cong et al., 2021b; Prat et al., 2019), manipulation and regula-
tion (e.g., Griffin and Shams, 2020; Li et al., 2021; Cong et al., 2021c, 2023), or digital currencies (e.g., Gans
et al., 2015; Bech and Garratt, 2017; Chiu et al., 2019; Cong and Mayer, 2021).

1 rewards and cause redistribution across agents with divergent trading horizons. We com-
2 plement this by endogenizing potential adopters' outside option, exploring agents' het-
3 erogeneity in wealth and usage preference, as well as considering DeFi staking in addition
4 to the PoS consensus. Also closely related is [Jermann \(2023\)](#) who develops a macrofinance
5 model specifically for Ethereum and quantitatively estimates the long-run staking ratio
6 of ETH and the implied money supply. While both studies pin down equilibrium staking
7 considering platform usage value relative to staking benefits, we endogenize the plat-
8 form productivity process whereas [Jermann \(2023\)](#) endogenizes the token supply. Conse-
9 quently, our focus is on token pricing instead of monetary policy. [Fanti et al. \(2021\)](#) is the
10 earliest to develop a cash-flow-based valuation framework of PoS cryptocurrencies to un-
11 derstand how the liquidity of validators' holdings, token valuation, and network security
12 relate to one another. Their focus is on long-run transaction fees, we focus on block re-
13 wards, endogenous reward rate, and transaction dynamics. Empirically, a recent article by
14 [Augustin et al. \(2022\)](#) characterizes the risk and return trade-offs of yield farming using
15 data from PancakeSwap. We offer likely the first theoretical framework to think about
16 returns to DeFi staking, UIP violations, and crypto carry, with empirical corroborating
17 evidence.

18 Differing from all aforementioned studies, we employ mean-field game analysis to
19 study agent heterogeneity and its interaction with general forms of staking in steady
20 states and transitions. In particular, we derive onchain and overall wealth distribution
21 in the long run, highlight the trade-off between platform development and equality, and
22 demonstrate how staking facilitates redistribution. Our study not only represents one of
23 the earliest adaptations of mean-field games and the master equation solution in finance,
24 but also innovates by introducing expected steady-states and transition path analysis.

25 Finally, studies in international finance examine uncovered interest rate parity (e.g.,
26 [Fama, 1984](#); [Lustig et al., 2019](#)). Carry and its predictability have been analyzed not only
27 for currencies but also for other assets such as equities (e.g., [Fama and French, 1998](#); [Grif-
28 fin et al., 2003](#); [Hou et al., 2011](#)), bonds (e.g., [Ilmanen, 1995](#); [Barr and Priestley, 2004](#)), and
29 commodities (e.g., [Bailey and Chan, 1993](#); [Casassus and Collin-Dufresne, 2005](#); [Tang and
30 Xiong, 2012](#)). [Kojien et al. \(2018\)](#) applies a general concept of carry and finds that carry
31 predicts returns in both the cross-section and time series. We add by documenting UIP
32 violations and carry among cryptocurrencies (and with fiat currencies). We theoretically

1 rationalize the observations and link carry to tokenomics, complementing recent empir-
2 ical work by [Franz and Valentin \(2020\)](#) that documents deviations from covered interest
3 parity among cryptocurrencies.

4 The remainder of this paper is structured as follows. Section 2 sets up a dynamic model
5 of staking and token pricing. Section 3 characterizes a homogeneous-agent equilibrium
6 to illustrate key mechanisms and convey economic intuition. Section 4 solves the full
7 model under heterogeneous settings and derives further implications in the mean-field
8 equilibrium. Section 5 introduces the data, stylized facts, and hypotheses to test. Sec-
9 tion 6 presents empirical evidence corroborating our theory. Section 7 concludes. The
10 appendices contain the institutional details of staking, introduction to mean-field games
11 (including the derivation of the master equation), formal proofs of propositions, numerical
12 procedures, and various extended discussions.

13 2 A Model of Tokenized Economy with Staking

14 2.1 Model Setup

15 In a continuous-time economy with infinite horizon, a continuum of agents optimally
16 allocate individual wealth between the offline real economy for consumption and a gen-
17 eral digital marketplace (e.g., a tokenized blockchain platform, henceforth referred to as
18 “the platform”) where they can conduct peer-to-peer transactions while participating in
19 staking programs for network services and contribution (e.g., consensus recordkeeping,
20 liquidity provision, or improving system security in DeFi protocols).⁵ A generic consump-
21 tion good serves as the numéraire and the medium of exchange in the digital network is
22 its native token.

23 **Platform productivity and token price.** As in [Cong et al. \(2021b,d\)](#), productivity A_t
24 captures the general usefulness and functionality of the platform, i.e., the convenience
25 users obtain by transacting on the platform using its tokens. We assume that A_t evolve
26 endogenously according to:

$$dA_t = \mu^A(\Theta_t)A_t dt, \quad (1)$$

27 where Θ_t is the endogenous staking ratio, i.e., the ratio of the aggregate number of staked
28 tokens to the total number of tokens, which constitutes a potential state variable that in-

⁵Our findings remain robust under finite horizons, though the numerical procedures have to be modified.

1 influences token prices and agent decisions. In base layers (pan-PoS consensus protocols)
 2 and/or higher layers (DeFi applications and Layer 2 projects), staked tokens contribute to
 3 the development of the platform by maintaining node operations, facilitating the achieve-
 4 ment of consensus, and increasing the security level of the network, respectively. There-
 5 fore, a higher staking ratio typically improves platform productivity, i.e., the drift of A_t is
 6 weakly increasing in Θ_t .⁶

7 Without loss of generality, we denote the token price (in units of the numéraire) as
 8 P_t , which is endogenously determined by A_t , the token issuance (total supply) Q_t , as well
 9 as external demand shocks (e.g., regulatory changes, market sentiment swings, and noise
 10 trading that are independent of (A_t, Q_t)) captured in a Markov stochastic process S_t sat-
 11 isfying $dS_t/S_t = \mu^S dt + \sigma^S dZ_t$ with one source of Brownian innovations $\{Z_t, t \geq 0\}$. In
 12 our setting, we treat S_t as a demand shifter so as to understand the impact of aggregate
 13 shocks.⁷

14 The token price, $P_t = P(A_t, Q_t, S_t)$, then follows a general diffusion process with en-
 15 dogenous and potentially time-varying μ_t and σ_t , which we shall solve for:

$$dP_t = P_t \mu_t dt + P_t \sigma_t dZ_t. \quad (2)$$

16 **Agents, adoption, and convenience.** We normalize the continuum of agents to be one
 17 unit measure and allow heterogeneity in their wealth. At time t , the economy wealth
 18 distribution is denoted as $m_t = m(w_t)$, where m_t is assumed to be an absolutely continuous
 19 density on $W = [\underline{w}, \infty] \subset \mathbb{R}^+$. Agent indexed by i is characterized by her current wealth
 20 $w_{i,t}$. Each agent makes consumption-portfolio choices among staked (locked) tokens, non-
 21 staked (tradable) tokens, and holding the numéraire (consumption goods or fiat). An agent
 22 becomes a platform user if she holds tokens either for staking or transactions on the
 23 platform. To simplify notations, we omit the subscript i in the general formulation of
 24 agents whenever feasible.

25 Users gain convenience from holding tokens and conducting economic activities on

⁶We could have introduced Brownian shocks to A_t directly, as we did in previous drafts, but they do not add new economic insights and are left out for parsimony and ease of numerical computation. Its effects are similar to aggregate demand shocks. Also, staking could hurt platform productivity if the staker competition is so fierce that fewer stakers participate. Instead of allowing μ^A to potentially decrease in Θ_t , we capture this by explicitly modeling the staking competition.

⁷If one allows S_t to be independently and identically distributed across individuals (e.g., capturing individual sentiments), the problem is further simplified without resorting to the Master Equation, as we show in earlier drafts of the paper. Correlations in individual sentiments or preferences can also be used to microfound the aggregate demand shock.

1 the platform. Since staked tokens are locked from the staker’s perspective, they can only
 2 derive transaction convenience from non-staked (tradable) tokens, which we model simi-
 3 larly as in [Cong et al. \(2021b,d\)](#): For an agent holding x_t (in numéraire, positive) worth of
 4 tradable tokens on the platform, she derives a utility flow:

$$dv(x_t) = dv_t = x_t^{1-\alpha}(N_t A_t U_t)^\alpha dt - \varphi dt. \quad (3)$$

5 With $\alpha \in (0, 1)$, the marginal transaction convenience $\frac{\partial v}{\partial x} > 0$ and decreases with x_t .
 6 $U_t = U_{i,t} = U(u_{i,t}, w_{i,t}) > 0$ is differentiable in $u_{i,t}$ and reflects transaction needs. $u_{i,t}$ indi-
 7 cates the agent’s idiosyncratic transaction preference at time t that is i.i.d. with bounded
 8 support. The individual’s transaction needs increase with wealth $w_{i,t}$, whereas the type
 9 varies the marginal needs. N_t is the measure of staked tokens so that a larger N_t cor-
 10 responds to an ecosystem with great effectiveness of validators that facilitate onchain
 11 transaction. For DeFi staking, especially the ones where token staking has contempora-
 12 neous network externality, N_t nicely maps to the concept of Total Value Locked (TVL) and
 13 the industry’s emphasis on it. In general, we only need N_t to be smoothly increasing in
 14 the amount of tokens staked and is zero when no token is staked.

15 At any time t , agents can choose not to participate, so that our results are not driven
 16 by switching costs. Agents adopting the platform need to incur a flow cost φ per unit of
 17 time for platform adoption to realize the transaction convenience as the second term in
 18 (3) shows. It captures the required effort and attention for participation.⁸ Even though
 19 we focus on token convenience as a medium of exchange, the reduced-form convenience
 20 could also include other utility flows such as governance and voting rights.

21 Following [Bansal and Coleman \(1996\)](#) and [Valchev \(2020\)](#), the convenience of holding
 22 numéraire is reflected in the reduction of transaction costs in consumption. Denote the
 23 cost as $\Psi_t = \Psi_t(y_t, n_t, A_t) \geq 0$, where y_t and n_t are consumption and numéraire holdings
 24 respectively. Naturally, $\frac{\partial \Psi}{\partial y} \geq 0$, $\frac{\partial \Psi}{\partial n} < 0$. Then $-\frac{\partial \Psi}{\partial n} > 0$ reflects the marginal convenience
 25 yield of holding the numéraire. Intuitively, when the platform productivity is lower, the
 26 relative convenience of numéraire is higher. Thus, we assume $\frac{\partial \Psi}{\partial A} \leq 0$.

27 Token transaction convenience and cost enter agents’ wealth dynamics rather than
 28 utility, for two reasons: First, token convenience flows and transaction costs are typically
 29 pecuniary in practice, corresponding to business profits and liquidity costs on real bal-

⁸It can also include the opportunity cost of earning risk-free interests offline, as in [Cong et al. \(2021b\)](#).
 If we take this interpretation, then the reward rate needs to be redefined to be in addition to the risk-free
 rate. For simplicity, we set the risk-free rate to zero.

ances, respectively. Second, this approach is functionally equivalent to accounting them in the utility function (Feenstra, 1986), and is a standard approach in the literature on convenience yields of bonds, for example.

Staking and staking rewards. Staking rewards incentivize agents to stake their tokens to either generate consensus records in a base layer or participate in some DeFi program, such as a liquidity pool or insurance pool. In practice, staking rewards come from fees others pay and additional token issuance (emission). To model staking rewards from newly issued blocks, we assume that the total amount of tokens at time t , Q_t , follows a general dynamic process: $dQ_t = E(L_t, A_t)Q_t dt$, where E is the “emission rate” function and L_t is the aggregate amount of staked tokens at t .⁹ This token supply dynamics reflect not only a potential “inflation” but also the redistribution of onchain wealth between transaction users and token stakers, in a similar spirit to that in John et al. (2022).

We denote the aggregate rewards generated by the transaction fees (e.g., ETH gas) as $F_t = F(L_t, A_t, Q_t)$. F_t is dependent on the current scale of validators in the ecosystem, as well as the platform productivity that reflects the capacity of processing transactions. Therefore, it also involves L_t and A_t .¹⁰ The total amount of tokens distributed as rewards R_t then becomes:

$$R_t = R(E_t Q_t, F_t) \equiv R(L_t, A_t, Q_t). \quad (4)$$

All staked tokens are fungible and consequently all stakers face an instantaneous reward rate akin to interest rates on bank deposits:¹¹

$$r_t \equiv \frac{R(L_t, A_t, Q_t)}{L_t}. \quad (5)$$

Here we only require that R_t being increasing in E and F (since they are both sources of staking rewards) and that r_t being weakly decreases with L_t , as is observed in practice.¹²

⁹The emission schedule is typically public information at the time of staking, and can be at least estimated based on real-time blockchain data (see details in Online Appendix OA1.2). Meanwhile, as Jermann (2023) proves, the equilibrium token supply could be well controlled by the ecosystem design. Therefore, we set the dynamic of Q_t without uncertainty terms. However, E could vary over time.

¹⁰The gas fee of a transaction in practice entails base and priority fees. The base fee is burned whereas the priority fee is paid to the validator as a tip, which varies across validators and users. L_t , as a proxy of the size of validators, does not equal the number of the validators, but reflects the staking scale competition across the validators, and is usually a good proxy in practice. Online Appendix OA1.2 contains more details.

¹¹For simplicity, we do not model the term structure of staking rewards—the focus of John et al. (2022). In our continuous-time setting, we only need staked tokens to be locked for dt . In our empirical tests, we only require agents to know the next period’s reward emission.

¹²For example, many programs fix the total amount of rewards, which implies that staking more tokens reduces the reward per token staked. More generally, L_t decreases the average unit staking rewards r_t

1 To capture the cost of node operation and risk of slashing, we assume that stakers incur
 2 costs at a rate $c_t < r_t$ proportional to their staking amount.¹³

3 It is straightforward to conclude that if someone stakes k_t tokens ($k_t P_t$ dollars), by Itô's
 4 Lemma, the wealth increments from staking satisfy:

$$d(k_t P_t) = k_t dP_t + P_t(r_t - c_t)k_t dt = (k_t P_t)[(\mu_t + r_t - c_t)dt + \sigma_t dZ_t]. \quad (6)$$

5 2.2 Agents' Problem and Staking as Optimal Control

6 Taking as given the system staking reward rate, r_t , each agent with personal wealth
 7 w_t decides at time t the consumption rate y_t and a portfolio consisting of l_t numéraire-
 8 equivalent amount of staked tokens, x_t numéraire-equivalent amount of tradable tokens
 9 and n_t numéraire, where $x_t, l_t, n_t \in [0, w_t]$, $n_t = w_t - x_t - l_t$. The individual stochastic control
 10 problem involves using (y_t, x_t, l_t) to optimize a discounted life-time utility:

$$\max_{\{y_s, x_s, l_s\}_{s=t}^{\infty}} \mathbb{E}_t \left[\int_t^{\infty} e^{-\phi(s-t)} \mathcal{U}(y_s) ds \right], \quad (7)$$

11 where $\mathcal{U}(y_t)$ is the agent's instant utility from consumption, which is strictly increasing
 12 and concave, and ϕ is the discount rate. Because staked tokens cannot be instantaneously
 13 liquidated, the agent also faces the budget constraint, $y_t \leq w_t - l_t$.

14 Meanwhile, the agent's overall wealth dynamics satisfy:

$$\begin{aligned} dw_t &= [(x_t + l_t)\mu_t + l_t(r_t - c_t) + v_t - y_t - \Psi_t]dt + (x_t + l_t)\sigma_t dZ_t \\ &= f(y_t, x_t, l_t; w_t, r_t, A_t)dt + g(y_t, x_t, l_t; w_t, r_t, A_t)dZ_t. \end{aligned} \quad (8)$$

15 Note that if we allow some of l_t to contribute towards x_t , our framework can be used
 16 to study the recent popular "liquid staking" that surpassed decentralized lending in TVL,
 17 where stakers can get staking rewards without being restricted by the lock-up.¹⁴

from both channels. For gas or service fees, since a higher L_t indicates the ecosystem has more validators and better capacity of validations, it generates competition on validating transactions, also depreciates the premium of prioritized transactions. Note that the definition and operation of priority fees are reported on [the official website of Ethereum](#), as well as third-party knowledge pages, e.g., [blocknative](#). As for emissions, the common practices mostly adopt such a reward offering strategy. Otherwise, staking would be more like cooperation and generate quite low liquidity to the ecosystem. For example, the corresponding reward rate of Ethereum EIP1559 takes the form of k/\sqrt{L} . This study scope setting is also a common practice. [Jermann \(2023\)](#) offers an in-depth analysis on optimal policies across a generalized form of $kL^{-1/s}$.

¹³The time-varying nature of c_t captures the fact that gas fees and risks of slashing could change over time. However, this is not crucial for our key economic insights.

¹⁴<https://www.coindesk.com/markets/2023/02/27/liquid-staking-replaces-defi-lending-as-second-largest-crypto-sector/>. This is achieved through wrapped tokens that allow unsupported assets to be traded, lent, and borrowed on DeFi platforms. Our earlier example of Solana is supported by liquid staking platforms such as Lido, as of 2022.

2.3 Staking Ratio, Reward Rate, and Market Clearing

Staking ratio. We define $\theta_{i,t}$ as the staking ratio given reward rate r_t at time t , then:

$$\theta_{i,t} = \theta(r_t, A_t, w_{i,t}, u_{i,t}) = \frac{l(r_t, A_t, w_{i,t}, u_{i,t})}{x(r_t, A_t, w_{i,t}, u_{i,t}) + l(r_t, A_t, w_{i,t}, u_{i,t})} = \frac{l_{i,t}}{q_{i,t}}, \quad (9)$$

where $q_{i,t} = x_{i,t} + l_{i,t}$ is the aggregate individual onchain value. The overall staking ratio, Θ , the ratio of the aggregate number of staked tokens to the total number of tokens, is a resulting control under system states, r , A , and the aggregation of agents' states,

$$\Theta_t = \Theta(r_t, A_t, \{w_{i,t}, u_{i,t}\}_{i \in [0,1]}) = \frac{L_t P_t}{Q_t P_t} = \frac{\int_W l(w_t) m_t(w_t) dw_t}{\int_W [x(w_t) + l(w_t)] m_t(w_t) dw_t}. \quad (10)$$

Agents stake taking as given the reward rate. That is, the staking ratio is a function of the current reward rate r_t . It can be shown that Θ_t is continuous in r_t . Staking ratio is important because it links individual choices with global states.¹⁵

Equilibrium reward. According to (5), r_t is influenced by the aggregate stake, L_t , and thus by the aggregation of agents' controls, Θ_t . At the same time, Θ_t is a function of r_t . Then the equilibrium staking reward rate, r_t^* , solves the fixed-point problem:

$$r_t^* = r(\Theta^*(r_t^*, A_t)). \quad (11)$$

Note that the reward rate decreases in Θ_t . We later show that all the agents' staking amount increases with r_t , which then gives a unique equilibrium r_t^* .

Define ρ_t as the staking reward ratio, then: $\rho_t \equiv \frac{R_t}{Q_t} \Rightarrow r_t = \frac{\rho_t}{\Theta_t}$. Since ρ_t has a one-to-one correspondence to the equilibrium r_t^* , the equilibrium staking ratio can also be represented as $\Theta^*(\rho_t, A_t)$. In our subsequent comparative statics analysis, we use $\Theta^*(\rho_t, A_t)$, while retaining the notation $\Theta(r_t, A_t)$ to highlight the output of agents' choices. When the system is at the equilibrium, $\Theta^*(r_t^*, A_t) = \Theta^*(\rho_t, A_t)$.

Token market clearing. The total quantity of tokens Q_t is equal to the sum of token holdings affected by the noisy demand shock:¹⁶

$$Q_t P_t = \int_W (x_t + l_t) m_t dw_t S_t. \quad (12)$$

¹⁵For notational simplicity, $\{w_{i,t}, u_{i,t}\}_{i \in [0,1]}$ are omitted in the remainder of the paper. In practice, Θ_t can be publicly tracked using data from websites such as *StakingRewards.com* or original platform networks.

¹⁶Naturally, the token price that satisfies the (onchain) market clearing condition should simultaneously clear both the staking and non-staking market. Otherwise, arbitrage opportunities arise. We simultaneously obtain the staking market clearing by combining (10) and (12), i.e., $P_t L_t = P_t Q_t \Theta_t = \int_W l_t m_t dw_t S_t$.

3 Equilibrium Characterization and Implications

To convey core economic intuitions, we first solve for a baseline Markovian equilibrium with homogeneous agents each having the same type u and non-negative (but finite) initial wealth, and set the transaction threshold to be zero. In a symmetric equilibrium, the evolution of individual wealth is the same across agents, which is denoted by w_t . Section 4 derives the equilibrium under the general settings with agent heterogeneity.

For homogeneous agents, we leave out the distribution m and write the indirect utility function (given that Q_t does not enter, as we show later):

$$J(t, w_t, A_t, r_t) = \max_{\{y_s, x_s, l_s\}_{s=t}^{\infty}} E_t \left[\int_t^{\infty} e^{-\phi(s-t)} \mathcal{U}(y_s) ds \right]. \quad (13)$$

We then derive the Hamilton-Jacobi-Bellman (HJB) equation:

$$\phi J(t, w, A, r) = \max_{\{y, x, l\}} \left\{ \mathcal{U}(y) + f(y, x, l; w, r, A) \frac{\partial J}{\partial w} + \frac{1}{2} g(y, x, l; w, r, A)^2 \frac{\partial^2 J}{\partial w^2} + \mu^A(\Theta) A \frac{\partial J}{\partial A} \right\}, \quad (14)$$

where we leave out the time subscript, t , for simplicity.

3.1 Rewards and Staking Activities

We start by analyzing the agents' optimal decisions. At the instant of decision-making, the agent takes the reward rate r_t as given. Intuitively, the marginal transaction convenience is decreasing with x_t , the value of tradable token held.

Proposition 1. Optimal individual staking. *For an agent with wealth w_t and type u under system states $\{A_t, r_t\}$, the optimal staking ratio, θ_t^* , is unique and satisfies:*

$$\theta_t^* = \max \left\{ 0, 1 - \frac{N_t A_t U_t}{q_t} \left(\frac{1 - \alpha}{r_t - c_t} \right)^{\frac{1}{\alpha}} \right\}. \quad (15)$$

The reward rate, r_t , appears in the denominator, implying that the individual staking ratio is weakly increasing in r_t . When the marginal transaction convenience becomes smaller than the staking reward rate, i.e., $r_t - c_t > (1 - \alpha) \left(\frac{N_t A_t U_t}{x_t^\alpha} \right)^\alpha$, an agent starts to stake excess tokens. Because to an individual, the benefits of staking is constant, an interior solution exists. Substituting the agents' individual optimal choices into (10), we obtain the aggregate staking ratio $\Theta(r_t, A_t, w_t, u)$. Market clearing guarantees the existence of this equilibrium staking ratio, which is weakly increases with reward rate r_t . $\{r_t, \Theta(r_t, A_t, w_t, u)\}$ satisfies (10) and (11). The equilibrium is determined by the aggregate staking reward ratio ρ_t . The following proposition states that the higher aggregate staking reward attracts agents to stake more, leading to a higher staking ratio.

1 **Proposition 2. Equilibrium staking ratio.** *The optimal token holding, $q_t = x_t + l_t$, is*
2 *unique, positive, and equal for any individual type u . The equilibrium overall staking ratio,*
3 *Θ_t^* , is unique and satisfies:*

$$\rho(\Theta_t^*) = \Theta_t^* \left\{ (1 - \alpha) \left[\frac{N(\Theta_t^*)A_t U_t}{q_t(1 - \Theta_t^*)} \right]^\alpha + c_t \right\}. \quad (16)$$

4 *In particular, when treated as a system state, higher total reward ratio ρ leads to a higher*
5 *aggregate staking ratio in equilibrium, i.e., $\forall \rho' > \rho > 0$,*

$$\Theta^*(\cdot, \rho') > \Theta^*(\cdot, \rho). \quad (17)$$

6 Proposition 2 gives a general characterization of how aggregate staking reward affects
7 staking ratio in equilibrium. The result (16) applies to both cross-sectional comparison and
8 time series analysis. Consider the economic meanings of the right hand. The aggregate
9 wealth inflow affects transaction convenience by two forces. The inflow from expected
10 price appreciation has a diminishing marginal transaction convenience on the one hand,
11 and thus moves to the stake pool, increasing the network effect therefore increasing the
12 convenience benefits, ultimately making the two forces in balance. Importantly, (17) gen-
13 erates comparative statics on ρ_t . For a given platform productivity A_t , as the aggregate
14 staking reward ratio ρ_t increases, the corresponding overall staking ratio increases.

15 3.2 Staking Ratio & Price Dynamics

16 We link staking activities to token prices. In general, the token price appreciates when
17 more agents' wealth flows into the platform, whether it is due to high platform produc-
18 tivity and thus large transaction convenience, or due to greater participation in staking.
19 We are interested in the drift term μ_t of token prices, which depends on both the platform
20 states and the agents' control cross-sectionally. For simplicity, we omit the subscript t
21 when there is no ambiguity.

22 By Proposition 2, a participating agent's optimal onchain wealth, q_t , is unique. Com-
23 bining with the market clearing condition, (12), as well as the equilibrium reward rate:

$$0 = \left(\mu + r(\Theta) - c + \frac{\partial \Psi}{\partial n} \right) \frac{\partial J}{\partial w} + \frac{PQ}{S} \sigma^2 \frac{\partial^2 J}{\partial w^2}, \quad (18)$$

24 where $\frac{\partial \Psi}{\partial n}$ may also be a function of P_t and Q_t . Further, as P_t is endogenously given by A_t ,
25 Q_t , and S_t . As the price dynamic, (2) defines, μ_t and σ_t are also endogenously determined.
26 Applying Itô's Lemma and matching the coefficients to (2), we obtain:

$$\mu_t = \frac{1}{P_t} \left(\frac{\partial P_t}{\partial A_t} A_t \mu_t^A + \frac{\partial P_t}{\partial Q_t} Q_t E_t + \frac{\partial P_t}{\partial S_t} S_t \mu_t^S \right), \quad \sigma_t = \frac{1}{P_t} \frac{\partial P_t}{\partial S_t} S_t \sigma_t^S. \quad (19)$$

1 Note that $\frac{\partial P_t}{\partial Q_t}$ is negative, thus the emission adds negatively to price drifts. In other words,
 2 emissions of staking rewards cause “inflation,” a concern token holders well recognize.

3 Combined with (19), the previous propositions, (18) can be rearranged as a partial
 4 differential equation with respect to A_t and Q_t , i.e., with $I = -\frac{\partial_{ww}J}{\partial_w J}$:

$$0 = \frac{\partial P}{\partial Q}EQ + \frac{\partial P}{\partial A}A\mu^A(\Theta^*) + \left[\frac{\partial P_t}{\partial S_t}S_t\mu_t^S - \frac{QI}{S} \left(\frac{\partial P}{\partial S}S_t\sigma^S \right)^2 \right] + [r(\Theta^*) - c + \partial_n\Psi]P, \quad (20)$$

5 (20) differs from a Black-Scholes-type partial differential equation (PDE): First, the
 6 “theta” term in Black-Scholes (BS) equation reflecting the variation of the derivative value
 7 over time is absent in (20). Instead, the term $\frac{\partial P}{\partial Q}EQ$ captures the expected inflation from
 8 token issuance. Second, since A_t , the productivity that drives token price, is not trad-
 9 able, the coefficient of $\frac{\partial P}{\partial A}$ is $A\mu^A$ instead of zero.¹⁷ Moreover, there is a “flow” term,
 10 $[r(\Theta^*) - c + \partial_n\Psi]P$, that reflects the excess gain from staking rewards offsetting the stak-
 11 ing cost and convenience loss. $\partial_n\Psi$, indicating the loss of numéraire convenience, is typi-
 12 cally negative and could be a function of A_t . $\left[\frac{\partial P_t}{\partial S_t}S_t\mu_t^S - \frac{QI}{S} \left(\frac{\partial P}{\partial S}S_t\sigma^S \right)^2 \right]$ captures the impact
 13 of external risk, where the later term features the impact of agents’ risk aversion, and does
 14 not appear in the risk-neutral BS equation.

15 (20) is a PDE involving derivatives w.r.t. A_t , Q_t , and S_t , which is hard to solve. The mar-
 16 ket clearing condition, (12), can be alternatively represented as a condition on aggregate
 17 wealth allocated to the platform, and is related to the emission rate, but not the aggregate
 18 amount of tokens, Q_t . Substituting the preceding equation into (20) converts the PDE into
 19 an ordinary differential equation (ODE). Moreover, to pin down a precise analytical ex-
 20 pression, we specify a log utility functional form for the agents given that the level risk
 21 aversion is not our focus, a Ψ_t linear in numéraire holding that captures the differential
 22 convenience direct consumption, and a zero sentiment (noise) drift μ^S .¹⁸

23 **Proposition 3. Token price and dynamic.** P_t is separable, $P_t = \frac{V(A_t)S_t}{Q_t}$, where $V(A_t)$
 24 captures the aggregate wealth allocated to the platform, and satisfies the ODE

$$0 = V'(A_t)A_t\mu^A(\Theta_t) + [r(\Theta_t) - c_t - E(\Theta_t, A_t) + \Psi_n(A_t)]V(A_t) - \frac{[\sigma^S(A_t)V(A_t)]^2}{w_t}, \quad (21)$$

25 where $\Theta_t = \Theta(A_t, V(A_t))$ and satisfies (16), w_t indicates the aggregation of agents’ wealth.
 26 Given the boundary condition $\lim_{A_t \rightarrow 0} V(A_t) = 0$, the ODE has a unique solution.

¹⁷If the fundamental productivity were tradable, the coefficient of $\frac{\partial P}{\partial A}$ would have been $r^f A$, where r^f is the risk-free rate and normalized to zero.

¹⁸We numerically verify that the model implications hold under general CRRA utilities.

1 The economic implications of (21) are similar to our previous discussion of (20). Under
 2 a fixed inflation rate, in equilibrium, the expected price drift, μ_t , and staking ratio, Θ_t ,
 3 are both functions of platform productivity, A_t . The boundary condition requires that a
 4 useless platform attracts no adopters.

5 Solving the ODE, we find that the equilibrium staking ratio Θ_t and expected price
 6 appreciation μ_t are positively related (Figure 1). Because staking ratio can be computed
 7 from onchain information, it can help predict price changes.

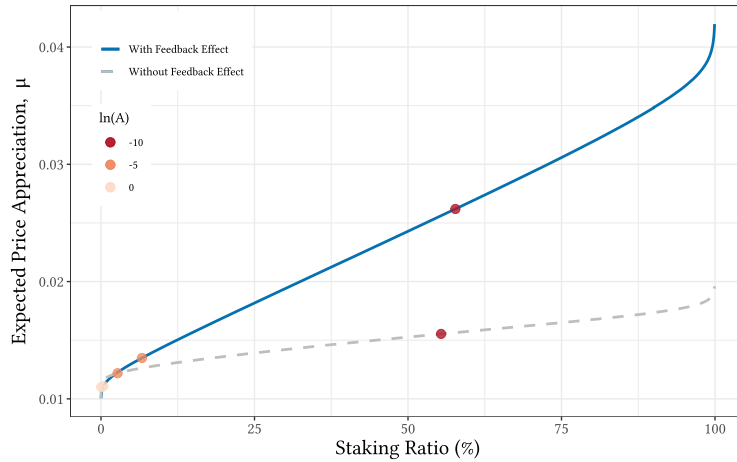


Figure 1: Staking ratio and price dynamics.

This graph shows the joint relationship between the system staking ratio Θ_t and the price drift μ_t . The blue curve is the case where the staking ratio feeds back the platform productivity A_t process (the main model), while the gray curve shows the case for comparison where the feedback effect does not exist. The colored scatter points on the two curves mark the corresponding point (Θ_t, μ_t) for different values of $\ln(A_t)$ respectively. As this graph shows, greater staking ratio relates to higher expected price appreciation.

8 There are two main economic driving forces. The first force comes directly from pro-
 9 ductivity A_t . On the one hand, μ_t declines in A_t . As A_t grows, agents allocate more wealth
 10 on the platform and less off-chain wealth, thus the potential future price appreciation is
 11 reduced, which generates the similar user-base stabilizing effect of tokens as Cong et al.
 12 (2021b). On the other hand, Θ_t also declines in A_t , because higher A_t results in a larger
 13 transaction convenience. Therefore, the joint dynamics of μ_t and Θ_t exhibit a positive re-
 14 lationship. This mechanism also explains the shape of the curve when the staking ratio
 15 is low. Such force does not rely on the feedback mechanism but in general a market phe-
 16 nomenon. Therefore, we can see from Figure 1 that even without the feedback effect (the
 17 grey curve), μ and Θ are positively related.

18 The second is the feedback effect of staking on the A_t process. As (1) and (19) show,
 19 a high staking ratio increases the productivity drift μ_t^A , and then leads to a large price

1 drift μ_t . This mechanism illustrates the role that staking plays in platform growth. In PoS,
 2 the system state with a relatively high staking ratio implies a strong network of highly
 3 engaged validators, so that the consensus and confirmation are efficiently reached. As for
 4 high-layer staking economy such as DeFi applications, with a certain capital value, a high
 5 staking ratio relates to a high TVL (total value locked), which is recognized as improving
 6 the security level of the platform. For both layers of the staking economy, the staking ratio
 7 positively impacts the growth of platform productivity A_t through the above-mentioned
 8 paths respectively, therefore resulting in a greater drift. As a reflection of the value of the
 9 platform, the price drift increases accordingly to (19). Online Appendix OA3.5 discusses
 10 further the implications of the feedback effect.

11 3.3 Token Excess Returns, UIP Violation, and Crypto Carry

12 Each token holder takes on the risk of token price fluctuation and loses the convenience of holding the numéraire. Denote the expected financial excess return of unit
 13 staked token over the numéraire by λ_t , $\lambda_t \equiv E_t [dP_t + P_t r^{staked\ token}] / P_t = \mu_t + r_t - c_t$.

14 **Proposition 4. Predictable excess return.** *The unit excess return, λ_t , satisfies*

$$15 \lambda_t = -\frac{\partial \Psi}{\partial n_t} + q_t^* \sigma_t^2 I > 0, \quad (22)$$

16 where $-\frac{\partial \Psi}{\partial n_t} > 0$ is the marginal convenience of holding numéraire, q_t^* is the optimal onchain
 17 wealth, $I = -\frac{\partial_{ww} J}{\partial_{wJ}} > 0$. RHS is positive, implying predictable excess returns.

18 Proposition 4 follows directly from the agents' optimization. The positive RHS of
 19 (22) implies predictable excess returns that arise as compensation for convenience losses
 20 and volatility risk. This phenomenon closely relates to the uncovered interest rate parity
 21 (UIP) in the foreign exchange market, since the token price in numéraire corresponds to
 22 the exchange rate, whereas the staking reward rate corresponds to the concept of interest
 23 rate. UIP implies that the expected returns on default-free deposits across currencies are
 24 equalized, and thus the expected excess return λ_t should be zero.¹⁹ However, (22) violates
 25 the UIP owing to the presence of two positive terms. First, when the relative convenience
 26 of numéraire increases, staked token is compensated with a higher financial return. This

¹⁹In relevant research on currency UIP, the more common notation reads $\lambda_t = E_t [dS_t/S_t + i_t^{foreign} - i_t^{local}]$, where S_t is the log exchange rate (foreign currency units per unit of local currency). The corresponding terms of S_t , $i_t^{foreign}$ and i_t^{local} are P_t , $r_t - c_t$ and the numéraire risk-free rate r_t^f (normalized to zero), respectively. In related empirical works, r_t^f is not always zero, and the time is discrete. The corresponding equation of UIP reads $E_t [\log P_{t+1} - \log P_t] = r_t^f - (r_t - c_t)$.

1 interpretation of UIP violation shares similar ideas with [Valchev \(2020\)](#); [Jiang et al. \(2021\)](#)'s
 2 explanation of the UIP puzzle in classical asset types such as bonds. The second term on
 3 the R.H.S represents the impact of volatility risk.²⁰

4 In a nutshell, the excess return of holding the token comes from both the staking re-
 5 ward and the price appreciation of tokens. But there is no free lunch. The excess return
 6 reflects the compensation for the missed convenience of holding the numéraire for con-
 7 sumption. This observation is general because convenience is a relative concept between
 8 any two assets. What this implies is that based on the same numéraire, the expected excess
 9 returns can be different for different tokens. Moreover, by using any of cryptocurrencies
 10 as numéraire, we can verify that UIP fails in general in the cryptocurrency market.

11 UIP violations naturally lead to profitable currency carry trades, which go long in
 12 baskets of currencies with high interest rates and short in low ones. In fact, carry is a
 13 general concept that applies in a host of asset classes, e.g., equities, bonds, commodities,
 14 Treasuries, credits, and options ([Kojien et al., 2018](#)). Its predictability of excess returns
 15 and investment performance are widely documented and studied (e.g., [Lustig et al., 2014](#);
 16 [Bakshi and Panayotov, 2013](#); [Burnside et al., 2011](#); [Menkhoff et al., 2012](#); [Kojien et al., 2018](#);
 17 [Daniel et al., 2017](#)). As a direct application to the violation of UIP, our model implies prof-
 18 itable crypto carry trades, where following [Kojien et al. \(2018\)](#), crypto carry is similarly
 19 defined as currency carry:

$$\text{carry}_t \equiv \frac{r_t - c_t - r^f}{1 + r^f}. \quad (23)$$

20 **4 Agent Heterogeneity and Mean-Field Equilibrium**

21 We now solve the full model under agent heterogeneity in both wealth and usage
 22 need for the platform. We find that all aforementioned model implications hold. We also
 23 derive the expected stationary wealth distribution, which exhibits a Pareto-like shape.
 24 While higher platform productivity offers greater transaction convenience, inequality also
 25 increases. We further subject the economy to aggregate shocks to examine its response
 26 dynamics, thereby elucidating the competitive dynamics among agents, rationalizing the

²⁰This explanation is related to studies using term structure models (e.g., [Bansal, 1997](#); [Lustig et al., 2019](#)), where the difference between domestic and foreign bond risk premia, expressed in domestic currency, is determined by the volatility difference of the permanent components of the stochastic discount factors. In addition, alternative relevant explanations for the UIP violation have been proposed in previous studies, ranging from time-varying risks including liquidity and volatility (e.g., [Bekaert, 1996](#); [Verdelhan, 2010](#); [Lustig et al., 2011](#); [Gabaix and Maggiori, 2015](#)) to peso problems (e.g., [Burnside et al., 2011](#)).

1 direct and indirect impact paths, etc.

2 Intuitively, poor agents with greater usage preference of the platform may stake less,
3 which in turn affects the aggregate staking ratio and token pricing. Further, introducing
4 wealth heterogeneity into the dynamic process enables us to discuss the evolution of the
5 wealth distribution and its long-run outcomes, and thus inequality and redistribution.

6 **4.1 The MFG Approach and Derivation of the Master Equation**

7 **Wealth heterogeneity and the mean-field game.** With wealth heterogeneity, the den-
8 sity m_t enters the determination of staking ratio and reward rate as (10) and (11) show.
9 Since agents solve their optimal control based on staking reward rates, m_t enters the value
10 function as an additional argument. For such a system involving the evolution of distri-
11 bution, we employ the so-called “backward-forward MFG system” for the system with
12 a backward HJB and a forward FP equation (law of motion).²¹ Because the external ag-
13 gregate (common) shock hits every agent, it adds randomness to the distribution so that
14 $\{m_t\}_{t \geq 0}$ is a random flow of measures.²² The resulting stochastic PDE system has been
15 thoroughly studied on its mathematical properties and applications, especially the equiv-
16 alent system defined by a so-called “master equation.” In the following, we build upon
17 Cardaliaguet et al. (2019) and Bilal (2023) to characterize the system with a master equa-
18 tion. For notational simplicity, we omit some arguments of a function whenever feasible.

²¹The mean field game (MFG) theoretical approach has been developed by Lasry and Lions (2007); Cardaliaguet et al. (2019), and applied in macroeconomics (e.g., Achdou et al., 2022) and related Bitcoin mining competition (Bertucci et al., 2020). Online Appendix OA3.1 provides a detailed review.

²²Let us compare aggregate shocks with another class of shocks that are also usually discussed, where each agent has an independent individual uncertainty. Although every agent randomly moves from her initial state, the stochasticity of directions and displacements is smoothed out after the summation of numerous agents, resulting in a deterministic evolution of the distribution. In contrast, the aggregate shock here randomly shifts system states and thus affects all agents systematically, despite the different exposures.

The standard time-dependent formulation of these coupled stochastic PDEs reads:

$$\begin{cases}
\phi J_t dt - dJ_t = \left\{ \begin{array}{l} \max_{y,x,l} \left[\mathcal{U}(y; w, m) + f(x, l; w, m) \frac{\partial J_t}{\partial w} + \frac{1}{2} g^2(x, l; w, m) \frac{\partial^2 J_t}{\partial w^2} \right] \\ + \mu^A A \frac{\partial J_t}{\partial A} - \frac{\partial g(w, m) v_t}{\partial w} \end{array} \right\} dt - v_t dZ_t \\
\equiv \left\{ \mathcal{U}(w, m) + L(w, m)[J] + \mu^A A \frac{\partial J_t}{\partial A} - \frac{\partial g(w, m) v_t}{\partial w} \right\} dt - v_t dZ_t, \\
dm_t = \left[-\frac{\partial}{\partial w} (f(w, m) m_t(w)) + \frac{\partial^2}{\partial w^2} \left(\frac{1}{2} g^2(w, m) m_t(w) \right) \right] dt - \frac{\partial}{\partial w} [g(w, m) m_t(w) dZ_t] \\
\equiv L^*(w)[m] dt - \frac{\partial}{\partial w} [g(w, m) m_t(w) dZ_t],
\end{cases} \tag{24}$$

where the second equal signs of the two equations define the notations for the optimized situation, including the utility \mathcal{U} , wealth drift f and diffusion g . $L(w)[J]$ is the Dynkin operator w.r.t. the individual state w . $L^*(w)[m]$ is also a useful operator, in which the star script reminds it is the adjoint operator of L . v_t is a function for penalty.²³

Regarding this system, the key of the master equation approach is to notice that the time-dependence of the value function dJ_t itself in (24) comes totally from the time-dependence of m_t .²⁴ As shown below, it treats J_t as $J(\cdot, m_t)$ and replaces dJ_t by the FP equation and the infinite-dimensional Itô's Lemma. As Bilal (2023) points out, though additional definitions introduced, the master equation brings substantial ease for discussion on economic insights, since it captures the system to be a Markovian representation of the agents' problem by a single equation. In this staking economy, the master equation reads:

$$\begin{aligned}
\phi J(w, m, A) &= \mathcal{U}(w, m) + L(w)[J] + \mu^A A \frac{\partial J}{\partial A} + \frac{\partial}{\partial w} \left[g(w) \int \frac{\delta J}{\delta m}(w, w', m) \frac{\partial g(w') m(w')}{\partial w'} dw' \right] \\
&+ \int \frac{\delta J}{\delta m}(w, w', m) L^*(w')[m] dw' \\
&+ \frac{1}{2} \int \int \frac{\delta^2 J}{\delta m^2}(w, w', w'', m) \frac{\partial g(w') m(w')}{\partial w'} \frac{\partial g(w'') m(w'')}{\partial w''} dw' dw''.
\end{aligned} \tag{25}$$

Without heterogeneous wealth and aggregate shocks, the master equation degenerates into the HJB equation, which corresponds to the first three terms on the right-hand

²³With the randomness in forward-backward SDEs, the HJB equation needs to involve a martingale as penalties to guarantee the solution is indeed adapted (according to the theory regarding forward-backward SDEs, see e.g., Pardoux and Răşcanu, 2014).

²⁴Put differently, $J_t = J(w_t, A_t, m_t)$ and the total derivative would include the time-dependence of all the state arguments. While in the HJB, the time-dependence of w_t and A_t have already been accounted for.

side. The next three terms intuitively capture the decomposition of the impact of m_t on the forward evolution of the MFG system: the first is derived from the penalty, i.e., it captures how the agents evaluate the impact of the realization of the evolutionary uncertainty of wealth distribution. The second represents the impact of the “deterministic” changes in the wealth distribution. Similar to the volatility risk (acts on wealth) of classical uncertainties, the evolutionary uncertainty of the distribution is volatile and results in a risk (the second-order term w.r.t. m), as the last term in (25) reflects.²⁵ The derivation is shown in Online Appendix OA3.2. The extra terms imply that aggregate shocks not only affect an individual agent w directly, but also affect other agents, whose responses in turn affect w .

4.2 Implications of Wealth Heterogeneity

Individual’s optimal staking. Heterogeneous agents differ in the trade-off between staking and convenience gains they face, some even quit the staking pool.

Proposition 5. Individual staking under heterogeneity. For agent i with wealth w_t and usage preference $u_{i,t}$, the optimal q_t^* is unique. The optimal individual staking ratio θ_t^* is heterogeneous w.r.t. agents’ transaction needs $U_t = U(u_t, w_t)$ and satisfies:

$$\theta_t^* = \max \left\{ 0, 1 - \left(\frac{1 - \alpha}{r_t - c_t} \right)^{\frac{1}{\alpha}} \frac{N_t A_t U_t}{q_t^*} \mathbb{I}\{U_t > U_0\} \right\}, \quad (26)$$

where \mathbb{I} is an indicator function, $U_0 = \frac{\varphi}{N_t A_t} \left(\frac{r_t - c_t}{1 - \alpha} \right)^{\frac{1 - \alpha}{\alpha}}$.

The indicator function captures the impact of the threshold φ . The unchanged, however, is all the agents weakly increase their staking under a higher reward rate. Figure 2 visualizes this implication and the determination of the cross-sectional equilibrium. As the aggregation of all the agents, the overall staking ratio (the blue curve) weakly increases with the given reward rate. Further, the resulting staking ratio leads to a new system reward rate (the gray curve). Then the equilibrium falls at the intersection.²⁶ In addition, we can see that big whales enter the staking pool first as the reward rate increases, since

²⁵Note that extra arguments w', w'' enter the derivatives. They are generated from infinite-dimensional Itô’ Lemma: $dJ_t = \langle \frac{\delta J}{\delta m}, dm_t \rangle + \frac{1}{2} \langle dm_t | \frac{\delta^2 J}{\delta m^2} | dm_t \rangle$. The inner product is defined in the appropriate functional space, $\langle f(x), g(x) \rangle = \int f(x)g(x)dx$. $\langle h | f(x, x') | g \rangle = \langle \langle f(x, x'), h(x) \rangle, g(x') \rangle$. The derivatives w.r.t. m refer to the Fréchet derivatives applied in infinite dimension, and appear to have extra arguments, i.e., $\frac{\delta J}{\delta m} = \frac{\delta J}{\delta m}(w, w', m)$, $\frac{\delta^2 J}{\delta m^2} = \frac{\delta^2 J}{\delta m^2}(w, w', w'', m)$. The rigorous definitions are described in Online Appendix OA3.1. One can roughly compare them with Jacobian and Hessian in the finite-dimensional case respectively.

²⁶When it falls in the gray area, some agents may not stake and only transact on the platform.

1 their marginal transaction needs are relatively lower. From another perspective, the re-
 2 tail agents are less likely to be interested in staking, since the staking reward, also their
 3 contribution to the platform by staking are relatively negligible.

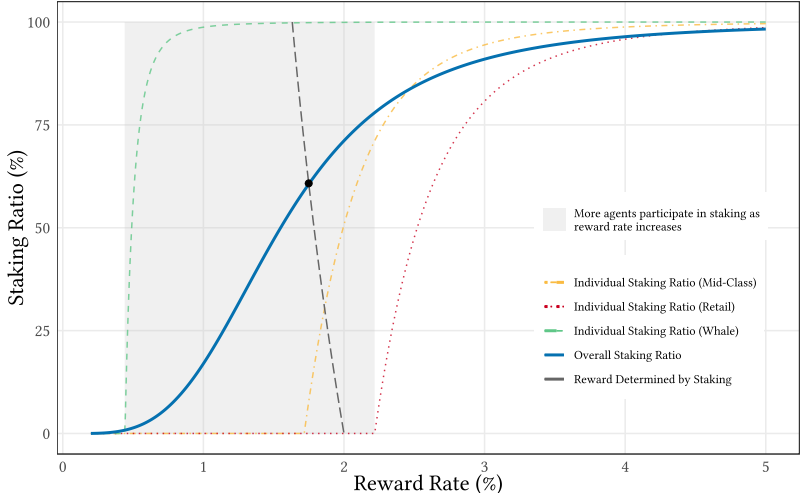


Figure 2: Individual staking decisions and equilibrium staking ratio.

The three dashed curves plot the individual staking ratios of retails (who own little wealth), rich whales, and the middle-class. The blue curve is the aggregated overall staking ratio. The staking ratio further leads to the resulting reward rate as the gray curve shows. Then, the equilibrium is the solution to the fixed point problem as visualized by the intersection of the blue and gray curves.

4 **System equilibrium states and redistribution.** The qualitative implications of the
 5 model remain intact despite the presence of heterogeneous agents.²⁷ However, the crucial
 6 difference is that the wealth distribution plays a pivotal role as an additional argument in
 7 shaping all the cross-sectional equilibrium states, leading to redistribution. Specifically,
 8 heterogeneity in wealth causes agents to have different tradeoffs between transaction us-
 9 age and staking rewards, leading to different individual staking ratios. Agents who value
 10 usage benefits more or have less wealth tend to stake less, and consequently suffer from
 11 emission inflation, whereas stakers, especially the wealthy ones, accumulate more to-
 12 kens, and thus onchain wealth. This insight shares the same spirit as in [John et al. \(2022\)](#),
 13 though the agent heterogeneity modeled there is different, and the redistribution is be-
 14 tween short-term and long-term holders. Under log utility, on-chain redistribution also
 15 corresponds to an overall wealth redistribution in equilibrium.

²⁷The essence that generates this assertion is that the system states are still calculated as aggregations across the crowd, whereas agents have the same direction of shifts in staking relative to different reward rates as mentioned above. Online Appendix provides a detailed discussion on the derivation process.

4.3 Expected Stationary State

The cross-sectional equilibrium exists under any given wealth distribution, while we further consider the steady state from the time dimension. With the continuous arrival of aggregate shocks, we should consider the expected steady state, $\mathbb{E}(dm_t) = 0$. It reflects the evolution on average and directly corresponds to the deterministic onchain steady state if there is no realized external shock. As discussed in Appendix OA3.5, if the agents obtain log utilities, $U_{i,t} = U(u_{i,t}, w_{i,t}) = u_{i,t}w_{i,t}$, and the random user type $u_{i,t}$ is independent of wealth, then all the agents' wealth change linearly. It is widely known that the resulting stationary distribution is a Pareto distribution.²⁸ We relax the above requirement by allowing for correlation between u and w , e.g., $u_{i,t} \sim \bar{u}\mathcal{N}(w_t^{\beta-1}, \sigma_X^2)$, where \bar{u} captures the tendency to transact (as opposed to stake). Then from the perspective of the whole crowd, there are different marginal benefits between staking (still constant return to scale given the reward rate r) and transaction (expectations affected by wealth). The following proposition solves for the general expected stationary distribution and shows it depends on the platform productivity.

Proposition 6. Expected stationary distribution. *The agents' wealth distribution in the expected stationary state is:*

$$m(w) = c_0 \frac{1}{w^{\phi\mathcal{V}}} \exp\left(\mathcal{V}\bar{u}\alpha\left(\frac{1-\alpha}{r-c}\right)^{\frac{1-\alpha}{\alpha}} NA \frac{w^{\beta-1}}{\beta-1}\right), \quad (27)$$

where $\mathcal{V} = \frac{2\sigma^2}{(\mu+r-c-\Psi_n)^2}$, $(\mu, r, \Psi_n, \sigma, N)$ are all functions of A at the cross-sectional equilibrium. c_0 is a normalization constant such that $\int_w^\infty m(w)dw = 1$. As $\beta \rightarrow 1$, the distribution is a Pareto distribution with tail parameter $a = \left[\phi - \alpha\left(\frac{1-\alpha}{r-c}\right)^{\frac{1-\alpha}{\alpha}} NA\bar{u}\right]\mathcal{V} - 1$.

We further investigate how the platform state influences the stationary wealth distribution as Figure 3 shows.²⁹ The distributions are Pareto-like, with a large amount of wealth concentrated in a few people. Panel A tells us that as the platform productivity increases, the distribution involves a fatter tail, implying the rising wealth inequality.

²⁸When the agent's wealth changes linearly over time, the law of motion generates a Pareto distribution (e.g., Wold and Whittle, 1957; Gabaix, 2009). It is worth pointing out that we make a methodological contribution by avoiding the common assumption in the literature of a representative agent that gives a deterministic evolution of the distributions.

²⁹To make the situations comparable, we normalize the wealth to the multiplier of the lowest onchain wealth in corresponding cases. Since in different cases, the agents have co-movements in on/off-chain trade-offs. The normalized onchain wealth allows us to focus on inequality issues.

1 Higher platform productivity generates larger benefits than the off-chain activities, while
 2 in this process, the richer has larger onchain allocation, and gains more wealth growth.
 3 Meanwhile, higher productivity increases the transaction convenience of all agents, which
 4 explains why many retail agents still use the platform.

5 Similarly, as demonstrated in Panel B, higher tendencies to stake (lower \bar{u}) reduce
 6 inequality. In fact, both user type (\bar{u} and β) and staking design (e.g., ρ) can alter the level
 7 of inequality. Platforms without staking or with less generous staking rewards (lower ρ)
 would not have as much staking participation, and therefore exhibit higher inequality.

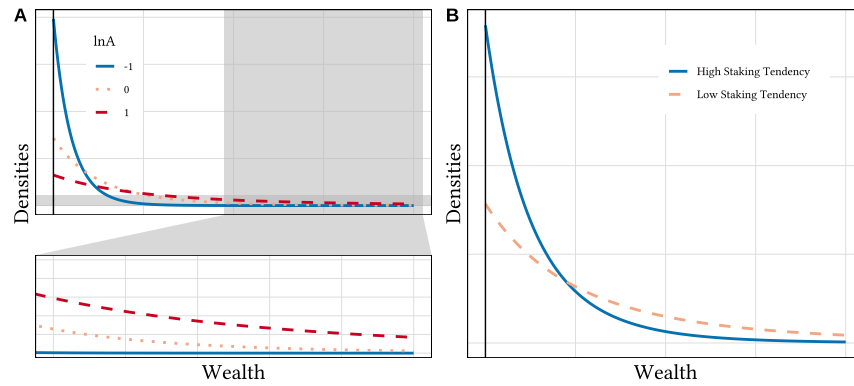


Figure 3: Expected stationary wealth distribution.

This graph shows the stationary wealth distribution under different platform states. The wealth is normalized to be the multiplier of the lowest wealth in each case. Panel A shows the comparison among different levels of platform productivity. Panel B compares different overall staking tendencies, which is examined by adjusting \bar{u} , the general scale of transaction demand in user types.

8
 9 **Wealth inequality and total welfare.** Just like in the real economy, inequality can be
 10 a double-edged sword. On the one hand, it results in a lower equilibrium staking reward
 11 rate and squeezes out retail agents from staking, which reduces their welfare. On the other
 12 hand, inequality is correlated with high platform productivity (and thus greater average
 13 user utility). Agents may still want to join a well-developed platform for usage, even in
 14 an economy with large onchain and overall wealth inequality.

15 These implications further help us understand the different stages of platform growth.
 16 In the initial stage, the tokenized economy is often accompanied by relatively low inequal-
 17 ity. Participating in staking can attract excess capital into the network and promote its
 18 development. As the platform grows, a few rich agents with larger marginal benefits in
 19 staking than transacting dominate staking activities, whereas other agents hold tokens
 20 mostly for onchain usage and speculation. This helps to rationalize why in practice, once
 21 platforms become large, a division of labor among participants emerges where valida-

1 tion is often done by prominent asset owners such as exchanges, who provide consensus
2 through PoS while earning staking revenues.

3 **4.4 System Trajectories and Aggregate Shocks**

4 According to the master equation (25), agents do not directly respond to any specific
5 shocks, but “internalize” them through the penalty term as well as the volatility risk of
6 penalty. To numerically solve (25), we obtain the value functions under shock series z ,
7 denoted as $J(w, m, A, z)$, and simulate all the possible series under the given stochastic
8 process to derive the origin $J(w, m, A)$. This idea offers additional potential to examine
9 the evolutionary paths under certain realized series of shocks. To solve J , we follow the
10 perturbation approach introduced in Bilal (2023), as detailed in Online Appendix OA2.

11 Figure 4 shows the impulse response paths when there are different series of shocks.
12 Panel A simulates a booming market with positive external demand shocks. The direct
13 and initial effect is a universal wealth growth across all agents, leading to a decrease in the
14 share of retail agents and, consequently, an increase in the overall staking ratio. As time
15 goes on, the growing productivity generates more benefits from transaction and reduces
16 the staking ratio. Panel B simulates a declining market with negative demand shocks, in
17 which the response paths are nearly symmetric. Panels C and D reveal the periods with
18 low and high oscillations. The whole system has immediate and violent response to each
19 round of external fluctuations. This is because the latest arriving shock brings the di-
20 rect impact, while the previous opposite shock only affects the current state indirectly
21 by the changes in the distribution.³⁰ Further, the changing nature of productivity obtains
22 quantitative-level differences among the rounds.

23 Panel E shows an experiment that involves a negative “MIT shock” to the platform
24 productivity at $t = 0$ and compare it to the steady benchmark. The deviations in the
25 staking ratio are similar to those in Panel B, but the explanation differs. Here, agents in-
26 crease their staking ratios relative to the benchmark not because they have more wealth,
27 but because transaction convenience drops. The higher staking ratio provides a larger
28 platform growth drift, which partially offsets the productivity loss caused by the shock.
29 However, when compared to the benchmark, agents continue to experience lower wealth
30 growth, gradually leading to relatively lower staking ratios. Consequently, the productiv-

³⁰At a specific period, the response can be roughly viewed as some combination of the continuous impacts of historical shocks. Online Appendix OA2 tests the impacts over time of a separate unit shock and also details the method that allows setting up a sequence of shocks.

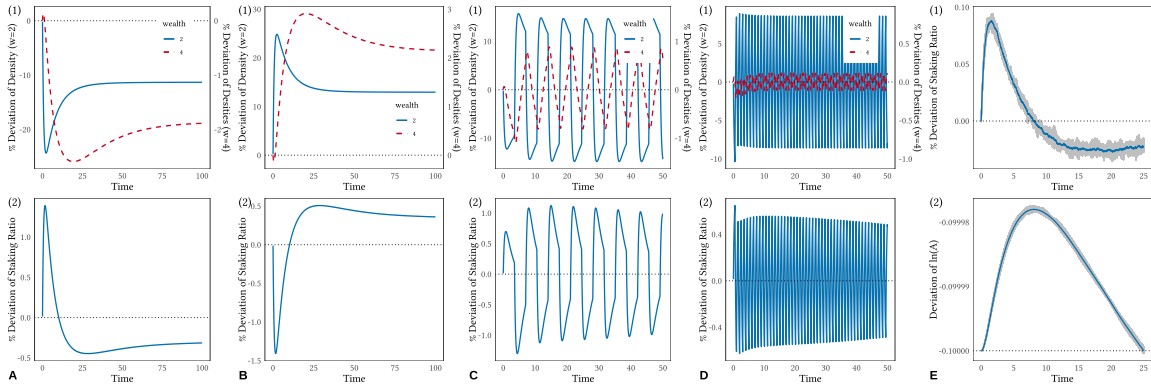


Figure 4: Impulse response paths under different realization of shocks.

Panels A-D show the impulse responses to different shock paths, i.e., continuous good and bad news, low and high-frequency oscillations, respectively. The time unit is roughly calibrated to one-day. In each panel, subplot (1) shows the response of $m_t(w)$, i.e. their deviations from the steady states, with different w . Subplot (2) shows the response of staking ratio. Panel E shows the Monte Carlo simulation of a -0.1 negative shock to $\ln(A)$, where the subplots show the deviations of staking ratio and log productivity. The grey region includes the curves under fewer simulations.

- 1 ity falls behind. This indicates that the staking mechanism plays a role in shaping platform
- 2 growth, yet it is insufficient to fully compensate for significant productivity shocks.

3 5 Data, Stylized Facts, and Hypotheses

4 5.1 Data on Stakable Tokens

5 Our main data source is *Stakingrewards.com*, arguably the largest collector of informa-
6 tion related to staking covering both historical and real-time data on most stakable assets.
7 Our sample covers daily observations of 66 stakable tokens including Ethereum 2.0. By
8 the end of 2021, our sample set makes up 37.78% of the total cryptocurrency market cap-
9 italization (64.34% when excluding Bitcoin), and respectively consists 80.35% of the PoS
10 market and 97.88% of the DeFi market.³¹ The sample period covers July 2018 through Nov
11 2022, covering the initial birth and rapid growth of “staking,” as well as the bear market
12 during 2022. Our sample includes all stakable assets with a market value of more than
13 100 million US dollars at a snapshot of Aug 2020 (as we initially wrote the paper), some
14 of which have collapsed in 2022. The additional information about staking is typically
15 aggregated from the official websites of each token, including details of staking participa-
16 tion methods (Online Appendix OA1.2), reward sharing rules, real-time staking amount
17 (staking ratio), etc.

³¹According to *CoinMarketCap* and *StakingRewards.com*. The sample set includes 48 base-layer pan-PoS protocols and 29 high-layer DeFi platform tokens. The two are not mutually exclusive as mentioned.

Table 1: Summary statistics.

Panel A summarizes the raw variables. We obtain means and standard deviations clustered by each token for the key variables, and report the statistics between groups in Panel B.

<i>Panel A: Raw variables.</i>									
	Daily			7-Day			30-Day		
	N	Mean	Std.Dev	N	Mean	Std.Dev	N	Mean	Std.Dev
Reward Rate, r (% Annual)	41003	13.42	17.78	5867	13.28	16.05	1387	13.16	15.69
Reward Ratio, ρ (%)	39546	6.31	8.86	5660	6.26	8.58	1339	6.20	8.47
Staking Ratio, Θ (%)	41706	46.37	23.06	5964	46.39	23.09	1415	46.36	23.13
Price Appreciation, r_{price} (%)	43114	-0.04	7.25	6091	-0.34	22.93	1391	-2.13	54.42
Δr	40788	-0.03	7.86	5745	-0.13	4.68	1301	-0.51	8.76
$\Delta \Theta$	41505	0.00	1.33	5851	0.03	3.37	1333	0.03	6.25

<i>Panel B: Group-summarized values.</i>								
	N	Mean	Std.Dev	Min	25%	Median	75%	Max
$mean(r)$	66	14.86	15.44	0.02	6.33	9.84	15.77	75.39
$sd(r)$	66	7.21	10.39	0.01	1.43	2.47	9.60	43.69
$mean(\Theta)$	65	44.05	22.22	2.78	27.26	44.22	59.61	97.77
$sd(\Theta)$	65	8.16	5.98	0.27	3.50	6.81	11.69	25.48
$mean(r_{price})$	66	-0.01	0.50	-1.17	-0.23	0.04	0.15	2.72
$sd(r_{price})$	66	6.76	3.05	3.89	5.53	6.25	6.80	23.88

1 Table 1 displays the summary statistics. In most analyses, we also aggregate the daily
 2 observations into weekly and monthly data for discussions and robustness. Panel B shows
 3 there is a large dispersion in reward rate, staking participation, and price returns among
 4 tokens: the mean staking reward rate ranges from 0.02% to 75.39%, while the mean staking
 5 ratio ranges from 2.78% to 97.77%.

6 5.2 Styled Facts About Staking and Token Pricing

7 **Aggregate trends.** For base layers, the shift of focus away from PoW and onto the PoS
 8 consensus algorithms have been evident and timely.³² The PoS share has increased sub-
 9 stantially over time from 5% in Oct. 2019 to over 20% in Oct. 2021. As of Oct. 2021, the
 10 PoS market cap is \$326.775 Billion, up from \$21.117 Billion a year ago. The annual growth
 11 rate reached 1,550%, while the overall crypto market cap is up by 673%. The entire staking
 12 economy has grown to over 4 million total users by the end of 2021.

13 **Staking rewards and token price returns.** The study of stakable tokens is related to
 14 international finance. Token price and staking reward rate can be compared to exchange
 15 rates and interest rates. If we treat the U.S. dollar as a local currency, then the change of
 16 token prices (denominated in US dollar) is equivalently considered as the change in foreign
 17 exchange rates. Moreover, earning staking reward rates is akin to earning interest rates.
 18 Figure 5 illustrates a plot of the excess return in the next week against the interest rate

³²According to 2021 Staking Ecosystem Report by StakingRewards.

1 spread calculated as the “foreign interest rate” minus the “local interest rate.” Each blue
 2 circle in the figure indicates a weekly data point for a particular token and the grey line
 3 shows a fitted line. The observed upward slope implies that an increase in the foreign
 4 interest rate relative to the local one is associated with an increase in the excess return
 5 on the cryptocurrency over the local currency, i.e., the crypto version of “the UIP puzzle,”
 6 which we formally test and discuss in Section 6.3.

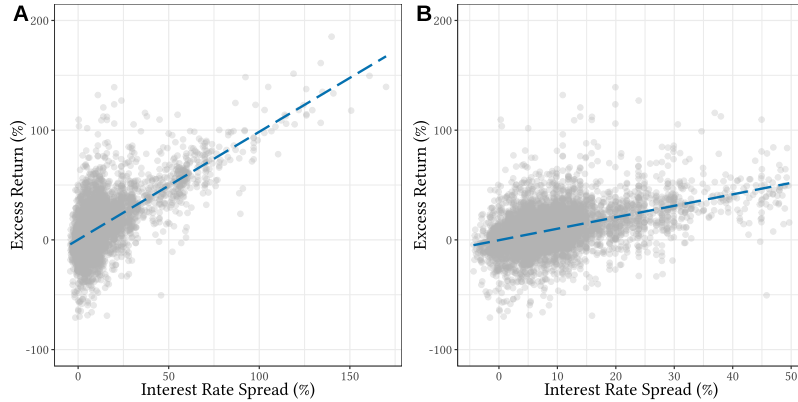


Figure 5: Reward rate spread and token exchange rate.

This figure shows the relationship between the reward rate spread (interest rate spread) and the crypto-token exchange rate (excess return). We treat the US dollar as local currency and the 1Y treasury interest rate as the local interest rate. The data is from the Federal Reserve. Each point in the figure indicates a weekly data point for a particular token. The staking reward rate (annualized) is treated as the foreign interest rate, and the x-axis, the interest rate spread, is calculated as the foreign interest rate minus the local interest rate. The y-axis is the excess return in the next week, including the interest rate spread and the price appreciation. Panel A shows the whole sample set, whereas Panel B focuses on the sub-sample set that limits the interest rate spread lies in a relatively common range ($< 50\%$). The blue lines show linear smoothing of the scatter points in two panels, respectively.

7 5.3 Hypothesis Formulation

8 Our model generates a rich set of predictions and reveals mechanisms underlying cer-
 9 tain empirical regularities. However, tests on the model implications concerning onchain
 10 and offchain wealth distribution, expected steady states, etc., are limited by data availabil-
 11 ity. We collect data to test the three main sets of model predictions. The first concerns
 12 the determination of staking ratio. Proposition 2 implies that **(H1a) A higher staking**
 13 **reward ratio ρ corresponds to a higher staking ratio Θ .** Proposition 5 suggests that
 14 heterogeneity also impacts equilibrium. In particular, **(H1b) A higher share of large**
 15 **investors is associated with a higher staking ratio.** In practice, it may take time to
 16 reach the cross-sectional equilibrium. Therefore, we expect: **(H1c) A higher reward rate**
 17 **r predicts an increase in staking ratio in the short term.**

1 Regarding token prices, Proposition 3 shows a positive predictability of staking ratio
2 on price appreciation, i.e., **(H2a) Staking ratio Θ positively predicts token returns.**

3 Finally, concerning crypto carry and interest rate parity, Proposition 4 shows: **(H3a)**
4 **Uncovered interest rate parity is violated among stakable tokens.** Consequently,
5 we expect: **(H3b) Crypto carry trade strategies are profitable.** Moreover, **(H3c) Carry**
6 **predicts excess return in tokens.**

7 **6 Empirical Findings**

8 **6.1 Linking Reward Rate and Wealth Concentration to Staking**

9 To test **(H1a)** empirically, we first calculate the daily average of aggregate staking
10 reward ratio ρ and staking ratio Θ for each token over its entire sample period. Figure
11 6 plots the relationship between staking reward ratio and staking ratio, in which each
12 token generates one scatter point. The grey dashed line shows the linear fit of the scat-
13 tered observations. The positive slope indicates that the reward is positively related to
14 the staking ratio.³³ This pattern corroborates Proposition 2, which also implicitly illus-
15 trates that averaging over the time series roughly conforms to the equilibrium. We also
16 visualize the relationship under earlier data coverage (up to Oct. 2020) as Panel B shows.
17 Although there are fewer stakable tokens in the earlier period, the significant positive
18 correlation between the staking ratio and staking reward ratio still exists, which suggests
19 the relationship is robust in the sample period.

20 We further test **(H1a)** in panel regressions (Table 2). We take the staking ratio, $\Theta_{i,t}$,
21 as a dependent variable, and the staking reward ratio, $\rho_{i,t}$, as the main explanatory vari-
22 able. As Column (1) shows, the value of estimation implies a 10-percentage-points higher
23 aggregate reward ratio is associated with a 7.79-percentage-points higher staking ratio.
24 After inducing time-varying platform controls and investment-related controls, the cor-
25 responding estimates decrease to about 3.7 points yet still significant. Different sample
26 periods and two-way fixed effects are considered. We cluster standard errors on both
27 token and time dimensions together with the fixed effects, which deals with the poten-
28 tial heterogeneity in the treatment effects as suggested by Petersen (2008); Abadie et al.
29 (2017). The positive correlation between staking reward and staking ratio remains robust.

³³After removing potential high-influential points (with mean staking reward ratio higher than 15%), the resulting blue dashed line shows that the positive correlation still holds, with an even larger slope.

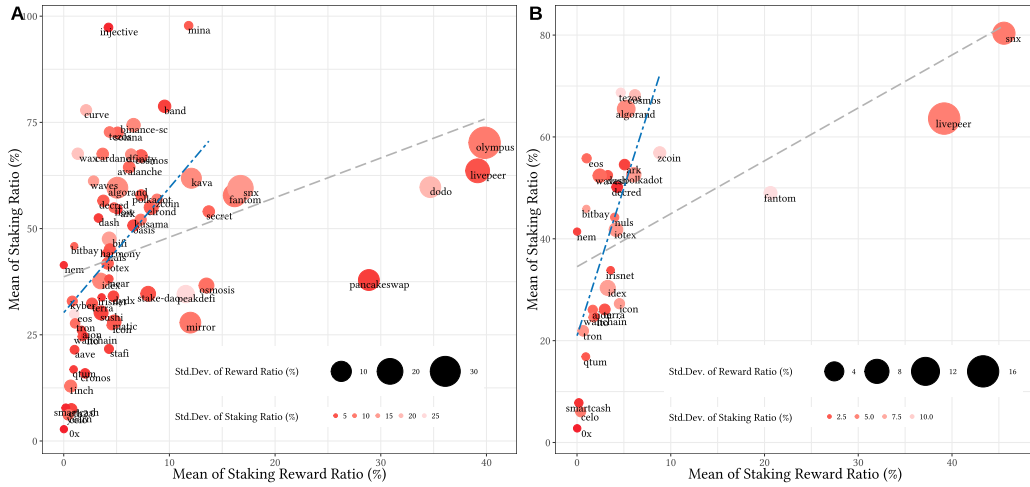


Figure 6: Staking ratio versus staking reward.

This figure corresponds to (H1a), the relationship between staking ratio Θ_t and staking reward ratio ρ_t . In Panel A, each token generates one point by calculating its mean Θ_t and ρ over the sample period. The size and color of the points indicate the standard deviations of ρ and Θ respectively. The gray dashed line is the linear smoothing. The blue line is the smooth after removing the influential points with ρ larger than 15%. In Panel B, we do the same thing under earlier data coverage (up to Oct. 2020).

- 1 Recall that staking essentially acts as an inflation tax, i.e., facilitates redistribution from
- 2 more usage-focused adopters to richer or investment-focused adopters. A larger staking
- 3 reward ratio corresponds to a heavier tax and, forces lower usage preference.

4 The time-varying token-specific controls bring alternative evidence for our theoret-

5 ical framework. $a_{i,t}$ is a proxy of platform productivity.³⁴ The model illustrates that the

6 equilibrium staking ratio negatively relates to the platform productivity, A_t , since it in-

7 creases transaction convenience with certain staking rewards. The share of large asset

8 users (big whales), $whale_{i,t}$, links to heterogeneity and Hypothesis (H1b), which will be

9 discussed specifically later. Token age is a concern it usually relates to reward designs.

10 We capture age effects by two dummies, $NotLaunched_{i,t}$ and $Y_{i,t}^0$, which equal 1 when the

11 token is in the stage before and within one year of launching on mainstream exchanges,

12 respectively. Younger platforms may have not distributed tokens to many agents, thus

13 should be associated with lower staking. Investment-related concerns are also controlled

³⁴The platform productivity is captured by the average onchain transaction processing per second. In practice, numerous platforms and blockchains aim to increase the transaction size of the flows processed on their chains, reflecting the platform productivity. Meanwhile, it is also influenced by the overall transaction needs, which means it does not necessarily to measure the hardware upper limits. However, both the two forces are closely related to the concept of transaction convenience and fit our main use for inducing platform productivity. Therefore, it is not necessary here to separate the two forces. Note that it may not capture the whole progress of platform development, such as transaction security and performance on specific financial services. It is beyond our scope to suggest an aggregated measurement.

1 e.g., platform size. Table 2 also corroborates these views.

Table 2: Staking ratio with respect to the staking reward ratio.

This table tests (H1a), i.e., the relationship between staking ratio, $\Theta_{i,t}$, and the aggregate staking reward ratio, $\rho_{i,t}$, in the same period. Controls are the token age, captured by two dummies, $NotLaunched_{i,t}$ and $Y_{i,t}^0$, which equal 1 when the token is before, and within one year of launching on mainstream exchanges, respectively; the proxy of platform productivity, $a_{i,t}$; the value share of tokens held by big-asset accounts, $Whale_{i,t}$, the token market cap, and price volatility. Token and time effects are fixed. Sample sets with different horizons (weekly and monthly) are tested. Standard errors clustered in both token and time dimensions in parentheses. ***, **, * indicate statistical significance at the 1%, 5% and 10% respectively.

Dependent:	<i>StakingRatio</i> _{<i>i,t</i>}								
	(1)	(2)	(3)	(4)	(5)	(6)	(7)	(8)	(9)
	7-Day				30-Day				
$\rho_{i,t}$	0.779*** (0.190)	0.428** (0.162)	0.429** (0.161)	0.360** (0.170)	0.374** (0.173)	0.794*** (0.188)	0.439*** (0.155)	0.413** (0.155)	0.431** (0.173)
$NotLaunched_{i,t}$			-0.076 (0.064)	-0.162** (0.063)	-0.183** (0.064)			-0.113** (0.053)	-0.130** (0.051)
$Y_{i,t}^0$			0.004 (0.030)	-0.059 (0.047)	-0.073 (0.045)			-0.028 (0.038)	-0.042 (0.037)
$a_{i,t}$				-0.747*** (0.158)	-0.417** (0.159)			-0.623*** (0.143)	-0.415*** (0.098)
$\frac{1}{100} \log(Cap)_{i,t}$				1.686 (1.756)	1.991 (1.719)			1.124 (1.843)	1.582 (1.809)
$\frac{1}{100} Volatility_{i,t}$				0.236 (0.344)	0.328 (0.397)			1.590 (1.806)	0.965 (1.459)
$Whale_{i,t}$					0.217*** (0.071)				0.171** (0.075)
Token FE		Yes	Yes	Yes	Yes		Yes	Yes	Yes
Time FE		Yes	Yes	Yes	Yes		Yes	Yes	Yes
Observations	5,660	5,660	5,660	1,364	1,364	1,339	1,339	308	308
R ²	0.088	0.811	0.812	0.917	0.920	0.089	0.801	0.929	0.931

2 The previous test focuses on contemporaneous correlations in equilibrium. As (H1c)
3 mentioned, it takes time to achieve equilibrium in practice, then the reward rate r should
4 predict future staking ratio Θ in short terms (transition process). Also, when agents face
5 multiple tokens, the predictability could appear in the cross-section. Table 3 reports the
6 tests for (H1c). We use the change in staking ratio, $\Delta\Theta_{i,t} = \Theta_{i,t} - \Theta_{i,t-1}$, as the dependent
7 variable, and the reward rate in the previous period, $r_{i,t-1}$, as the main independent. Its
8 estimated coefficients are all positive, implying that a larger reward rate predicts a positive
9 change in staking ratio, e.g., column (6) shows that if the annual reward rate increases by
10 one percentage point, then the overall staking ratio will increase by 0.026 percentage
11 points in the following week. This can be a large effect considering the magnitude of the
12 changes in the rewards rate in the staking economy and the size of the time window. The
13 lag staking ratio is controlled to capture the potential diminishing marginal effects. Time-

1 varying platform controls are also considered, which do not exhibit significant influences.
2 This is reasonable since the platform characteristics enter the equilibrium clearly, but
3 their impact on the transition process could be complex. In addition, the statistical power
4 of such predictability decreases as the time window expands. This is partly due to the
5 aggregation of noise over a longer time period. More importantly, the longer period makes
6 the predicted impact already reflected in the formation of new equilibrium.

Table 3: Staking ratio with respect to the staking reward rate.

This table tests **(H1c)**, i.e., how people’s staking choices are affected by the reward rate. The dependent is the change of overall staking ratio, $\Delta StakingRatio_{i,t}$, and the main independent is the reward rate in the previous period, $r_{i,t-1}$. Controls include: the token age, the proxy of previous platform productivity, the previous percentage of tokens held by big-asset accounts that are similar in previous tables, and the previous staking ratio, $StakingRatio_{i,t-1}$ that capturing potential diminishing marginal effect. Token and time effects are fixed. Sample set with different horizons (weekly and monthly) are tested. Standard errors clustered in both token and time dimensions in parentheses. ***, **, * indicate statistical significance at the 1%, 5% and 10% respectively.

Dependent:	$\Delta StakingRatio_{i,t}$								
	Daily				7-Day		30-Day		
	(1)	(2)	(3)	(4)	(5)	(6)	(7)	(8)	(9)
$r_{i,t-1}$	0.002*** (0.000)	0.003*** (0.001)	0.001** (0.001)	0.001** (0.001)	0.002* (0.001)	0.026* (0.015)	0.030 (0.024)	0.049** (0.020)	0.006 (0.019)
$StakingRatio_{i,t-1}$			-0.009*** (0.002)	-0.009*** (0.002)	-0.016*** (0.004)		-0.103*** (0.028)		-0.294*** (0.057)
$NotLaunched_{i,t}$				-0.001 (0.001)	-0.002* (0.001)		-0.009 (0.006)		-0.029 (0.021)
$Y_{i,t}^0$				0.000 (0.000)	-0.001 (0.001)		-0.006 (0.005)		-0.012 (0.016)
$a_{i,t-1}$					0.005 (0.006)		0.018 (0.047)		0.046 (0.107)
$Whale_{i,t-1}$					0.003 (0.002)		0.019 (0.011)		-0.002 (0.036)
Token FE		Yes	Yes	Yes	Yes	Yes	Yes	Yes	Yes
Time FE		Yes	Yes	Yes	Yes	Yes	Yes	Yes	Yes
Observations	39,359	39,359	39,359	39,359	10,636	5,559	1,511	1,266	344
R ²	0.0006	0.043	0.049	0.049	0.172	0.063	0.197	0.124	0.322

7 **Wealth concentration and aggregate staking.** As Section 4 illustrates, agents are het-
8 erogeneous in staking propensities. In particular, large-asset agents (whales) tend to stake
9 more, implying that when the tokens are more concentrated in whales, the equilibrium
10 staking ratio would be higher **(H1b)**. We test this hypothesis in Columns (5) and (9) of
11 Table 2, where the coefficients of $whale_{i,t}$ are significantly positive. That is, concentration
12 implies additional general tendencies to staking. Importantly, if staking benefits the plat-
13 form in a fundamental way (such as enhanced network security), wealth concentration

1 may not be all bad — large stakeholders are more interested in becoming facilitators of
2 the platform’s services than pure users. Agents, on the other hand, may have incentives
3 to pursue larger usage benefits at the cost of more concentration, as discussed earlier.
4 In practice, staking/voting pools for prominent platforms are often backed by large ex-
5 changes and foundations, which is consistent.

6.2 Equilibrium Staking Ratio and Token Price Dynamics

7 Table 4 reveals the tests for **(H2a)**, i.e., staking ratio positively predicts token price
8 changes. We calculate the log token price change at time t for token i , $r_{price_{i,t}} = \log(\frac{P_{i,t}}{P_{i,t-1}})$,
9 and regress it on the previous staking ratio. We consider the factors in the cryptocurrency
10 market, including market and market value factors that have important impacts on price
11 changes as discussed in Liu et al. (2019). The estimated coefficient of staking ratio is sig-
12 nificantly positive, which implies that a higher staking ratio predicts larger token price
13 appreciation. As column (4) shows, if the staking ratio of a token increases by one percent-
14 age point, its price will appreciate by 0.066% in the next week. Considering there is often
15 a large variation in the staking ratio, this effect can have a significant impact on price. The
16 significant positive estimates also suggest that this effect is robust against different time
17 windows. With the inclusion of more control variables that have been suggested to affect
18 the token’s pricing in recent studies, staking ratio has incremental predictive power. The
19 additional controls include platform controls (token age, productivity, and whale share)
20 for possible predictable price appreciation from platform characteristics, the previous re-
21 turns for the potential phenomenon of momentum, and the influence of onchain network
22 activities, $\Delta Network_{i,t-1}$.³⁵ To further consider the time-series auto-correlation, we adopt
23 two-way fixed effects regression in columns (3), (6), and (9), where the estimated rolling
24 CAPM β captures the forces from market fluctuations. The estimated coefficients remain
25 significant and positive with two-way clustered standard errors.

26 Further discussion may lie in the differences in the predictive power of staking ratio
27 across market sentiment, as well as among the roles played in platform development of
28 staking. We test the same specification on multiple sub-samples, including bull and bear
29 periods, pan-PoS and DeFi groups in Online Appendix OA3.6 and OA3.7. The estimated
30 coefficients of $\Theta_{i,t-1}$ are all positive, among which only the bear-period sub-sample ex-

³⁵It is the lagged log differences in the total amount of addresses with non-zero balance on the platform. As Cong et al. (2021b) discusses, cryptocurrency returns exhibit network adoption premia. The estimated coefficient of the network adoption term is positive and consistent with prior research.

Table 4: Staking ratio and token prices.

This table tests (H2a), i.e. staking ratio predicts token price appreciation. The dependent $r_{price_{i,t}}$ is the log price change. The main independent is the staking ratio of the previous period, $StakingRatio_{i,t-1}$. Controls include the market return MKT_t , the log market cap $\log(Cap)_{i,t-1}$, the proxy of network adoption $\Delta Network_{i,t-1}$, the price return of the previous period $r_{price_{i,t-1}}$, and rolling CAPM beta, $\hat{\beta}_{i,t}$. Token characteristic controls include the token age, platform productivity, and the previous percentage of tokens held by big-asset accounts that are similar to previous tables. We also do the test in different horizons and with token-specific and time fixed effects. Standard errors clustered in both token-specific and time dimensions in parentheses. ***, **, * indicate statistical significance at the 1%, 5% and 10% respectively.

Dependent:	$r_{price_{i,t}}$								
	Daily			7-Day			30-Day		
	(1)	(2)	(3)	(4)	(5)	(6)	(7)	(8)	(9)
$StakingRatio_{i,t-1}$	0.009** (0.004)	0.027*** (0.007)	0.022** (0.008)	0.066*** (0.023)	0.172** (0.068)	0.138* (0.071)	0.208* (0.121)	0.347* (0.197)	0.372** (0.139)
MKT_t	0.968*** (0.031)	1.029*** (0.043)		0.844*** (0.264)	0.685* (0.352)		2.445* (1.435)	2.201 (1.496)	
$\hat{\beta}_{i,t}$			-0.002 (0.002)			-0.037 (0.031)			-0.132 (0.104)
$\log(Cap)_{i,t-1}$	-0.002*** (0.000)	-0.002** (0.001)	-0.005*** (0.001)	-0.027*** (0.006)	-0.031*** (0.009)	-0.038*** (0.009)	-0.120*** (0.034)	-0.121*** (0.043)	-0.113*** (0.021)
$r_{price_{i,t-1}}$		0.021 (0.050)	0.035 (0.060)		0.008 (0.040)	-0.075* (0.042)		0.127* (0.062)	-0.076 (0.074)
$\Delta Network_{i,t-1}$		0.167*** (0.058)	0.224*** (0.068)		0.195 (0.207)	0.366 (0.259)		0.992 (1.393)	0.996 (1.216)
$a_{i,t-1}$		0.047 (0.030)	0.069 (0.041)		0.603** (0.258)	0.306 (0.235)		1.007 (0.825)	0.614 (0.946)
$Whale_{i,t-1}$		-0.010 (0.009)	-0.013 (0.009)		-0.006 (0.086)	-0.103 (0.073)		-0.179 (0.341)	-0.253 (0.201)
$NotLaunched_{i,t}$		-0.003 (0.002)	0.011*** (0.004)		0.075*** (0.024)	0.108** (0.040)		0.119 (0.154)	0.159 (0.126)
$Y_{i,t}^0$		0.002 (0.002)	0.007** (0.003)		0.021 (0.021)	0.056** (0.020)		-0.073 (0.084)	0.114 (0.107)
Token FE	Yes	Yes	Yes	Yes	Yes	Yes	Yes	Yes	Yes
Time FE			Yes			Yes			Yes
Observations	41,544	10,887	9,991	5,872	1,530	1,434	1,347	334	322
R ²	0.267	0.346	0.478	0.043	0.054	0.507	0.120	0.207	0.640

1 hibits lower statistical significance. This suggests the positive relationship between stak-
2 ing ratio and price appreciation to be a generally existing phenomenon in our sample. As
3 applications to such predictability, we also discuss the portfolio performance sorted by
4 staking ratio in Online Appendix OA3.8.

5 6.3 UIP Violation and Crypto Carry

6 **UIP violation.** We test Hypothesis (H3a), i.e., whether UIP is violated, using the regres-
7 sion specification in Fama (1984): let the excess return $\lambda_{i,t} = \log P_{i,t+1} - \log P_{i,t} + (r_{i,t} - c_{i,t}) - r_t^f$,
8 i represents token i , and regress $\lambda_{i,t+1}$ on $r_t^f - r_{i,t} + c_{i,t}$ with coefficient B , where P_t is the
9 price denominated in local currency, r^f is the local interest. Under UIP, $B = 0$, i.e. the ex-

cess return is not forecastable by current interest rate differences. We examine different time horizons as Valchev (2020) does, and use different assets as local, including US dollar, Bitcoin, Ethereum and stakable ETH 2.0. Table 5 reports the findings.³⁶ All the results show significantly negative estimated B . Moreover, $B < 0$ and is close to -1 , implying that a higher interest rate will predict a positive appreciation of the exchange rate. This leads to potential arbitrage opportunities. We also use each single token as local currency, respectively. The regression results (reported in Online Appendix OA3.9) all violate the UIP, i.e., the phenomenon also exists within the token market.

Table 5: Test of UIP violation.

This table tests (H3a), i.e., the panel regression results of UIP test. In each row, we use a different asset as local currency and report the estimated coefficients of B with different data horizons. Estimated coefficients of B and the corresponding robust standard errors clustered by tokens are reported.

Local Currency	Horizon: 7-day			Horizon: 30-day		
	Coef., B	Std. Err.	R^2	Coef., B	Std. Err.	R^2
US Dollar	-1.02	(0.044)	0.33	-1.12	(0.176)	0.11
Bitcoin	-1.02	(0.034)	0.37	-1.08	(0.134)	0.11
Ethereum	-1.04	(0.033)	0.37	-1.09	(0.126)	0.12
Eth 2.0	-1.04	(0.014)	0.42	-1.25	(0.059)	0.17

UIP violations naturally prompt us to examine the predictability of crypto carry to token excess return and the performance of the crypto carry trade portfolio.

Crypto carry trades. We test the performance of carry-trade strategies (H3b). Tokens in the asset pool are ordered by their carry in the previous period, and then divided into the top $X\%$ of assets, the bottom $X\%$ and the middle group. Then we construct a carry trade portfolio by going long high carry group with equal weight and going short low with equal weight at the end of each week. For long tokens, we also stake them to earn staking reward rate, while for the short assets, we also compensate for the staking reward rate. The portfolio is rebalanced every week.³⁷ The performance of such crypto carry trade mainly measures the cross-sectional effect. Since we long high carry and short

³⁶While in practice, there are various ways to stake (e.g., delegating and running a node), which corresponds to different reward rates and costs, the staking programs mostly feature delegation/voting (that our data correspond to), which incurs negligible operational costs. We therefore normalize $c_{\{i,t\}}$ for all tokens to a constant (we use zero because only their relative magnitude matters).

³⁷The choice of X does not affect our observation of the main characteristics of the carry trade portfolio. We also assume that the staking rules allow a one-week stake period. Most stakable tokens do offer such flexible staking options, and our data for reward rates are also selected in the corresponding options. For some rare exceptions, we can assume the existence of some derivatives that would enable such an asset allocation. Such derivatives are gradually appearing in practice. Considering the abnormal fluctuation of token price and staking ratio when a staking project is first launched, our weekly asset pool does not include new staking projects that come out within a week.

1 low carry, the portfolio carry is always positive. If the portfolio always achieves positive
2 returns, it means that in the cross-section, assets with higher carry have greater aggregate
3 returns. We also report related strategies for comparison: (i) hold the same portfolio but
4 without stake (and not compensate for staking); (ii) apply the same strategy but adjust
5 the portfolio every month; (iii) Considering the potential short-selling limits, examine the
6 average return of equal-weighted full-sample / (top 50%) high-carry / low-carry tokens.

7 Table 6 reports the statistics of these strategies. The carry strategy has a significantly
8 greater positive return and yields a Sharpe ratio of 1.60. For higher moments, the strong
9 positive skewness is associated with the currency carry trade shown by Brunnermeier
10 et al. (2008). Moreover, the carry strategy exhibits excess kurtosis, indicating fat-tailed
11 positive and negative returns, which is consistent with Kojien et al. (2018)'s findings for
12 currencies and commodities. The long-short carry trade strategy exhibits relatively stable
13 returns, especially considering the high volatility of cryptocurrency markets and the circle
14 of bulls and bears during 2020-2022. The non-staking strategy also yields positive returns,
15 implying that the carry strategy earns excess returns not only from carry (staking reward)
16 but also from price appreciation. Moreover, the monthly-rebalanced strategy exhibits
17 fewer returns. There are two potential explanations. (i), the reward rate decreases with
18 contemporaneous staking ratio mechanically. Therefore, investors cannot consistently
19 earn high carry over a long period without timely position adjustments. (ii), the reversal
20 of reward rate further influences the staking ratio, which then weakens the effect on price
21 appreciation. In addition, long-only strategies corroborate the carry premia: longing top
22 50% tokens with high carry still outperforms the simple equal-weighted benchmark, while
23 the bottom 50% performs the worst. Their cumulative returns are also plotted in Figure
24 OA3.9, ensuring the above observations.

25 **Excess return predicted by carry.** In (H3c), the return predictability can come from
26 both the crypto carry itself and any price appreciation that is related to or predicted by
27 carry. We follow Kojien et al. (2018) to regress the overall excess return on the previous
28 carry. Table 7 reports the estimations of the coefficient of carry, C . The results in Table
29 7 imply that carry is a strong predictor of expected return. In Columns (1) and (3), with-
30 out crypto specific fixed effect, the estimated coefficient is around 1, which means that
31 high staking reward rate tokens neither depreciate nor appreciate on average.³⁸ Hence,

³⁸If the expected return moves one for one with carry, $C = 1$; if the total return is unpredictable, $C = 0$.

Table 6: Statistics of carry strategies.

This table corresponds to (H3b) and reports the statistics of carry trade strategies. The first three rows report the results of the long-short carry strategies. The rows below report long strategies. Annualized mean, standard deviations, skewness, kurtosis, maximum drawdown (MDD), and Sharpe ratio are reported.

Strategy	Mean (Annual, %)	St.dev. (Annual, %)	Skewness	Kurtosis	MDD (%)	Sharpe Ratio (Annual)
<i>Long-short Strategy:</i>						
1W-Carry Trade (Staking)	65.820	41.095	1.410	18.772	29.966	1.602
1W-Carry Trade (Non-staking)	52.497	41.104	1.404	18.719	35.920	1.277
1M-Carry Trade (Staking)	45.051	56.929	1.260	20.508	69.497	0.791
<i>Long Strategy:</i>						
EW All assets	15.577	78.244	-1.576	7.672	92.934	0.199
EW High Carry	49.416	81.309	-1.103	4.687	90.419	0.608
EW Low Carry	-16.404	80.444	-1.804	9.907	95.645	-0.204

- 1 investors can earn reward rate differential using carry trade (e.g., [Kojien et al., 2018](#)).

Table 7: Carry and excess returns.

This table tests (H3c). The dependent variable is the excess return, and the independent variable is the carry in the previous period. Standard errors that clustered in both token-specific and time dimensions in parentheses. ***, **, * indicate statistical significance at the 1%, 5% and 10% respectively.

Dependent:	ExcessReturn _{i,t}							
	7-Day				30-Day			
	(1)	(2)	(3)	(4)	(5)	(6)	(7)	(8)
Carry _{i,t-1}	0.956*** (0.053)	0.901*** (0.095)	0.968*** (0.042)	0.917*** (0.071)	0.968*** (0.296)	0.773 (0.534)	1.009*** (0.216)	0.846** (0.383)
Token FE	Yes				Yes			
Time FE	Yes				Yes			
Observations	5,745	5,745	5,745	5,745	1,301	1,301	1,301	1,301
R ²	0.230	0.239	0.441	0.447	0.038	0.094	0.333	0.374

- 2 Once the token-fixed-effect is added, the estimated C is less than 1 and even insignif-
3 icant, especially when the time window expands.³⁹ The time series carry predicts less
4 expected return:⁴⁰ Despite a high reward rate leads to a high staking ratio, and thus a
5 higher price appreciation, there is a *downward adjustment effect* of the reward rate in the
6 time series. As the sum of carry (approximately equal to the reward rate) and the price
7 appreciation, the excess return is then influenced by the adjustment. Comparing the re-
8 sults of weekly data with those of 30-day data, the downward adjustment effect is also
9 magnified when the time window becomes larger, and thus the estimated C decreases.

³⁹Without token-specific and time-fixed effects, C represents the total predictability of returns from carry from both its passive and dynamic components. Token fixed effects will remove the predictable return component of carry that comes from passive exposure to tokens with different unconditional average returns.

⁴⁰This phenomenon is similarly found in commodities ([Kojien et al., 2018](#)): when a commodity has a high spot price relative to its futures price, implying a high carry, the spot price tends to depreciate on average, thus lowering the realized return on average below the carry.

7 Conclusion

Staking has become a hallmark feature in many distributed networks involving hundreds of billions of dollars. In addition to offering a convenience yield for transactions, blockchain-based tokens are frequently staked for base-layer consensus generation or for incentivizing economic activities in DeFi protocols and platform development, and consequently earn staker's rewards. We build the first dynamic model of a token-based economy where agents endogenously allocate wealth on and off a digital platform and use tokens either to earn rewards or to transact. We solve this mean-field game with stochastic controls and systematic shocks, and identify staking ratio as a fundamental variable linking staking to the endogenous reward rate and token price. The staking ratio is proportional to the reward rates in the cross-section but negatively correlated to reward rates in the time series; it positively predicts the returns of cryptocurrencies. Furthermore, the model rationalizes violations of the uncovered interest rate parity, and the significant crypto carry premia that we empirically document.

The framework can be explored further for studying the utilities of platform tokens. For example, DeFi projects increasingly lock up both native and non-native tokens. Allowing multiple tokens to be used within a network may cause the payment utility of native tokens to decline. But stable tokens entitle the holders to instead collect rewards (fees and subsidies), while providing functionalities such as security or liquidity for the networks. Given that many platforms use staking to foster adoption and demand, partially designing the various utilities of tokens and understanding their implications on token prices constitute interesting future research. Similarly, it remains an open question how to jointly design token supply policy and staking protocols, especially with multiple types of tokens.

Appendix

Proof of Proposition 1. The marginal utility of staked and non-staked tokens are

$$MU_l = MU_o + (r_t - c_t) \frac{\partial J}{\partial w}, MU_x = MU_o + (1 - \alpha) \left(\frac{N_t A_t U_t}{x_t} \right)^\alpha \frac{\partial J}{\partial w}, \quad (\text{A.1})$$

where $MU_o = (\mu_t + \frac{\partial \Psi}{\partial n_t}) \frac{\partial J}{\partial w} + q_t \sigma_t^2 \frac{\partial^2 J}{\partial w^2}$, $q_t = x_t + l_t$. is the common part of MU_l and MU_x . Note that $MU_l - MU_o$ stays the same in l , while $MU_x - MU_o$ decreases in x . Thus, when treat q_t , is given, there exists at most a unique $\tilde{x}_t \leq q_t$ that satisfies $MU_l = MU_x$, i.e.,

$\tilde{x}_t = \left(\frac{1-\alpha}{r_t-c_t}\right)^{\frac{1}{\alpha}} N_t A_t U_t$.⁴¹ Substitute (10) and note the boundaries, then (1) is obtained.

Proof of Proposition 2. When there is an inner point solution of individual staking ratio, the on-chain allocation is already in optimal, i.e., $MU_l = MU_x$, Then the marginal onchain utility in optimal reads $MU_q = (\mu + r - c + \partial_n \Psi) \partial_w J + q \sigma^2 \partial_{ww} J$, where the subscript of time t is omitted. By risk aversion and the definition of Ψ_t , MU_q decreases in q . Note that under a risk-aversion setting, when $q \rightarrow \infty$, $MU_q \rightarrow -\infty$. Thus, there exists a unique $q^* \geq 0$ that satisfies the first-order condition, $MU_q = 0$, if $MU_q(q = 0) \geq 0$. Otherwise, $q^* = 0$.⁴² Consider the case when $q = x$. Similarly, the marginal transaction convenience is decreasing, leading to decreasing MU_q and a unique solution to the F.O.C.

In equilibrium, $\int_i x_i^* di = \left(\frac{1-\alpha}{r_t-c_t}\right)^{\frac{1}{\alpha}} N_t A_t \int_i U_{it} di = \left(\frac{1-\alpha}{r_t-c_t}\right)^{\frac{1}{\alpha}} N_t A_t U_t$.⁴³ Then $\Theta^* = 1 - \left(\frac{1-\alpha}{r_t-c_t}\right)^{\frac{1}{\alpha}} \frac{N_t A_t U_t}{q_t^*} \equiv \Theta^*(r_t)$. r_t^* fits (11). Substituting into agents' optimization, we obtain

$$0 = (1 - \alpha) \left[\frac{N_t(\Theta_t^*) A_t U_t}{q_t^*(1 - \Theta_t^*)} \right]^\alpha - \frac{\rho}{\Theta^*} + c_t \equiv h_1(\Theta^*(\rho)) q^*(\rho)^{-\alpha} - h_2(\rho). \quad (\text{A.2})$$

The notations above indicate the fact that both Θ^* and q^* are affected by the reward ratio ρ given A and w .

$$\Theta'(\rho) = \frac{\Theta^* + \Theta^{*2} \alpha h_1(\Theta^*(\rho)) q^*(\rho)^{-\alpha-1} q^{*\prime}(\rho)}{\Theta^{*2} h_1'(\Theta^*(\rho)) q^*(\rho)^{-\alpha} + \rho}, \quad (\text{A.3})$$

where the denominator is positive. Consider $q^{*\prime}$. $\frac{\partial MU_q}{\partial \rho} = (1 - \Theta) \partial_w J + \sigma^2 \partial_{ww} J q^{*\prime}(\rho)$. Suppose there is an ρ , s.t. $q^{*\prime}(\rho) < 0$. Under risk-aversion, $\partial_{ww} J < 0$ and thus $\frac{\partial MU_q}{\partial \rho} > 0$ for all q . Since q^* is the solution of F.O.C., $q^{*\prime}(\rho) > 0$, leading to contradiction. Back to (A.3), we obtain $\Theta'(\rho) > 0$. Thus if there is a $\Theta(\rho)$ satisfies (A.2), it must be unique. For existence: the first term on the R.H.S. of (A.2) tends to infinite when $\Theta \rightarrow 1$, thus the R.H.S. must be positive. $\Theta \rightarrow 0$, N_t tends to zero and thus the R.H.S. must be negative.

Proof of Proposition 3. Substituting the derivatives w.r.t. $V(A_t)$ into (20), we obtain

$$0 = V'(A_t) A_t \mu^A(\Theta_t) + [r(\Theta_t) - c_t - E(\Theta_t, A_t) + \Psi_n(A_t)] V(A_t) - [\sigma^S V(A_t)]^2. \quad (\text{A.4})$$

Then, we show that under current specific forms assumed in Section 3.2, I and Θ_t are both at most functions of A_t and $V(A_t)$, but do not contain any derivatives of A_t . Precisely,

⁴¹The only case where such \tilde{x}_t does not exist is that $MU_l \leq MU_x$ even when $l_t = 0$. Then, the individual staking ratio is zero. The entry cost in (3) avoids the case where l and x both tend to zero.

⁴²Note that q^* could be larger than individual wealth since self-financing is allowed.

⁴³We focus on the inner case, since the corner solution leads to a trivial equilibrium of $\Theta^* = 0$ and $\Theta^{*\prime}(\rho) = 0$. The integral seems unnecessary under a representative-agent setting; it, however, helps understand the aggregation of on-chain tradable allocation in the general case with heterogeneity. Also note that $\int_i U_{it} di$ equals to U_t since agents are homogeneous and in a unit measure.

$\Psi_t = \psi(A_t)(w_t - n_t)$. From the first-order derivatives of the HJB equation, we obtain $\partial_w J = \mathcal{U}'(y_t) = \frac{1}{y_t}$. Agents with log-utilities face changing investment opportunities, $I = -\partial_{ww} J / \partial_w J = \frac{1}{w_t}$, and the on/off-chain allocation is linear in agent's wealth.⁴⁴ Meanwhile, (16) implies that Θ_t satisfies $\rho(\Theta_t, A_t) = \Theta_t \left\{ (1 - \alpha) \left[\frac{N(\Theta_t)A_t U_t}{V(A_t)(1 - \Theta_t)} \right]^\alpha + c_t \right\}$ and thus uniquely exists as a function of A_t and $V(A_t)$ without any derivatives. Therefore, we obtain (21). It follows the form $V'(A) = F(A, V(A))$, where F is continuously differentiable. Therefore, the ODE has a unique solution given the boundary condition.

Proof of Proposition 4. Rearrange the formula of MU_q to obtain (4).

Proof of Proposition 5. Similar to previous proofs, there exists a unique $\tilde{x}_{i,t}$ s.t. $MU_l = MU_x$.⁴⁵ Based on the proof of Proposition 2, we denote the unique solution of $MU_q = 0$ as $q_{i,t}^*$. Agents may vary in trade-offs between convenience benefits and the fixed entry cost φ . When $\tilde{x}_{i,t} < q_{i,t}^*$, (3) yields $dv(\tilde{x}) = \left[\left(\frac{1-\alpha}{r-c_t} \right)^{\frac{1-\alpha}{\alpha}} N_t A_t U(u_{i,t}, w_{i,t}) - \varphi \right] dt$. Only when $U(u_{i,t}, w_{i,t})$ are large enough s.t. $dv_t > 0$, i.e., $U_t > \frac{\varphi}{NA} \left(\frac{r-c}{1-\alpha} \right)^{\frac{1-\alpha}{\alpha}} \equiv U_0$, transaction is applicable. Otherwise, the optimal θ_{it} is always 1. Then (26) is obtained.⁴⁶

Proof of Proposition 6.

Lemma 1. The penalty function. *The penalty function $v(w)$ satisfies*

$$v(w) = - \int \frac{\delta J(w, w', m)}{\delta m} \frac{\partial g(w') m(w')}{\partial w'} dw'. \quad (\text{A.5})$$

Proof. Treat J_t as $J(\cdot, m_t)$, and use Itô's Lemma, $dJ_t = \langle \frac{\delta J}{\delta m}, dm_t \rangle + \frac{1}{2} \langle dm_t | \frac{\delta^2 J}{\delta m^2} | dm_t \rangle$. \square

(A.5) always holds even the non-stationary states. Consider the value function.

Lemma 2. *With log utility, the value function J is separable: $J = \frac{\log(w)}{\phi} + F(m, A)$, where F satisfies $\forall w, w', \forall w'', \frac{\delta F}{\delta m}(w, w'', m, A) = \frac{\delta F}{\delta m}(w', w'', m, A) \equiv \hat{F}(w'', m, A)$.*

Proof. Consider $J(w, m, A) = b \log(w) + F(m, A)$ as a trial form. Then the optimal $y = 1/\partial_w J = \frac{w}{b} \cdot q = \frac{\mu+r-c+\Psi_n}{\sigma^2} w \equiv \frac{k_1}{\sigma^2} w$, where k_1 could be a functional of m and A , but definitely

⁴⁴Proof of Proposition 6 precisely proves this in a more general (heterogeneous) setting. The general solution can be found in Merton (1971) and Duffie (2010). Because the main results do not depend on risk-aversion, we assume log utility for simplicity. For general utilities such as HARA, agents have extra terms to hedge the changes of investment opportunity. The numerical approach still applies.

⁴⁵Note that \tilde{x} reflects the trade-off threshold of switching to staking, while both the two on-chain allocations need to satisfy $MU_q \geq 0$. $\tilde{x}_{i,t} = \left(\frac{1-\alpha}{r-c_t} \right)^{\frac{1}{\alpha}} N_t A_t U(u_{i,t}, w_{i,t})$.

⁴⁶Similarly, other implications with heterogeneity are proved in Online Appendix OA3.3. In brief, the key observation is that heterogeneity changes the proofs by entering m , while the overall variables are integrated values over m , then the monotonicity of the staking ratio precludes a great deal of concern about uniqueness.

does not involve w , since the endogenous variables, μ and r , are determined by the whole crowd rather than any atomic agent. $x = \left(\frac{1-\alpha}{r-c}\right)^{\frac{1}{\alpha}} NAu_i w$. Substituting these optimal controls and the derivatives of J into the HJB equation, we obtain

$$\begin{aligned} \phi b \log(w) + \phi F = \log(w) - \log(b) + f(w) \frac{b}{w} - \frac{1}{2} g(w)^2 \frac{b}{w^2} + \mu^A A \partial_A F \\ + \frac{\partial}{\partial w} \left(g(w) \int \frac{\delta F}{\delta m}(w, w', m) \frac{\partial g(w') m(w')}{\partial w'} dw' \right), \end{aligned} \quad (\text{A.6})$$

where $g(w) = \frac{k_1^2}{\sigma} w$, $f(w) = \frac{k_1^2}{\sigma^2} w - \frac{w}{b} + \alpha \left(\frac{1-\alpha}{r-c}\right)^{\frac{1-\alpha}{\alpha}} NAu_i w \equiv \left(\frac{k_1^2}{\sigma^2} - \frac{1}{b} + k_{2i}\right)w$. By the property of F , the last term can be rearranged as $\frac{k_1}{\sigma} \tilde{F}(m, A)$. Since (A.6) holds for all w , the coefficient of $\log(w)$ should be zero, $b = \frac{1}{\phi}$ and satisfies the supposed form of b . Then

$$\phi F = \log(\phi) + \frac{k_1^2}{2\phi\sigma^2} - 1 + \frac{k_{2i}}{\phi} + \mu^A A \partial_A F + \frac{k_1 \tilde{F}}{\sigma}, \quad (\text{A.7})$$

indicating that F does not involve w ,⁴⁷ i.e., the separable trial form is indeed valid. \square

With the lemmas in hand, we consider the steady-state law of motion,

$$0 = L^*(w)[m] = -\frac{\partial}{\partial w} \left(\widehat{f(w, m)} m_t(w) \right) + \frac{\partial^2}{\partial w^2} \left(\frac{1}{2} g^2(w, m) m_t(w) \right), \quad (\text{A.8})$$

where $\widehat{f(w, m)}$ is the average f_i among different types $u_{i,t}$ whose wealth w_i equals to w :

$$\widehat{f(w, m)} = \mathbb{E}[f_i(w_i, m) | w_i = w] = \left(\frac{k_1^2}{\sigma^2} - \frac{1}{b} + \mathbb{E}(k_{2i}) \right) w = \left(\frac{k_1^2}{\sigma^2} - \frac{1}{b} + k_2 w^{\beta-1} \right) w, \quad (\text{A.9})$$

where $k_2 = \alpha \left(\frac{1-\alpha}{r-c}\right)^{\frac{1-\alpha}{\alpha}} NA\bar{u}$. Rearrange the law of motion (A.8), we obtain

$$\left(\frac{k_1^2}{\sigma^2} - \phi \right) \frac{\partial}{\partial w} [wm(w)] + k_2 \frac{\partial}{\partial w} [w^\beta m(w)] = \frac{k_1^2}{2\sigma^2} \frac{\partial^2}{\partial w^2} [w^2 m(w)]. \quad (\text{A.10})$$

Let $h(w) = w^2 m(w)$. We obtain a 2nd-order ODE w.r.t. h (let $a_1 = 2 - \frac{2\phi\sigma^2}{k_1^2}$, $a_2 = \frac{2k_2\sigma^2}{k_1^2}$):

$$h''(w) = a_1 \frac{h'(w)w - h(w)}{w^2} + a_2 \frac{h'(w)w - (2 - \beta)h(w)}{w^{3-\beta}}. \quad (\text{A.11})$$

Solve this ODE and note m is a p.d.f. with bounded integral, we obtain h and further (27).

References

- ABADI, JOSEPH AND MARKUS BRUNNERMEIER (2018): ‘‘Blockchain economics,’’ Tech. rep., National Bureau of Economic Research.
- ABADIE, ALBERTO, SUSAN ATHEY, GUIDO W IMBENS, AND JEFFREY WOOLDRIDGE (2017): ‘‘When should you adjust standard errors for clustering?’’ Tech. rep., National Bureau of Economic Research.

⁴⁷The precise solution to $F(m, A)$ needs the determination of how k_1 , k_{2i} , μ^A , and σ depends on m and A . This further requires the combination with the pricing formula. However, whatever the precise solution is, (A.7) already indicates that F does not involve w .

- ACHDOU, YVES, JIEQUN HAN, JEAN-MICHEL LASRY, PIERRE-LOUIS LIONS, AND BENJAMIN MOLL (2022): “Income and wealth distribution in macroeconomics: A continuous-time approach,” The review of economic studies, 89 (1), 45–86.
- AUGUSTIN, PATRICK, ROY CHEN-ZHANG, AND DONGHWA SHIN (2022): “Yield Farming,” Available at SSRN 4063228.
- BAILEY, WARREN AND KALOK C CHAN (1993): “Macroeconomic influences and the variability of the commodity futures basis,” The Journal of Finance, 48 (2), 555–573.
- BAKSHI, GURDIP AND GEORGE PANAYOTOV (2013): “Predictability of currency carry trades and asset pricing implications,” Journal of financial economics, 110 (1), 139–163.
- BANSAL, RAVI (1997): “An exploration of the forward premium puzzle in currency markets,” The Review of Financial Studies, 10 (2), 369–403.
- BANSAL, RAVI AND WILBUR JOHN COLEMAN (1996): “A monetary explanation of the equity premium, term premium, and risk-free rate puzzles,” Journal of Political Economy, 104 (6), 1135–1171.
- BARR, DAVID G AND RICHARD PRIESTLEY (2004): “Expected returns, risk and the integration of international bond markets,” Journal of International money and finance, 23 (1), 71–97.
- BASU, SOUMYA, DAVID EASLEY, MAUREEN O’HARA, AND EMIN SIRER (2019): “StableFees: A Predictable Fee Market for Cryptocurrency,” Available at SSRN 3318327.
- BECH, MORTEN L AND RODNEY GARRATT (2017): “Central bank cryptocurrencies,” BIS Quarterly Review September.
- BEKAERT, GEERT (1996): “The time variation of risk and return in foreign exchange markets: A general equilibrium perspective,” The Review of Financial Studies, 9 (2), 427–470.
- BENHAIM, ALON, BRETT HEMENWAY FALK, AND GERRY TSOUKALAS (2021): “Scaling Blockchains: Can Elected Committees Help?” arXiv preprint arXiv:2110.08673.
- BERTUCCI, CHARLES, LOUIS BERTUCCI, JEAN-MICHEL LASRY, AND PIERRE-LOUIS LIONS (2020): “Mean field game approach to bitcoin mining,” arXiv preprint arXiv:2004.08167.
- BIAIS, BRUNO, CHRISTOPHE BISIERE, MATTHIEU BOUVARD, AND CATHERINE CASAMATTA (2019): “The blockchain folk theorem,” Review of Financial Studies, 32 (5), 1662–1715.
- BIAIS, BRUNO, CHRISTOPHE BISIERE, MATTHIEU BOUVARD, CATHERINE CASAMATTA, AND ALBERT J MENKVELD (2020): “Equilibrium bitcoin pricing,” Available at SSRN 3261063.
- BILAL, ADRIEN (2023): “Solving heterogeneous agent models with the master equation,” Tech. rep., National Bureau of Economic Research.
- BRUNNERMEIER, MARKUS K, STEFAN NAGEL, AND LASSE H PEDERSEN (2008): “Carry trades and currency crashes,” NBER macroeconomics annual, 23 (1), 313–348.
- BURNSIDE, CRAIG, MARTIN EICHENBAUM, ISAAC KLESHCHELSKI, AND SERGIO REBELO (2011): “Do peso problems explain the returns to the carry trade?” The Review of Financial Studies, 24 (3), 853–891.
- CAPPONI, AGOSTINO AND RUIZHE JIA (2021): “The Adoption of Blockchain-based Decentralized Exchanges: A Market Microstructure Analysis of the Automated Market Maker,” Available at SSRN 3805095.
- CARDALIAGUET, PIERRE, FRANÇOIS DELARUE, JEAN-MICHEL LASRY, AND PIERRE-LOUIS LIONS (2019): “The master equation and the convergence problem in mean field games,” in The Master Equation and the Convergence Problem in Mean Field Games, Princeton University Press.
- CASASSUS, JAIME AND PIERRE COLLIN-DUFRESNE (2005): “Stochastic convenience yield implied from commodity futures and interest rates,” The Journal of Finance, 60 (5), 2283–2331.

- CHIU, JONATHAN, SEYED MOHAMMADREZA DAVOODALHOSSEINI, JANET HUA JIANG, AND YU ZHU (2019): “Bank market power and central bank digital currency: Theory and quantitative assessment,” Available at SSRN 3331135.
- CONG, LIN WILLIAM AND ZHIGUO HE (2019): “Blockchain disruption and smart contracts,” Review of Financial Studies, 32 (5), 1754–1797.
- CONG, LIN WILLIAM, ZHIGUO HE, AND JIASUN LI (2021a): “Decentralized mining in centralized pools,” Review of Financial Studies, 34 (3), 1191–1235.
- CONG, LIN WILLIAM, GEORGE ANDREW KAROLYI, KE TANG, AND WEIYI ZHAO (2021b): “Value Premium, Network Adoption, and Factor Pricing of Crypto Assets,” Network Adoption, and Factor Pricing of Crypto Assets (December 2021).
- CONG, LIN WILLIAM, WAYNE LANDSMAN, EDWARD MAYDEW, AND DANIEL RABETTI (2023): “Tax-loss harvesting with cryptocurrencies,” Journal of Accounting and Economics, 101607.
- CONG, LIN WILLIAM, XI LI, KE TANG, AND YANG YANG (2021c): “Crypto wash trading,” arXiv preprint arXiv:2108.10984.
- CONG, LIN WILLIAM, YE LI, AND NENG WANG (2021d): “Token-based platform finance,” Journal of Financial Economics.
- (2021e): “Tokenomics: Dynamic adoption and valuation,” Review of Financial Studies, 34 (3), 1105–1155.
- CONG, LIN WILLIAM AND SIMON MAYER (2021): “The Coming Battle of Digital Currencies,” Available at SSRN 3992815.
- CONG, LIN WILLIAM, KE TANG, YANXIN WANG, AND XI ZHAO (2022): “Inclusion and Democratization Through Web3 and DeFi? Initial Evidence from the Ethereum Ecosystem,” Working Paper.
- DANIEL, KENT, ROBERT HODRICK, AND ZHONGJIN LU (2017): “The Carry Trade: Risks and Drawdowns,” Critical Finance Review, 6 (2), 211–262.
- DUFFIE, DARRELL (2010): Dynamic asset pricing theory, Princeton University Press.
- EASLEY, DAVID, MAUREEN O’HARA, AND SOUMYA BASU (2019): “From mining to markets: The evolution of bitcoin transaction fees,” Journal of Financial Economics, 134 (1), 91–109.
- FAMA, EUGENE F (1984): “Forward and spot exchange rates,” Journal of monetary economics, 14 (3), 319–338.
- FAMA, EUGENE F AND KENNETH R FRENCH (1998): “Value versus growth: The international evidence,” The journal of finance, 53 (6), 1975–1999.
- FANTI, GIULIA, LEONID KOGAN, AND PRAMOD VISWANATH (2021): “Economics of proof-of-stake payment systems,” in Working paper.
- FEENSTRA, ROBERT C (1986): “Functional equivalence between liquidity costs and the utility of money,” Journal of Monetary Economics, 17 (2), 271–291.
- FRANZ, FRIEDRICH-CARL AND ALEXANDER VALENTIN (2020): “Crypto Covered Interest Parity Deviations,” Available at SSRN 3702212.
- GABAIX, XAVIER (2009): “Power laws in economics and finance,” Annu. Rev. Econ., 1 (1), 255–294.
- GABAIX, XAVIER AND MATTEO MAGGIORI (2015): “International liquidity and exchange rate dynamics,” The Quarterly Journal of Economics, 130 (3), 1369–1420.
- GANS, JOSHUA S, HANNA HALABURDA, ET AL. (2015): “Some economics of private digital currency,” Economic analysis of the digital economy, 257–276.
- GRIFFIN, JOHN M, XIUQING JI, AND J SPENCER MARTIN (2003): “Momentum investing and business cycle risk: Evidence from pole to pole,” The Journal of finance, 58 (6), 2515–2547.
- GRIFFIN, JOHN M AND AMIN SHAMS (2020): “Is Bitcoin really untethered?” Journal of Finance, 75

- (4), 1913–1964.
- HARVEY, CAMPBELL R, ASHWIN RAMACHANDRAN, AND JOEY SANTORO (2021): DeFi and the Future of Finance, John Wiley & Sons.
- HINZEN, FRANZ J, KOSE JOHN, AND FAHAD SALEH (2019): “Proof-of-work’s limited adoption problem,” NYU Stern School of Business.
- HOU, KEWEI, G ANDREW KAROLYI, AND BONG-CHAN KHO (2011): “What factors drive global stock returns?” The Review of Financial Studies, 24 (8), 2527–2574.
- HOWELL, SABRINA T, MARINA NIESSNER, AND DAVID YERMACK (2020): “Initial coin offerings: Financing growth with cryptocurrency token sales,” Review of Financial Studies, 33 (9), 3925–3974.
- HUBERMAN, GUR, JACOB D LESHNO, AND CIAMAC MOALLEMI (2021): “Monopoly without a monopolist: An economic analysis of the bitcoin payment system,” Review of Economic Studies, 88 (6), 3011–3040.
- ILMANEN, ANTTI (1995): “Time-varying expected returns in international bond markets,” The Journal of Finance, 50 (2), 481–506.
- JERMANN, URBAN J (2023): “A Macro Finance Model for Proof-of-Stake Ethereum,” Available at SSRN 4335835.
- JIANG, ZHENGYANG, ARVIND KRISHNAMURTHY, AND HANNO LUSTIG (2021): “Foreign safe asset demand and the dollar exchange rate,” The Journal of Finance, 76 (3), 1049–1089.
- JOHN, KOSE, THOMAS J RIVERA, AND FAHAD SALEH (2020): “Economic implications of scaling blockchains: Why the consensus protocol matters,” Available at SSRN 3750467.
- (2022): “Equilibrium staking levels in a proof-of-stake blockchain,” Available at SSRN 3965599.
- KOGAN, LEONID, GIULIA FANTI, AND PRAMOD VISWANATH (2021): “Economics of proof-of-stake payment systems,” .
- KOIJEN, RALPH SJ, TOBIAS J MOSKOWITZ, LASSE HEJE PEDERSEN, AND EVERT B VRUGT (2018): “Carry,” Journal of Financial Economics, 127 (2), 197–225.
- LASRY, JEAN-MICHEL AND PIERRE-LOUIS LIONS (2007): “Mean field games,” Japanese journal of mathematics, 2 (1), 229–260.
- LEHAR, ALFRED AND CHRISTINE A PARLOUR (2020): “Miner collusion and the bitcoin protocol,” Available at SSRN 3559894.
- LI, TAO, DONGHWA SHIN, AND BAOLIAN WANG (2021): “Cryptocurrency pump-and-dump schemes,” Available at SSRN 3267041.
- LI, TAO, CHUYI SUN, DONGHWA SHIN, AND BAOLIAN WANG (2022): “The Dark Side of Decentralized Finance,” Working Paper.
- LIU, YUKUN, ALEH TSYVINSKI, AND XI WU (2019): “Common risk factors in cryptocurrency,” Tech. rep., National Bureau of Economic Research.
- LUSTIG, HANNO, NIKOLAI ROUSSANOV, AND ADRIEN VERDELHAN (2011): “Common risk factors in currency markets,” The Review of Financial Studies, 24 (11), 3731–3777.
- (2014): “Countercyclical currency risk premia,” Journal of Financial Economics, 111 (3), 527–553.
- LUSTIG, HANNO, ANDREAS STATHOPOULOS, AND ADRIEN VERDELHAN (2019): “The term structure of currency carry trade risk premia,” American Economic Review, 109 (12), 4142–77.
- LYANDRES, EVGENY, BERARDINO PALAZZO, AND DANIEL RABETTI (2019): “Do tokens behave like securities? An anatomy of initial coin offerings,” SSRN Electronic Journal.

- MENKHOFF, LUKAS, LUCIO SARNO, MAIK SCHMELING, AND ANDREAS SCHRIMPF (2012): “Carry trades and global foreign exchange volatility,” The Journal of Finance, 67 (2), 681–718.
- MERTON, ROBERT C (1971): “Optimum consumption and portfolio rules in a continuous-time model,” Journal of Economic Theory, 3 (4), 373–413.
- PARDOUX, ETIENNE AND AUREL RÂȘCANU (2014): Stochastic differential equations, Backward SDEs, Partial differential equations, vol. 69, Springer.
- PARK, ANDREAS (2021): “The conceptual flaws of constant product automated market making,” Available at SSRN 3805750.
- PETERSEN, MITCHELL A (2008): “Estimating standard errors in finance panel data sets: Comparing approaches,” The Review of financial studies, 22 (1), 435–480.
- PRAT, JULIEN, VINCENT DANOS, AND STEFANIA MARCASSA (2019): “Fundamental pricing of utility tokens,” .
- SALEH, FAHAD (2021): “Blockchain without waste: Proof-of-stake,” Review of Financial Studies, 34 (3), 1156–1190.
- TANG, KE AND WEI XIONG (2012): “Index investment and the financialization of commodities,” Financial Analysts Journal, 68 (6), 54–74.
- TANG, KE AND HAOXIANG ZHU (2016): “Commodities as collateral,” The Review of Financial Studies, 29 (8), 2110–2160.
- VALCHEV, ROSEN (2020): “Bond convenience yields and exchange rate dynamics,” American Economic Journal: Macroeconomics, 12 (2), 124–66.
- VERDELHAN, ADRIEN (2010): “A habit-based explanation of the exchange rate risk premium,” The Journal of Finance, 65 (1), 123–146.
- WOLD, HERMAN OA AND PETER WHITTLE (1957): “A model explaining the Pareto distribution of wealth,” Econometrica (Pre-1986, Journal of the Econometric Society), 591–595.

Online Appendices for “The Tokenomics of Staking”

OA1 Institutional Background of Staking

OA1.1 Staking Mechanisms

Blockchain-based staking in general involves two broad categories of activities: those related to pan-PoS consensus protocols and those in higher layer DeFi applications.⁴⁸ Even on non-blockchain-based or centralized platforms, various programs that involve escrows or crowd funds can be analyzed as a form of business layer staking through the lens of our framework. Fundamentally, a blockchain functions to generate a relatively decentralized consensus record of system states to facilitate economic interactions such as value or information exchanges (e.g., [Cong and He, 2019](#)). PoS protocols have gained popularity and momentum with major market players such as Ethereum adopting them. Under PoS, agents stake native tokens to compete for the opportunity to record transactions, execute smart contracts, append blocks, etc., to earn block rewards and fees. Meanwhile, various staking programs have become popular means to encourage desirable behavior in higher layer applications, escrowing a balance of tokens under custody in a smart contract, or deploy them to enable network economic functionalities.

Consensus generation in PoS. Fundamentally, blockchain functions to generate a relatively decentralized consensus to enable economic interactions such as value or information exchanges (e.g., [Cong and He, 2019](#)). Permissionless blockchains have historically relied on variants of the PoW protocol. Because of scalability and environmental issues of PoW ([Cong et al., 2021a](#); [John et al., 2020](#)), PoS protocols have gained popularity and momentum for both permissioned and permissionless blockchains, with major market players adopting and incumbents such as Ethereum contemplating a conversion ([Irresberger et al., 2021](#)).

Under PoS, agents who stake native tokens have the opportunity to append blocks and earn block rewards and fees as compensation. The more one stakes, the more likely one is to be selected and compensated for their participation ([Saleh, 2021](#), contains more details). Note that holding a token does not necessarily mean participating in staking. In practice, agents incur negligible physical costs (as opposed to the high entry cost of PoW mining or directly maintaining a node in PoS). Our study includes all protocols using pan-PoS protocols, such as Proof-of-Credit (POC) used in Nuls, which are variants of the above mechanisms. Online Appendix [OA1.2](#) provides more background information and examples in practice.

Staking in DeFi. Staking programs are a popular means for incentivizing desirable behavior and guarding against misbehavior in DeFi applications. It escrows a balance of tokens under custody in a smart contract and stakers receive rewards similar to interest payments from their tokens staked ([Harvey et al., 2021](#)). Synthetix is an example of an open-source DeFi protocol with staking where users can create and trade derivative tokens and gain exposure to assets like gold, bitcoin, and euros without having to actually own them. These derivative assets are collateralized by the platform tokens (SNX) which, when locked in the contracts, enables their issuance. In return, SNX stakers earn rewards from both newly issued tokens and small fees transactions generate.⁴⁹ Another salient form of staking is yield farming, which allows investors to earn yield by temporarily locking tokens in a decentralized application (dApps). Yield farming often entails shorter lock-up (some allows withdrawal at any time), uncertain yields, and higher risks. (see, [Augustin et al., 2022](#), for more institutional details).

Without getting bogged down with specific eligibility requirements and operational differences across various DeFi protocols and smart contracts, DeFi staking can be characterized as simply earning rewards by collateralizing the tokens for some functionalities in the network.

⁴⁸The two are not mutually exclusive. Solana, for example, uses both PoS and DeFi staking. The classification we use follows mainstream cryptocurrency data aggregators such as CoinMarketCap.

⁴⁹DeFi staking may involve multiple tokens. For example, in MakerDAO, the profits generated from DAI can be viewed as a yield on ETH staking, and our framework can be used to understand the price impact on ETH.

Reward determination and slashing. In most staking programs, the total rewards used to incentivize staking or its determination mechanism are pre-specified and announced. In PoS, the blockchain branch is randomly selected from the whole staking pool. Then the staking reward is randomly distributed to stakeholders based on the number of staked coins they hold as a probability weight.⁵⁰ Similarly, on DeFi platforms, stakers share the rewards from transaction fees or predetermined emissions (minting of new tokens).

Staking reward rate can be naturally compared to interest rate or yield of other financial assets. However, unlike deposit rates set by the banks, staking reward rate is jointly determined by the announced staking reward and the aggregate tokens staked. Online Appendix OA1.2 details the staking programs for the tokens in our sample. Stakers face the risk of losing the staked tokens due to possible security attacks, illegal verification, and storage failures. To discourage the misbehavior of the validator, most projects also propose a punishment mechanism known as *slashing*. A pre-defined percentage of a validator's tokens are lost when it does not behave consistently or as expected on the network (e.g., downtime and double signing).

Market and information. In PoS, validators compete in the amount of staking to earn rewards. To incentivize more delegates, they develop a reward distribution plan at the node level. Potential delegates can freely choose among these nodes or delegate through some intermediaries. Therefore, nodes engage in price competition for delegated stakes. For DeFi platforms, staking reward rates are typically equal for participants, but some white-listed groups may have priority in staking. Most stakable tokens are launched on mainstream cryptocurrency exchanges. Investors can easily invest in these staking projects and trade these tokens with cryptocurrency assets such as Bitcoin and Ethereum.

Information on staking programs, including participation rules, reward distribution plan, total staked value (or total value locked, TVL, which includes non-native tokens), and even information of all the validators, are open and can be easily obtained on official websites of projects. Third-party websites also specialize in collecting real-time information on staking projects, e.g., *Stakingrewards.com*. In particular, the *staking ratio*, which captures the total number of tokens staked as a fraction of the total number of tokens, is typically public knowledge.

OA1.2 Forms of Staking in Our Sample

PoS staking. Under PoS, agents who stake native tokens have opportunities to append blocks and earn block rewards and fees as compensation. There are mainly two ways to participate. The first is to *run a validator node, staking pool, or masternode* by holding native tokens and incurring the costs including hardware costs and time spent on maintenance. The more one stakes, the more likely one is to be selected and compensated for their participation (Saleh, 2021, contains more details). Note that holding a token does not necessarily mean participating in staking. The second way is through *delegation*. Agents only need to delegate their tokens to an existing node or a pool to receive a reward earned by the node/pool. This route is flexible and friendly for players with fewer tokens and allows them to share risk (Cong et al., 2021a). In practice, agents incur negligible physical costs (as opposed to the high entry cost of PoW mining or directly maintaining a node in PoS).

Solana is a concrete example of pan-PoS staking.⁵¹ Solana is an open-source project that implements a new, high performance, permissionless blockchain. It enables transactions to be ordered as they enter the network, rather than by block, which makes Solana one of the fastest blockchains in the world and the rapidly growing ecosystem in crypto, with thousands of projects spanning DeFi, NFTs, Web 3.0 and more. Solana uses Proof-of-Stake (PoS) as its consensus mechanism. The performance is improved by its innovative protocol, Proof-of-History (PoH). Solana's Proof-of-Stake is designed to quickly confirm the current sequence of transactions produced by the PoH generator, vote and select the next PoH generator, and punish misbehaving validators. A

⁵⁰For example, if an investor stakes 10 coins while the aggregate staked amount of this branch is 100, then the investor has a 10% probability of appending to the branch and receiving the staking reward.

⁵¹For references, see <https://docs.solana.com>, blockdaemon.com, and <https://blockdaemon.com/platform/validator-node/how-solana-staking-works/>.

block in the context of Solana is simply the term used to describe the sequence of entries that validators vote on to achieve confirmation. *Validators* within Solana's PoS consensus model are the entities responsible for confirming if these entries are valid. *SOL* is the name of Solana's native token, which can be passed to nodes in a Solana cluster in exchange for running an on-chain program or validating its output. *Stakers* delegate SOL to validators to help increase these validators' voting weight. Such action indicates a degree of trust in the validators. Stakers delegate to ensure validators cast honest votes and hence ensure the security of the network. The more stake delegated to a validator, the more often this validator is chosen to write new transactions to the ledger, and then the more *rewards* the validator and its delegators earn.

Staking DeFi native tokens. Incentivizing desirable behavior and guarding against misbehavior are crucial in DeFi applications. To this end, staking programs are popular and important in practice, which applies to a balance of tokens under custody in a smart contract. Users on DeFi platforms receive staking rewards as a form of interest payment from their token balance staked (Harvey et al., 2021).

In practice, DeFi staking may involve different lock-up periods and multiple tokens.⁵² The risks of being slashed and losing the staked tokens are also different. Without getting bogged down with specific threshold requirements and operational differences across various DeFi protocols and smart contracts, DeFi staking can be characterized as simply earning rewards by collateralizing the tokens for some functionalities in the network. From the stakers' perspective, staking shares the spirit of certificates of deposit or risky illiquid investments.

Transaction gas fees and Rewards. We summarize the gas fee foundations of Ethereum (EIP 1559) as an example. The major of contents are extracted from the official webpage of Ethereum and the third-party page, *blocknative*.⁵³

Gas refers to the unit that measures the amount of computational effort required to execute specific operations on the Ethereum network. Since each Ethereum transaction requires computational resources to execute, each transaction requires a fee. Gas thus refers to the fee required to execute a transaction on Ethereum.

Every block has a *base fee* which acts as a reserve price. To be eligible for inclusion in a block the offered price per gas must at least equal the base fee. The base fee is calculated independently of the current block and is instead determined by the blocks before it - making transaction fees more predictable for users. When the block is mined this base fee is "burned", removing it from circulation. The base fee is calculated by a formula that compares the size of the previous block (the amount of gas used for all the transactions) with the target size. The base fee will increase by a maximum of 12.5% per block if the target block size is exceeded. This exponential growth makes it economically non-viable for block size to remain high indefinitely.

In origin, miners would receive the total gas fee from any transaction included in a block. With the new base fee getting burned, the London Upgrade introduced a *priority fee* (tip) to incentivize miners to include a transaction in the block. Without tips, miners would find it economically viable to mine empty blocks, as they would receive the same block reward. Under normal conditions, a small tip provides miners a minimal incentive to include a transaction. For transactions that need to get preferentially executed ahead of other transactions in the same block, a higher tip will be necessary to attempt to outbid competing transactions.

Staking rewards are the combination of gas fees and the emission of new tokens. Together with the gas fee policies summarized above, as well as the mechanism of rewards from emission described in the main text, the main take-away is that the reward distribution design is widely under the platform's control, whereas the crowd decisions and interactions provide influence under the designed structure. In practice, the staking rewards may also involve the phenomenon of multilevel distribution, as some agents can delegate tokens to larger nodes. The holders of the larger nodes thus need to have a process for deciding on the distribution of benefits. Therefore,

⁵²MakerDAO is a good example. The profits generated from DAI can be viewed as a yield on ETH staking, and our framework can be used to understand the price impact on ETH.

⁵³Please see <https://ethereum.org/en/developers/docs/gas/>, and <https://www.blocknative.com/blog/eip-1559-fees>, respectively.

there may exist multiple staking participation methods for one token. In relevant empirical tests, we always choose the participation method with the lowest capital threshold and risk, such as delegating, voting, etc.

Examples in practice.

We summarize representative staking programs involving tokens in our sample. Most information is accessed from *Stakingrewards.com*. There is also information from official websites of corresponding tokens. Many tokens have similar mechanisms, thus we do not repeat the description. These descriptions are excerpted in 2022. There may be changes over time in the specific mechanisms of some programs, whereas these descriptions apply to the time intervals covered by the data in our paper.

- The individual AION rewards depends on the Block Reward, Block Time, Daily Network Rewards and Total Staked. Every block one validator is randomly selected to create a block, whereas 1 staked or delegated token counts as one “lottery ticket”. The selected validator has the right to create a new block and broadcast them to the network. The Validator then receives the 50% of the block reward and the fees of all transactions (network rewards) successfully included in this block, whereas the PoW Miner receives the other 50%.
- Rewards in the form of algos are granted to Algorand users for a variety of purposes. Initially, for every block that is minted, every user in Algorand receives an amount of rewards proportional to their stake in order to establish a large user base and distribute stake among many parties. As the network evolves, the Algorand Foundation will introduce additional rewards in order to promote behavior that strengthens the network, such as running nodes and proposing blocks.
- The individual BitBay rewards depends on the Block Reward, Block Time, Daily Network Rewards and Total Staked. Every block is randomly selected whereas 1 staked coin counts as one “lottery ticket”. The selected staker has the right to create a new block and broadcast it to the network. He then receives the block reward and the fees of all transactions successfully included in this block.
- Dash blockchain consensus is achieved via Proof of Work + Masternodes. Investors can leverage their crypto via operating masternodes. Miners are rewarded for securing the blockchain and masternodes are rewarded for validating, storing and serving the blockchain to users.
- Eos has a fixed 5% annual inflation. 4% goes to a savings fund, which might distribute the funds to the community later on. 1% goes to Block producers and Standby Block Producers. Out of the 1% that are given to block producers, only 0.25% will go to the actual 21 producers of the blocks. The other 0.75% will be shared among all block producers and standby block producers based on how many votes they receive and with a minimum of 100 EOS/day.
- The individual reward of staking fantom depends on the Total Staked ratio. Transactions are packaged into event blocks. In order for event blocks to achieve finality, event blocks are passed between validator nodes that represent at least 2/3rds of the total validating power of the network. A validator’s total validating power is primarily determined by the number of tokens staked and delegated to it. A validator earns rewards each epoch for each event block signed according to it’s validating power. By delegating, investors can increase the share of their validator proportionally to the balance of their account. They will receive rewards accordingly and share them with investors after taking the commission.
- The effective yield for staking IDEX depends on the actual Trading Volume on IDEX Market. The higher the trading volume on IDEX, the higher are the actual rewards. The second metric to watch is the total amount of AURA currently staking. Fewer tokens on stake result in higher rewards.
- Every livepeer (LPT) token holder has the right to delegate their tokens to an Orchestrator node for the right to receive both inflationary rewards in LPT and fees denominated in ETH from work completed by that node.

- The individual LTO rewards depends on the Network Rewards (Transaction Fees spent on the Network) and the Total Staked. Every block one staking node operator is randomly selected to create a new block, whereas 1 staked token counts as one “lottery ticket”. The staker receives the fees of all transactions successfully included in this block. Staking Node Operators share the rewards with their delegators after deducting a commission.
- NEM blockchain consensus is achieved via Proof of Importance. Investors can leverage their crypto via harvesting. To harvest NEM coins it is recommended to run the official NEM Core wallet with an entire copy of the blockchain on the stakers’ computer or a Virtual Private Server (VPS). The individual NEM harvesting rewards depends on the Daily Network Rewards and Total Staked. For every block, the staker is randomly selected whereas 1 staked coin counts as one “lottery ticket”. The selected staker has the right to create a new block and broadcast it to the network. The staker then receives the fees of all transactions successfully included in this block.
- Everyone who holds NEO will automatically be rewarded by GAS. GAS is produced with each new block. In the first year, each new block generates 8 GAS, and then decreases every year until each block generates 1 GAS. This generation mechanism will be maintained until the total amount of GAS reaches 100 million and no new GAS will be generated.
- Nuls blockchain consensus is achieved via Proof of Stake + Masternodes. Investors can leverage their crypto via staking. The amount earned is variable based on the current blockchain metrics like the amount of stakers (Total Staked ratio). Investors can stake Nuls into a project’s nodes and earn their token as a reward, while the project earns Nuls as a reward. Some projects offer to stake with just 5 Nuls as the minimum.
- Delegators in Polkadot are called Nominators. Anyone can nominate up to 16 validators, who share rewards if they are elected into the active validators set. The process is a single-click operation inside the wallet. The current reward rate for validators is determined by the current Total Staked ratio. The less DOT is being staked, the higher are the rewards.
- Qtum blockchain consensus is achieved via Proof of Stake 3.0. The individual reward depends on the Block Reward, Block Time, Daily Network Rewards and Total Staked. Every block is randomly selected whereas 1 staked coin counts as one “lottery ticket”. The selected staker has the right to create a new block and broadcast it to the network. The staker then receives the block reward and the fees of all transactions successfully included in this block.
- Synthetix Network Token blockchain consensus is achieved via the Ethereum Blockchain. Investors can leverage their crypto via staking. SNX holders can lock their SNX as collateral to stake the system. Synths are minted into the market against the value of the locked SNX, where they can be used for a variety of purposes including trading and remittance. All Synth trades on Synthetix Exchange generate fees that are distributed to SNX holders, rewarding them for staking the system.
- Tezos blockchain consensus is achieved via Liquid Proof of Stake. Investors can leverage their crypto via baking or delegating. There are a number of tokens that use a similar mechanism, including iotex, irisnet, etc.
- Tron reward depends on the Block Rewards, Endorsement Rewards, Block Time, Daily Network Rewards and Total Staked. Every block is randomly selected to bake a block and 32 stakers are selected to endorse a block, whereas 1 staked coin counts as one “lottery ticket”. The selected stakers have the right to create or endorse new block and broadcast them network. The Baker then receives the block reward and the fees of all transactions successfully included in this block. The Endorsers receive the endorsement rewards.

- Wanchain blockchain consensus is achieved via Galaxy Proof-of-Stake. The individual WAN rewards depends on the Foundation Rewards, Daily Network Rewards and Total Staked. At the beginning of each protocol cycle (epoch), two groups, the RNP (Random Number Proposer) group and the EL (Epoch Leader) group, are selected from all validators. 1 staked or delegated token counts as one “lottery ticket” to be selected. The two groups equally share the Foundation Rewards and Transaction Fees (Network Rewards). The Foundation Rewards consists of 10% of the outstanding Wanchain Token Supply and are decreasing by 13.6% each year, whereas the Network Rewards are expected to rise alongside wider network usage.

OA2 Notes on Numerical Solutions

We document the numerical approaches in Section 4.4. In brief, we connect Bilal (2023)’s idea of analytical perturbation and the approximation using instantaneous arriving shocks, and then derive a system that solvable by the finite difference (FD) method.

In the master equation (25), the agents do not respond to any specific shocks, but only “internalize” them by the penalty term as well as the volatility risk of penalty. To better comprehend the trajectory of the economy after specific shocks, we adopt the underlying simulation idea. Suppose once an agent decides on an allocation, she cannot adjust her portfolio choice within a short time interval dt , regardless of the magnitude of the shock that realizes during this brief period. Thus, z is presumed when solving optimization problems and enters the wealth dynamic as well as the penalty function as an external parameter. In simpler terms, the uncertainty over the entire future time horizon is dissected into two components as $dt \rightarrow 0$: the part that remains unrealized, which operates as a risk affecting agents’ retrospective evaluation, and the part that corresponds to the realized shock z . This realized shock z is incorporated into the optimization process as an additional external parameter influencing wealth dynamics and the penalty structure. This inclusion is essential since, given a specific z , agents can only hypothesize its value when solving optimization problems.

Then we show how z enters the value function J . Take $dt \rightarrow 0$ and the weighted traversal of any possible z into account, the resulting value function is proved to be an appropriate approximation of that in the initial master equation. Recall the master equation (25) contains the derivatives w.r.t. m . Though it is conceptually not difficult to calculate the approximation of the second-order derivative, it generates a large bracket of terms but bring relatively unclear general insights. What we clearly know is that it comes from the Brownian uncertainty on the distribution, i.e., $\frac{\partial}{\partial w}[g(w)m(w)dZ_t]$. Alternatively, we first approximate the master equation from the economic perspective, i.e., consider the following scenario. At time t and near the steady state, each agent solves the optimization problem given the current platform productivity A and distribution m . The difference from the background of the above master equation is that once she determines the allocation, she cannot change her portfolio choice in a short time dt , no matter what degree the shock in this short period realizes. In other words, the uncertainty in the whole future time dimension is divided into two parts as $dt \rightarrow 0$: The unrealized part performs as a risk that affects agents’ backward induction. The realized shock z enters the optimization directly as an extra exogenous argument, since for any given z , agents can only presuppose its value when solving optimization problems. An implicit requirement that allows this approach to be a proper approximation is that the generator of uncertainty is memoryless. Also, this approach shares a similar idea with Bertucci (2021), which rigorously proves that under the situation as our model introduces, i.e., all the agents are pushed by the same Brownian motion, it is a good approximation by introducing a transformation that is going to affect all players in the game at random times.

Then the law of motion is

$$dm_t/dt = L^*(w)[m] - \frac{\partial}{\partial w}g(w)m(w)z \equiv L^*(w)[m] + zG^*(w)[m], \quad (\text{OA.1})$$

where $G^*(w)[m] = -\frac{\partial}{\partial w}[g(w)m(w)]$. In addition, by the separate form of the value function J , we only focus on the part that does not involve A and denote the resulting part of the value function as the new J for simplicity.

Then substituting into the master equation above and calculating the penalty term, we obtain

$$\begin{aligned} \phi J(w, m, z) = & \mathcal{U}(w, m, z) + L(w)[J] + \int \frac{\delta J}{\delta m}(w, w', m) L^*(w')[m] dw' \\ & + \frac{\partial}{\partial w} \left[g(w) \int \frac{\delta J}{\delta m}(w, w', m) \frac{\partial g(w') m(w')}{\partial w'} dw' \right] + \mathcal{Z}(z)[J], \end{aligned} \quad (\text{OA.2})$$

where $\mathcal{Z}(z)[J] = \frac{1}{2} \frac{\partial^2 J}{\partial z^2}$. This term is obtained from the fact that agents also take the generation of such a shock into account. That is, the agent not only presupposes the case of such z , but also takes into account the possibility of such a presupposition. Note that the direct impact of z , i.e. the corresponding term in (OA.1) is offset by the penalty vz , while the penalty generates the additional term $\frac{\partial}{\partial w} g(w)v(w)$. Also, the precise form of $\mathcal{Z}(z)[J]$ is determined by the generator of Z_t . Since we have accounted for σ in $g(w, m)$, the rest part is a standard Brownian motion.

So far, we have obtained a version of value function that contains a presumed shock z . By combining all the possible shocks, we simulate the original value function. Thus, the only thing to do is to solve $J(w, m, z)$ in (OA.2). On solving $J(w, m, z)$, we follow Bilal (2023) to adopt a perturbation method near the steady state. Let $v(w, w') = \frac{\delta J}{\delta m}(w, w', m^{SS})$ (“SS” refers to the steady state), which can be also understood as the “deterministic” impulse value function. Apply the similar method of analytical perturbation in Bilal (2023), we set a small distributional shock h as well as a relatively small scale to the shock $\epsilon = \tilde{Z}/z$, $\epsilon h = m - m^{SS}$, then the first order solution to the master equation (OA.2) reads

$$J(w, m, z) = J^{SS}(w) + \epsilon \left\{ \int v(w, w') h(w') dw' + \omega(w, z) \right\} + \mathcal{O}_w(\|h\|_{H^2}^2), \quad (\text{OA.3})$$

where $v(w, w')$ refers to the deterministic part of the impulse value, whereas $\omega(w, z)$ is the stochastic part of the impulse. Bilal (2023) provides the complete explanation of the above process. The difference here is that both the deterministic and stochastic part come from the aggregated distributional shock, and correspond to the two parts of uncertainties as we mentioned above.⁵⁴ That is, the value function J is a linear functional of h to the first order.

The next step is then to solve the two impulse functions, $v(w, w')$ and $\omega(w, z)$. For $v(w, w')$: substituting into the master equation, we will obtain an equation w.r.t. the impulse value function, $v(w, w')$. Precisely, around the steady state, the associated vector that integrates against h must be zero. Then the approximate master equation is calculated by letting the first-order coefficients of h satisfy the equation that L.H.S. = R.H.S. We omit the expansions of those terms w.r.t. h but note the following observations: $\partial_J \mathcal{U}, \delta_m \mathcal{U}, \partial_J f, \partial_J g, \delta_m g = 0$, $\partial_w v(w, w')$ is second-order w.r.t. h , and the property of adjoint operators, $\int L(w)[a]b(w)dw = \int a(w)L^*(w)[b]dw$, and finally obtain

$$\begin{aligned} \phi v(w, w') = & \mathcal{L}_m(w, w')[J^{SS}] + \mathcal{L}(w)[v(\cdot, w')] + \mathcal{L}(w')[v(w, \cdot)] + \mathcal{G}(w')[v(w, \cdot)] \\ & + \int v(w, w'') \left\{ \mathcal{L}_m^*(w'', w')[m^{SS}] + \mathcal{L}_y^*(w'', \mathcal{M}(w'', w', v))[m^{SS}] \right\} dw'', \end{aligned} \quad (\text{OA.4})$$

and similarly, $\omega(w, z)$ satisfies

$$\phi \omega(w, z) = z \left\{ \mathcal{U}_z^{SS}(w, z) + \mathcal{L}_z(w)[J^{SS}] \right\} + \mathcal{L}(w)[\omega(\cdot, z)] + \mathcal{Z}(z)[\omega(w, \cdot)] + z \mathcal{G}_z^*(w')[m^{SS}], \quad (\text{OA.5})$$

where \mathcal{M} is the distributional marginal propensity to control, implying how individual controls respond to a small distributional impulse, $\mathcal{G}^*(w')[m^{SS}] = -\frac{\partial}{\partial w'} (g(w')m^{SS}(w'))$, the subscripts of the operators are the Fréchet derivatives, e.g., $\mathcal{L}_m(w, w')[J^{SS}] = \frac{\delta}{\delta m} L(w, w')[J^{SS}]$.

⁵⁴Note that the first-order approximation is additive in the response to a distributional impulse h and the aggregate shock z . Any pairwise perturbation involving the both is second-order.

Then, we only need to numerically solve (OA.4) and (OA.5). Note that they only contain the unknown matrices (in numerical processes), $v(w, w')$ and $\omega(w, z)$, and the terms at SS. Therefore, they are much easier to solve. Substituting into OA.2, the value function presuming z is solved. Then the original value function is obtained as the weighted aggregation of the cases presuming all possible z . However, the derivation of the impulse response for a particular sequence of shocks does not need to go this far — recall the resulting key changes, distributional disparity h . The perturbation method suggests that near the SS, the deterministic and stochastic impulse kernel, D and S , respectively satisfy

$$D(w, w') = \mathcal{L}_m^*(w, w')[m^{SS}] + \mathcal{L}_c^*(w_i, \mathcal{M}(w_i, w_j, v))[m^{SS}]; S(w, z) = z\mathcal{G}_z^*(w'')[m^{SS}]. \quad (\text{OA.6})$$

Further, the impulse in the distribution h_t follows the SPDE,

$$dh_t(w, z) = \{\mathcal{L}^*(w)[h_t] + D(w)[h_t] + S(w, z_t)\} dt. \quad (\text{OA.7})$$

Then, given a series of realized shock $\{z\}_{t=1}^T$ and the initial h_0 , the discretized distributional impulse is obtained by numerically solving the above equation.

*Supplementary Discussion on the impulse responses. Figure OA.1 visualizes the impulse value functions, as well as the impulse response paths of unit shock. Panel A.(1)-(2) visualize the results of $v(w, w')$ and $\omega(w, z)$. The deterministic impulse value is widely negative, indicating the agents are competitive with each other. Further, the whales (agents with large w) are virtually unaffected by the retails, while their entry has huge impact to the retails. The only exception is the agents near the lowest threshold.⁵⁵ They are less affected by any other agents, since they have less onchain allocation. In subplot (2), for similar reasons, the retails have smaller exposure to the realized shock z .

As discussed, the numerical solving process allows us to simulate any given arrived series of shocks. On the other hand, standing at any period, the response is, to some extends, the combination of the continuous impacts of historical shocks. As such, we simulate the impulse sequence of a unit shock separately, which helps understand the relationship between continuously-arriving shocks and the continuously-moving states. Precisely, we assume a unit negative shock at $t = 0$, and zero shocks for any $t > 0$. As Figure OA.1 Panel (B) shows, the initial effect is a universal loss of money across all agents, leading to an increase in the share of retail agents and a decrease in the proportion of wealthier agents. Consequently, the overall staking ratio experiences a decline. As the response progresses, two driving forces come into play. Firstly, the affluent agents are compelled to further increase their wealth through both staking and transactions, thereby reinforcing their financial positions. Secondly, the positive adjustment of staking reward rates contributes to the staking ratio's response dynamics. Interestingly, there is an over-response to the staking ratio. In addition to the complex aggregation among the changing crowd, it is also explained by the platform development: Due to the decrease in staking, the progression of the platform's productivity A_t decelerates. As time advances, the value of A_t remains lower than it would be without the occurrence of such a shock. In comparison to the steady state, agents exhibit relatively higher preference in staking. This propensity persists until the developmental disparity is filled.

The numerical approach can also be used for simulating the direct impulse on the distribution. It could, for example, correspond to the cases where the economy suddenly changes by an unintended entry of external groups, especially the whales. This is also within the scope of our framework. That is, we suppose there is an unanticipated distributional shock h and examine its influence. As Figure OA.1 Panel (C) shows, the entry of a crowd of whales initially definitely induces a large rise in the proportion of affluent agents and an accompanying decline in the share of retail participants. This shift triggers a substantial increase in the staking ratio. However, the subsequent evolution of the wealth distribution exhibits a fatter tail, which aligns with Figure 3. This suggests

⁵⁵Recall (27), the distribution is similar with Pareto distribution, in which the minimal w is also needed. From the economic perspective, agents with too little wealth will be blocked by the threshold of transaction, φ , and have no onchain activities.

that the primary benefit stemming from the entry of large funds lies in its potential to stimulate platform growth. Nevertheless, the competitive interaction among agents implies that such an entry invariably exerts impact on the on-chain inequality.

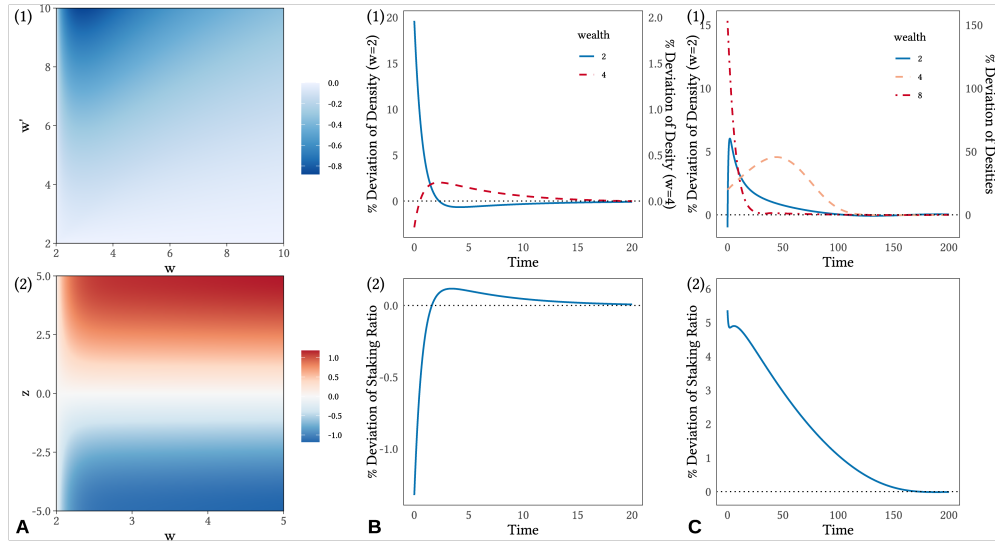


Figure OA.1: Impulse values and response functions: Supplementary tests.

Panel A.(1)-(2) show the deterministic and stochastic impulse value functions, $v(w, w')$ and $\omega(w, z)$, respectively. Panel B shows the impulse responses of a unit negative shock at $t = 0$, in which subplot (1) shows the response, i.e, the deviations comparing with the steady state of density $m(w)$ of different w , and subplot (2) shows the response of the staking ratio. Time unit is roughly calibrated to one-day. Similarly, Panel C shows the experiment when there is a crowd of whales near $w = 5$ enters the economy.

OA3 Background and Extended Discussions

OA3.1 Mean Field Game and the Master Equation

Mean field games (MFGs), introduced in the pioneering works of [Lasry and Lions \(2007\)](#), offer a powerful framework for analyzing strategic interactions in large populations when each individual agent has only a small impact on the behavior of other players. MFG supposes that the rational agents are indistinguishable and individually have a negligible influence on the game, and that each individual strategy is influenced by some averages of quantities depending on the states of the other agents. A very nice introduction to the theory of MFGs is supplied in the notes of [Cardaliaguet \(2010\)](#), including theoretical results on the existence and uniqueness of classical solutions, and also discussions on weak solutions.

MFG has a wide range of potential applications in economics. In macroeconomics, it has been applied to the studies that connects represent agent's optimization and the dynamics of macro interests, such as the income distribution ([Achdou et al., 2022](#)). It also allows heterogeneous settings, such as the heterogeneous-agent model ([Krusell and Smith, 1998](#)). Literatures also attempt to model financial problems using MFG. [Brunnermeier and Sannikov \(2016\)](#) compare the historical evolutions of macroeconomic and finance models, arguing that properly framed, the analysis of continuous time stochastic models should provide a unifying thread for these subfields of economics which so far, developed in parallel.⁵⁶ To this end, the authors introduce models of the economy comprising households maximizing consumption like in classical macroeconomic growth models, as well as investors trading in financial markets. Some applications have been discussed, including trade crowding ([Cardaliaguet and Lehalle, 2018](#)) and crypto mining ([Li et al., 2019](#)).

In many interesting situations in financial studies, it is important to allow for systematic risks (or systematic/common shocks). Such applications call for a more general framework in theory. Fortunately, the MFG

⁵⁶This is also reviewed by [Carmona \(2020\)](#).

system can be written in the most general case in terms of a so-called “Master Equation” (Cardaliaguet et al., 2019). The master equation is an equation on the space of measures; i.e. it is an equation that is set in infinite-dimensional space. The logic why the problem with aggregate uncertainty becomes infinite-dimensional is that the cross-sectional distribution across agents becomes a state variable in agents’ dynamic programming problems and that distribution is an infinite-dimensional object.⁵⁷ The master equation is first introduced by Lions (2011). The most related research advances include the proof of the existence and uniqueness of a classical solution to the master equation (Cardaliaguet et al., 2019), monotonous solutions in several specific cases of common shocks (Bertucci, 2021), the case without idiosyncratic but with Brownian-type common shock (Cardaliaguet and Souganidis, 2020), and the corresponding weak solutions (Cardaliaguet and Souganidis, 2021).

The relationship between MFGs and the master equation. There are two lines for understanding the relationship between the two: The first one is in line with the development of the theory, whereas the second is relatively smoother from the perspective of applications in economics.

Consider the first logic. A MFG system is enough to handling situations where heterogeneous players solve optimal decisions even with idiosyncratic shocks and the crowd evolves dynamically. Although they can also be rearranged in the master equation form, the couple of PDEs shows clearly the respective dynamics of J and m , and fits mathematical tools for forward-backward PDEs. Therefore, the MFG system is usually described by the HJB equation together with the law of motion (FP equation). However, when the shock is not idiosyncratic but universal, it directly adds uncertainty to the distribution. Thus the system of PDEs both becomes stochastic as shown in (24). Even worse, the appearance of the extra “penalty” term makes the respective dynamics unclear in the separate PDEs. Therefore, the convenience of the coupled-PDEs form no longer exists. To this end, the master equation is presented as a more generalized representation that applicable to aggregate shocks, while at the cost of the value equation needing to be defined over infinite dimensions.

The second logic is more in line with economic research. Many theoretical frameworks consider the representative agent who solves optimal choices under system states with shocks. The distribution of the crowd m_t could be one of the system states and enters the value function as an argument. From the formal perspective, we still totally differentiate the value function to obtain the “HJB equation”. The thing is that m_t is a function itself and dm_t is actually the law of motion. Ignoring the technical details for the moment, we notice that the total differential involves the law of motion, and the resulting new “HJB equation” is essentially (at least formally) the master equation.

The two understanding logics also make slight differences in the derivations of the master equation. The total differential approach seems natural while faces with more rigor considerations, whilst the former aims to rearrange the PDEs and find the solution to the MFG system. The master equation is finally the equation that characterize the solution.

OA3.2 Derivation of the Master Equation

Relevant definitions and requirements. In the main text, we mentioned the notations, $\frac{\delta J}{\delta m}$ and $\frac{\delta^2 J}{\delta m^2}$, i.e., the first and second Fréchet derivatives applied in infinite dimension w.r.t. the density m . They appear to have extra arguments, i.e.,

$$\frac{\delta J}{\delta m} = \frac{\delta J}{\delta m}(w, w', m), \quad \frac{\delta^2 J}{\delta m^2} = \frac{\delta^2 J}{\delta m^2}(w, w', w'', m). \quad (\text{OA.8})$$

One can roughly compare them with Jacobian and Hessian in the finite-dimensional case respectively. To gain rigorous requirements of the derivatives in a more generalized way, we introduce the Monge-Kantorovich dis-

⁵⁷This is also reviewed in the online Appendix of Achdou et al. (2022).

tance first. The set $\mathcal{P}(\mathbb{R})$ of measures on \mathbb{R} is endowed with the Monge-Kantorovich distance,

$$d(m, m') = \sup_{\Xi} \int_{\mathbb{R}} \Xi(y) d(m - m')(y), \quad (\text{OA.9})$$

where the sup term is taken over all Lipschitz continuous maps $\Xi : \mathbb{R} \mapsto \mathbb{R}$ with a Lipschitz constant bound by 1.⁵⁸ Then the formal definitions are provided below, which also follow [Cardaliaguet et al. \(2019\)](#).

Definition 1. We say that $J : \mathcal{P}(\mathbb{R}) \rightarrow \mathbb{R}$ is C^1 , if there is a continuous map $\frac{\delta J}{\delta m} : \mathcal{P}(\mathbb{R}) \times \mathbb{R} \rightarrow \mathbb{R}$ such that, for any $m, m' \in \mathcal{P}(\mathbb{R})$,

$$\lim_{s \rightarrow 0^+} \frac{J((1-s)m + sm') - J(m)}{s} = \int_{\mathbb{R}} \frac{\delta J}{\delta m}(m, y) d(m' - m)(y). \quad (\text{OA.10})$$

Definition 2. We say that $J : \mathcal{P}(\mathbb{R}) \rightarrow \mathbb{R}$ is C^2 , if for a fixed $y \in \mathbb{R}$, the map $m \mapsto \frac{\delta J}{\delta m}(m, y)$ is C^1 . Moreover, denote its derivative as $\frac{\delta^2 J}{\delta m^2} : \mathcal{P}(\mathbb{R}) \times \mathbb{R} \times \mathbb{R} \rightarrow \mathbb{R}$. It satisfies

$$\frac{\delta J}{\delta m}(m', y) - \frac{\delta J}{\delta m}(m, y) = \int_0^1 \int_{\mathbb{R}} \frac{\delta^2 J}{\delta m^2} \left((1-s)m + sm', y, y' \right) d(m' - m)y' ds. \quad (\text{OA.11})$$

*Derivation. We adopt the second logic mentioned in Appendix [OA3.1](#), which shares the similar idea with [Bilal \(2023\)](#). The key observation is to apply the Itô's Lemma to the value function J_t and especially note the time-dependence of m_t . As the time-dependence of w_t and A_t have been accounted in the HJB equation, the rest time-dependence could be replaced by the dependence on the distribution m .

$$dJ_t = \left\langle \frac{\delta J}{\delta m}, dm_t \right\rangle + \frac{1}{2} \langle dm_t | \frac{\delta^2 J}{\delta m^2} | dm_t \rangle, \quad (\text{OA.12})$$

where the inner product is defined in the appropriate functional space, $\langle f(x), g(x) \rangle = \int f(x)g(x)dx$. $\langle h | f(x, x') | g \rangle = \langle \langle f(x, x'), h(x) \rangle, g(x') \rangle$. Substituting into the HJB equation, we obtain

$$\phi J(w, m, A) dt = \left\{ \begin{array}{l} \mathcal{U}(w, m) + L(w)[J] + \mu^A A \frac{\partial J}{\partial A} + \frac{\partial}{\partial w} g(w)v(w) \\ + \int \frac{\delta J}{\delta m}(w, w', m) L^*(w')[m] dw' \\ + \frac{1}{2} \int \int \frac{\delta^2 J}{\delta m^2}(w, w', w'', m) \frac{\partial g(w')m(w')}{\partial w'} \frac{\partial g(w'')m(w'')}{\partial w''} dw' dw'' \\ - \left(v(w) + \int \frac{\delta J}{\delta m}(w, w', m) \frac{\partial g(w')m(w')}{\partial w'} dw' \right) dZ_t. \end{array} \right\} dt \quad (\text{OA.13})$$

By the definition of the penalty, v guarantees that J is adapted with respect to the filtration generated by the shock, i.e., the same idea as Lemma 1, v lets the diffusion term zero. Substituting into [\(OA.13\)](#), the master equation [\(25\)](#) is derived.

*Linking with the derivation process in literature. As mentioned in Section 4, a more standard and rigorous way to derive the master equation in MFG theory papers, e.g., as [Cardaliaguet et al. \(2019\)](#) does, is to make a change of variable, $\tilde{J}(w) = J(w + g(w)Z_t)$, $\tilde{m}(w) = m(w + g(w)Z_t)$,⁵⁹ implying that \tilde{m} is the conditional law of the motion

⁵⁸As the online Appendix of [Achdou et al. \(2022\)](#) also discusses, in the theoretical literatures, the space is often specified as the n -dimensional torus \mathbb{T}^n rather than \mathbb{R}^n . The only reason is to sidestep the discussion of boundary conditions in the space dimension.

⁵⁹As [Cardaliaguet et al. \(2019\)](#) illustrates, the formally equivalent but more rigorous definition of \tilde{m} is to let it be a push-forward of m_t by the shift $w \mapsto w - g(w)Z_t$. This definition is completely licit. m_t reads as a conditional measure given the aggregate shock. Therefore, since conditioning consists of freezing the shock Z_t , such a shift is considered as a “deterministic” mapping.

of the wealth process $w_t - g(w_t)Z_t$. When Z_t is relatively small, there is an approximation:

$$d(w - g(w)Z_t) = [f(w) - Z_t g'(w)dw]dt \approx f(w)dt.$$

Then \tilde{m}_t satisfies:

$$d\tilde{m}_t = -\frac{\partial}{\partial w} (\tilde{f}(w, \tilde{m})\tilde{m}_t(w)) dt, \quad (\text{OA.14})$$

where $\tilde{f}(w) = f(w + g(w)Z_t)$, and the tilde scripts below indicates similar meanings w.r.t. different functional without specific instructions. The HJB equation similarly becomes

$$\phi\tilde{J}_t dt - d\tilde{J}_t = \left[\tilde{V}(w, \tilde{m}) + \tilde{f}(w, \tilde{m}) + \mu^A A \frac{\partial \tilde{J}_t}{\partial A} \right] dt + \tilde{v}dZ_t = \left[\tilde{V}(w, \tilde{m}) + \tilde{f}(w, \tilde{m}) + \mu^A A \frac{\partial \tilde{J}_t}{\partial A} \right] dt + d\tilde{M}_t, \quad (\text{OA.15})$$

where $\tilde{v}_t(w) = \tilde{g}(w)\partial_w \tilde{J} + v_t(w + g(w)Z_t)$. Denote the realization of shocks generated by $(Z_t)_{t \geq 0}$ as an information set $(\mathcal{F}_t)_{t \geq 0}$. Then $(\tilde{M}_t(w))_{t \in [0, T]}$ is an $(\mathcal{F}_t)_{t \in [0, T]}$ martingale. (24), the boundary conditions $\tilde{m}_0 = m_0$, and \tilde{J}_∞ bounded, jointly construct the standard expression of the MFG with aggregate shocks.

Discussion on the solution to the master equation. The classical solution to the second order master equation is, naturally, a map $J(w, m, A) : \mathbb{R} \times \mathcal{P}(\mathbb{R}) \times \mathbb{R} \mapsto \mathbb{R}$, which satisfies all the requirements in the relevant definition part in this section, and satisfies the master equation. The definition of the weak solution introduced by [Cardaliaguet and Souganidis \(2021\)](#) focuses on the master equation with no idiosyncratic shock, i.e., the case in our paper.⁶⁰ The relationship between the weak solution and the classical solution is that if J^ is a weak solution, and $J, \frac{\partial J}{\partial w}, \frac{\delta J}{\delta m}, \frac{\partial^2 J}{\partial w^2}, \frac{\delta^2 J}{\delta m^2}$ and $\frac{\partial}{\partial w} \frac{\delta}{\delta m} J$ are continuous in w and m . Then J^* is a weak solution when the classical solution J^* can be expressed as J^* combining with a continuous function of $m, c^*(m)$, i.e.,

$$J^*(w, m, A) = J^{**}(w, m, A) + c^*(m). \quad (\text{OA.16})$$

It is because the definition of the weak solution actually characteristics $\frac{\partial J}{\partial w}$ and not J . Under proper assumptions, the existence and uniqueness of the weak solution have been proved in literature.

OA3.3 Implications Under Heterogeneity

Consider the implications, i.e., the propositions in Section 3, under heterogeneity. Similar with the homogeneous case, the aggregate equilibrium value of tradable tokens is

$$\int_i x_i^* di = \left(\frac{1 - \alpha}{r_t - c_t} \right)^{\frac{1}{\alpha}} N_t A_t \int_{\tilde{W}} \bar{U}_t(w_t) m(w_t) dw_t \equiv \left(\frac{1 - \alpha}{r_t - c_t} \right)^{\frac{1}{\alpha}} N_t A_t M_{1t}, \quad (\text{OA.17})$$

where $\bar{U}_t = \mathbb{E}[U(u_{i,t}, w_t) | w_t]$ is a function of w_t , $\arg_{w_t} \{\bar{U}(w) > U_0\} = \tilde{W} \subset W$. Then $\Theta^* = 1 - \left(\frac{1 - \alpha}{r - c} \right)^{\frac{1}{\alpha}} \frac{N A M_1}{q^*} = \Theta^*(r)$, where r fits the fixed point problem (11). Then we can see that the rest of proof are the same as Proposition 2 but only replace \bar{U} with M_1 . It is with no extra difficult to prove (17) under heterogeneity. Further, note that the additional terms in (25) does not enter the optimization, also the optimal q^* is not involved in extra terms. The derivation of pricing DE then still starts from the market clearing condition (further settings in Section 3.2 are

⁶⁰The solution is solved by the Hilbert space approach introduced by [Lions \(2011\)](#), the detailed notion of the weak solution is provided in [Cardaliaguet and Souganidis \(2021\)](#). Here we no longer repeat existing work.

adopted):

$$\begin{aligned}
0 &= \mu + r(\Theta) - c + \frac{\partial \Psi}{\partial n} + PQ_1 \sigma^2, \\
0 &= (1 - \alpha) \int_{\hat{W}} \left(\frac{NA\bar{U}(w)}{q(w)} \right)^\alpha \frac{\partial_w J}{\partial_{ww} J} m(w) dw + \left(\mu + \frac{\partial \Psi}{\partial n} \right) \int_{\tilde{W}} \frac{\partial_w J}{\partial_{ww} J} m(w) dw + PQ_2 \sigma^2,
\end{aligned} \tag{OA.18}$$

where $Q_1 + Q_2 = Q$, $\hat{W} = W \setminus \tilde{W}$. The second equation refers to the aggregation of agents with zero staking. Denote the two integrals as $M_2 = M_2(A; m)$ and $M_3 = M_3(A; m)$, respectively, and sum up the two equations, we obtain

$$0 = (\mu + \Psi_n)(1 + M_3(A)) + r(\Theta) - c + (1 - \alpha)M_2(A) + PQ/S\sigma^2. \tag{OA.19}$$

Then, apply Itô's Lemma to P_t and substitute the resulting (μ, σ) into the above equation, the pricing PDE is obtained and is similar with (20) but only involves M_s , $s = 1, 2, 3$ (M_3 enters Θ). The rest process is all similar with the baseline. Finally, $V(A)$ still satisfies an ODE. Further, M_2 and M_3 enters the "flow" term of the PDE, whereas M_1 is independent of A . Therefore, they do not qualitatively affect the relationship between the drift and the staking ratio.

To generate an intuitive understanding, we consider two specific cases. First, when all the agents have "extra" wealth to invest in staking, then $\hat{W} = \emptyset$ and $M_2 = M_3 = 0$, then (OA.19) is in the same form as (18). Second, if the transaction need is also linear in wealth, e.g., $U(u_{i,t}, w_{i,t}) = u_{i,t} w_{i,t}$, then it is not difficult to show that for agents with wealth $w_{i,t} \in \hat{W}$, $q(w_{i,t}) = x(w_{i,t}) = c_0 w_{i,t}$, where $c_0 > 0$ is independent of w , and $\partial_w \left(\frac{\partial_w J}{\partial_{ww} J} \right) = 0$. Denote $\int_{\hat{W}} E(u_{i,t}^\alpha | w) m(w) dw = \hat{M}_2$, $\int_{\hat{W}} m(w) dw = \hat{M}_3$, then the summation of the two equations in (OA.18) yields

$$0 = (\mu + \Psi_n)(1 + \hat{M}_3) + r(\Theta) - c + c_1(1 - \alpha)(NA)^\alpha \hat{M}_2 + PQ/S\sigma^2. \tag{OA.20}$$

Finally, the violation of UIP is directly obtained rearranging agents' optimal control and the aggregation across populations, and even without the assumption of log utilities. For agents with wealth $w \in \hat{W}$, they do not participate in staking and thus their optimal control problems do not involve r , i.e. their marginal excess return is the price appreciation plus the marginal transaction convenience. For agents with wealth $w \in \tilde{W}$, $\lambda_t = -\frac{\partial \Psi}{\partial n} + q_t^* \sigma^2 I$, which is completely in the same form as the baseline. As an aggregation, the system excess return of staking is

$$\lambda_t = -\Psi_n + \sigma^2 \int_{\tilde{W}} q^*(w) I(w) m(w) dw, \tag{OA.21}$$

where $I(w) = \frac{\partial_{ww} J}{\partial_w J}(w) > 0$, $q^*(w) \geq 0$, $-\Psi_n$ is the marginal convenience of numéraire and is positive.

OA3.4 Discussion on the Properties of Stationary Distribution

To generate a better understanding of the stationary $m(w)$ (6), we consider the case when $\beta \rightarrow 1$, i.e., the transaction needs tends to be linear in wealth. $\frac{w^{\beta-1}}{\beta-1} \rightarrow \log(w)$ and thus

$$m(w) \rightarrow \bar{m}(w) = \bar{c}_0 \frac{1}{w^{(\phi-k_2)\mathcal{V}}} = \frac{[(\phi - k_2)\mathcal{V} - 1] w^{[(\phi-k_2)\mathcal{V}-1]}}{w^{(\phi-k_2)\mathcal{V}}}, \tag{OA.22}$$

where the upper bar $\bar{\cdot}$ indicates the case at the limit. $\bar{m}(w)$ is a Pareto distribution with the tail parameter $(\phi - k_2)\mathcal{V} - 1$.

According to the properties of the tail parameter, when $(\phi - k_2)\mathcal{V} \leq 1$, there is no stationary situation. Considering the economic meaning of k_2 and \mathcal{V} , it corresponds to the situations that the benefits from on-chain activities or price appreciation are so large that the whole crowd continues to earn money. When $0 < (\phi - k_2)\mathcal{V} - 1 \leq 1$, the stationary distribution has infinite expectation, implying that the wealthier earn more from beneficial

on-chain activities and price appreciation. When $(\phi - k_2)\mathcal{V} - 1 > 1$, the distribution has a finite expectation. The general case can be seen as a slight transformation of the Pareto distribution, which could roughly have similar different situations that corresponding to different on-chain convenience and price fluctuations.

On the other hand, the Pareto case can be easily solved by substituting $\beta \rightarrow 1$ into (A.9). Then it indicates that in expectation among all the types, the wealth corresponding to transaction benefits changes linearly. Then by letting $h = m/w^2$, we obtain an ODE, $0 = a_2 w^2 h''(w) - a_1 w h'(w) + a_1 h(w)$, which finally results in a Pareto p.d.f. Since it is widely known that when the wealth of all people changes linearly, the resulting distribution by the law of motion follows the Pareto distribution, the above property also shows the consistency of the form of the general case. Also, it is worth pointing out that the general distribution has no contradiction with existing studies. Here, each agent's wealth still changes linearly. However, the slope varies among the crowd, which is affected by the user type $u_{i,t}$, whereas the randomness of $u_{i,t}$ is not independent on wealth. This cause the aggregation among populations to perform a slight difference from Pareto distribution.

OA3.5 Extended Discussion on the Feedback Effect

In the beginning of our setup, we introduce the feedback effect, which captures the “ideal” efforts of staking in incentivizing participation of the consensus or increasing the security level, etc., and thus enters the growth dynamic of platform productivity. The main relevant interest is how does the feedback effect influence token pricing. In Section 3, we have obtained the general positive relationship between staking ratio and expected price drift, which are both functions of the platform productivity (and some additional static arguments). Interestingly, the positive relationship exists no matter whether there is a feedback effect, but leads to different magnitudes of impact. Such a comparison is meaningful, since the feedback effect is not necessarily present in every stakable project. Also, it is somewhat difficult to verify its existence and size in practice. Then, the comparison shows general implications of that holds despite the existence or absence of feedback effects.

Further, the different magnitudes of impact are explained by two forces, in which the feedback force is that higher staking ratio leads to a higher drift of platform productivity, and then enters the price drift according to Itô's Lemma. Knowing such an extra benefit, agents will be slightly tilted towards staking in the on-chain trade-off. Thus, we see from Figure 1 that the equilibrium staking ratio is different under the same platform productivity. Figure OA.2 (A) shows such a variation more clearly. On the other hand as Subplot (B) shows, the aggregate on-chain wealth naturally increases with platform productivity, which is a corollary of the positive drift. The higher staking ratio is associated with higher drift, implying that there is more wealth allocated in as the platform grows.

The above two findings are also meaningful for discussing the feedback effect. However, it may rely on more assumptions or relatively narrow parameter choices. For the staking ratio, the setup of agents should not be too simplified to allow them to be able to anticipate the feedback effect, i.e. the growing platform, on themselves. If the utility is logarithmic and the transaction need is linear, then there would be no incentive to hedge against the changing investment opportunities presented by the dynamics of A , also they would be too myopia to see the benefits of future A growth. This setup would result in two overlapping curves for the numerical simulation of Subplot (A). As for the impact on the aggregate allocation, it generally holds that V increases with A , and when A is sufficiently large, the allocated wealth with feedback effects is larger, shown in Subplot (B). In periods where A is small, i.e., generally the initial phase of the platform, however, we observe in numerical simulations that platforms with feedback effects may instead have relatively small total wealth. This echoes the similar logic with the first force, i.e., there is a seesaw effect between already allocated wealth and potentially entering wealth. This is also comprehensively discussed in Cong et al. (2021b). The more in-depth discussion is however beyond the main focus of the present paper.

Overall, when staking is truly involved in building the platform rather than a purely speculative choice, with agents realizing that the platform development is beneficial to them, this feedback effect appears to work, and

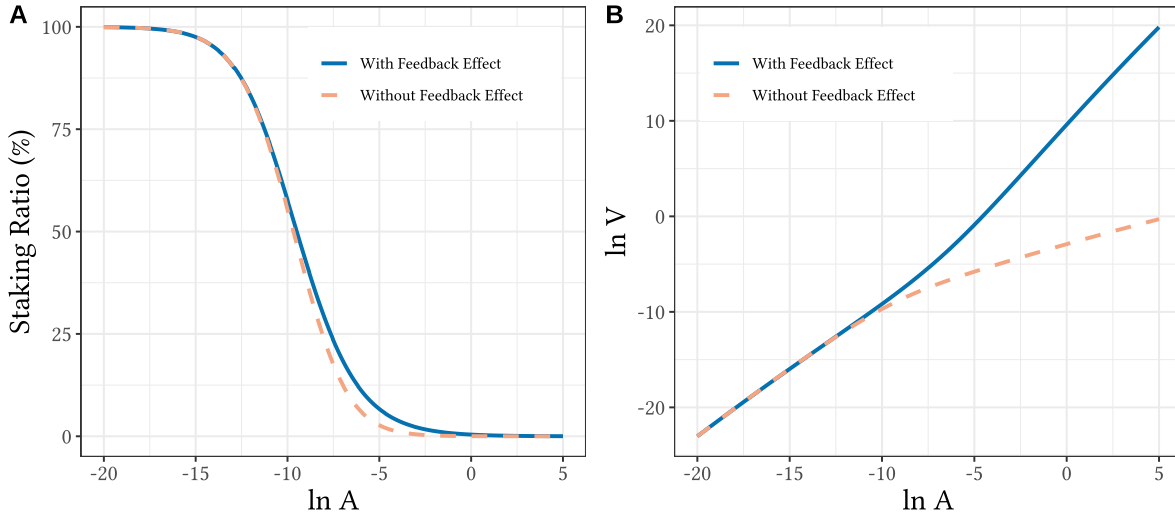


Figure OA.2: Platform productivity, staking ratio and aggregate on-chain wealth.

This plot shows how do the staking ratio and the aggregate on-chain wealth endogenously vary under different levels of platform productivity. The x-axis is the log productivity, $\ln A$. Subplot (A) and (B) show the corresponding curves of staking ratio and log on-chain wealth $\ln V$, respectively. The blue lines show the situations with feedback effects, whereas the orange dashed line are the situations without feedback.

brings a greater influx of on-chain wealth to the platform, especially for well-developed platforms.

In addition, there are some different way to model the feedback effect. For example, since the growth of platforms may be accompanied by a broadening of usage scenarios, this effect can enter the differences between on-chain and off-chain convenience. It is worth pointing out that although we do some comparison the presence and absence of the feedback, however, our primary focus is still on how the on-chain actions are shaped in different platform states when there is such an effect.

OA3.6 Robustness in Sub-samples: Bulls and Bears

Table OA.1 A common concern related to pricing factors is the different predictability in bulls and bears. Fortunately, our data set includes a complete bull and bear market cycle. Overall speaking, the cryptocurrency market was roughly in a bull market in 2020 and 2021, and entered into a bear market in the end of 2021. A more precise and simple way to classify market bulls and bears refers to Lunde and Timmermann (2004) with the corresponding amplitude thresholds set to 35% (bulls) and 25% (bears). We use Bitcoin price as the indicator of the market, which is a common approach in practical investments. Also, as Ethereum is playing an increasingly important role, especially with its significant place in the staking economy, we alternatively use Ethereum price as the indicator for robustness. Figure OA.3 visualizes the segmentation of bulls and bears during the whole in-sample periods. We then regress the main empirical specification in Table 4 on sub-samples of bulls and bears. Columns (1)-(8) of Table OA.1 reports the regression results. In general, the estimated coefficients of $StakingRatio_{i,t-1}$ are all positive across bulls and bears that divided by different indicators, as well as different horizons (daily and weekly). This suggests that the implication that staking ratio positively predicts price appreciation generally holds in bulls and bears. It is worth noting that, however, the estimated value and significance are lower in bears.

OA3.7 Robustness in Subsamples: PoS Tokens and DeFi Tokens

As mentioned in the introduction, our model evolve both base layer pan-PoS staking mechanisms and higher layer DeFi stakable tokens. We model the common features and introduce several implications. In the empirical analysis, we use a sample containing the tokens from both the two layers. To empirically illustrate that these

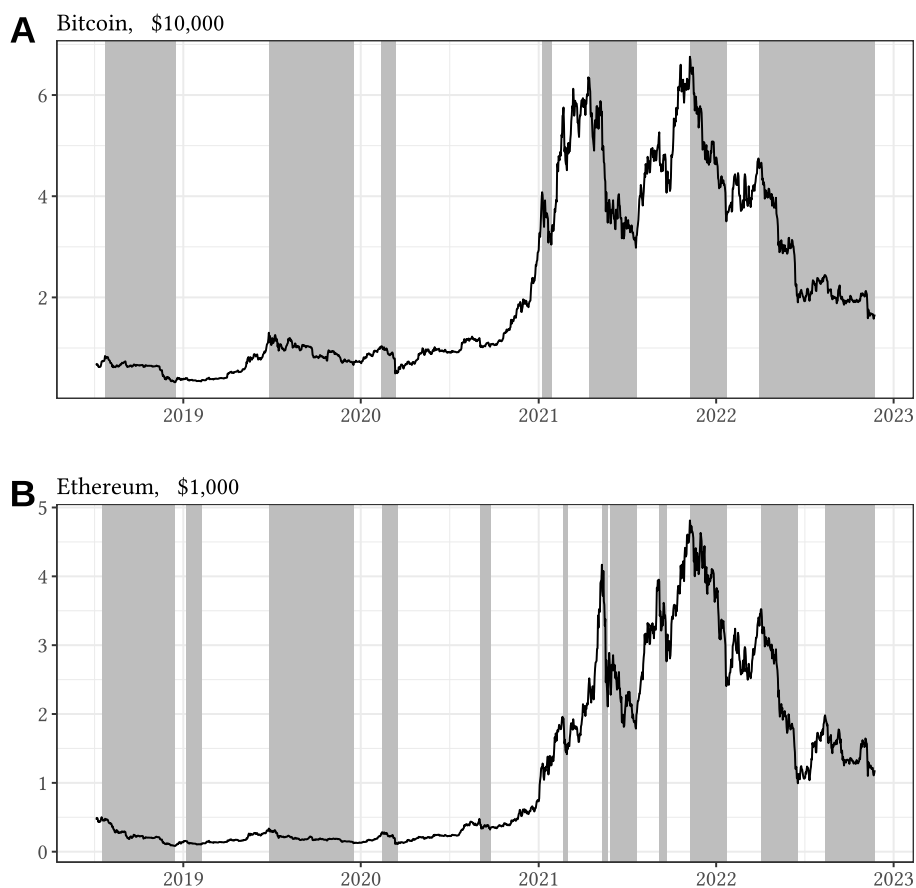


Figure OA.3: Identification of bull and bear markets.

Grey background denotes detected bear periods. In Subplot (A) and (B), we use the price of Bitcoin and Ethereum as indices, respectively. The identification algorithm refers to [Lunde and Timmermann \(2004\)](#) with the corresponding amplitude thresholds set to 35% (bulls) and 25% (bears).

implications are common for both the pan-PoS and DeFi tokens, we divide our sample into two subsets based on the category of tokens, and repeat the main tests of Table 4.

Columns (9)-(12) of Table OA.1 reports the results of these robustness tests. We regress pan-PoS and DeFi sub-samples on both daily and the weekly data sets. The dependent is log price change $r_{price_{i,t}}$ on the staking ratio in the previous week. The estimated coefficients of the staking ratio are both positive and consist with our main empirical result, which suggest that the staking ratio predicts price appreciation. The daily data shows both significant estimations, whereas in the weekly data, the statistical power is lower. This also consists with the main regression in Table 4. Also, it could be partly explained by the small sample size since the raw weekly sample set is further divided into two subsamples.

Table OA.1: Robustness test for Table 4: Staking ratio and token prices.

This table presents the robustness test on the analysis of how the staking ratio predicts token price appreciation. The regression model Column (2) of Table 4, in which the main independent is the staking ratio of the previous period, $StakingRatio_{i,t-1}$, and the dependent is the price appreciation, $r_{price_{i,t}}$. The difference is that we replicate the test on subsets of bulls, bears, PoS tokens, and DeFi tokens. The bulls and bears are detected based on (2004)'s algorithm. Due to the lack of a recognized index for the cryptocurrency market, we refer to the common approach used in practice as a market indicator. We also repeat with Ethereum as an indicator for robustness. The detected bulls and bears are visualized in Figure 1 and DeFi tokens are sorted based on tokens' nature. We also do the test in different horizons and with fixed effects to show the robustness. Clustered in both token-specific and time dimensions are reported in parentheses. ***, **, * indicate statistical significance at the 1%, 5% and 10% level, respectively.

Sub-sample:	Dependent:		Bull-Bear						Daily			
			Daily				7-Day				Daily	
			Bitcoin as Indicator		Ethereum as Indicator		Bitcoin as Indicator		Ethereum as Indicator			
	Bull	Bear	Bull	Bear	Bull	Bear	Bull	Bear	Bull	Bear	pan-PoS	DeFi
	(1)	(2)	(3)	(4)	(5)	(6)	(7)	(8)	(9)	(10)		
$StakingRatio_{i,t-1}$	0.040*** (0.009)	0.010 (0.012)	0.025** (0.011)	0.018 (0.012)	0.290*** (0.098)	0.017 (0.094)	0.135 (0.091)	0.124 (0.109)	0.028** (0.012)	0.019* (0.010)		
$\hat{\beta}_{i,t}$	-0.002 (0.003)	0.000 (0.004)	0.004 (0.003)	-0.011** (0.005)	-0.051 (0.043)	-0.016 (0.025)	0.034 (0.021)	-0.169* (0.082)	-0.003 (0.003)	-0.002 (0.003)		
$\log(Cap)_{i,t-1}$	-0.006*** (0.002)	-0.006*** (0.002)	-0.004*** (0.001)	-0.009*** (0.003)	-0.044*** (0.012)	-0.050*** (0.016)	-0.032*** (0.008)	-0.069*** (0.020)	-0.004*** (0.001)	-0.010** (0.002)		
$r_{price_{i,t-1}}$	0.085* (0.049)	-0.055 (0.098)	0.019 (0.027)	0.044 (0.130)	-0.116** (0.045)	-0.004 (0.075)	-0.053 (0.039)	-0.195 (0.125)	0.066 (0.046)	0.098** (0.040)		
$\Delta Network_{i,t-1}$	0.203*** (0.062)	0.353* (0.178)	0.198*** (0.065)	0.412** (0.190)	0.524 (0.314)	-0.284 (0.332)	0.421 (0.262)	-0.107 (0.357)	0.158*** (0.047)	0.259** (0.111)		
$a_{i,t-1}$	0.053 (0.035)	0.151 (0.116)	0.052* (0.027)	0.114 (0.121)	0.448* (0.245)	0.224 (0.771)	0.230 (0.198)	0.253 (0.895)	0.049 (0.044)	0.940*** (0.227)		
$Whale_{i,t-1}$	-0.018 (0.012)	0.006 (0.022)	-0.011 (0.013)	-0.011 (0.016)	-0.130 (0.120)	-0.107 (0.139)	-0.094 (0.096)	-0.141 (0.125)	-0.008 (0.006)	0.004 (0.024)		
$NotLaunched_{i,t}$	0.031*** (0.007)	0.001 (0.005)	0.021*** (0.005)	0.016 (0.014)	0.286*** (0.071)	0.075*** (0.025)	0.151*** (0.043)	0.270 (0.168)		0.006 (0.007)		
$Y_{i,t}^0$	0.007* (0.004)	0.007 (0.006)	0.005 (0.003)	0.012 (0.008)	0.078** (0.027)	0.046 (0.049)	0.038 (0.025)	0.115 (0.070)	0.010* (0.004)	0.007* (0.004)		
Token FE	Yes	Yes	Yes	Yes	Yes	Yes	Yes	Yes	Yes	Yes		
Time FE	Yes	Yes	Yes	Yes	Yes	Yes	Yes	Yes	Yes	Yes		
Observations	5,692	4,299	6,204	3,787	795	639	897	537	5,529	6,173		
R ²	0.382	0.577	0.406	0.529	0.477	0.546	0.535	0.496	0.579	0.547		

OA3.8 Staking Ratio and Returns

The predictability of price appreciation suggests that high staking ratio tokens should bring excess returns over the low ones. We test it by creating a long-short strategy, that is, sort the tokens by their staking ratio by the end of previous period, equal-weighted long the top 50% and short the bottom. The allocation is adjusted every week. Figure OA.4 and Table OA.2 document that the portfolio provides relatively stable positive cumulative returns with a Sharpe ratio of 0.865. To show that this is not another manifestation of the size effect, we test the same sorted strategy within the large-cap and small-cap token groups, respectively. The implication remains qualitatively robust. Table OA.2 suggests that the large-cap group performs weaker. It is partly because the staking ratio of these tokens are relatively low in general, and thus with smaller differences among each other. The corresponding effect is therefore minor.⁶¹ Considering the limitations on shorting in practice, we also test the long-only strategies, i.e., borrow US dollars and equal-weighted long top (bottom) 50% tokens sorted by staking ratio. The top group outperforms the bottom group, and also the full-sample benchmark.⁶²

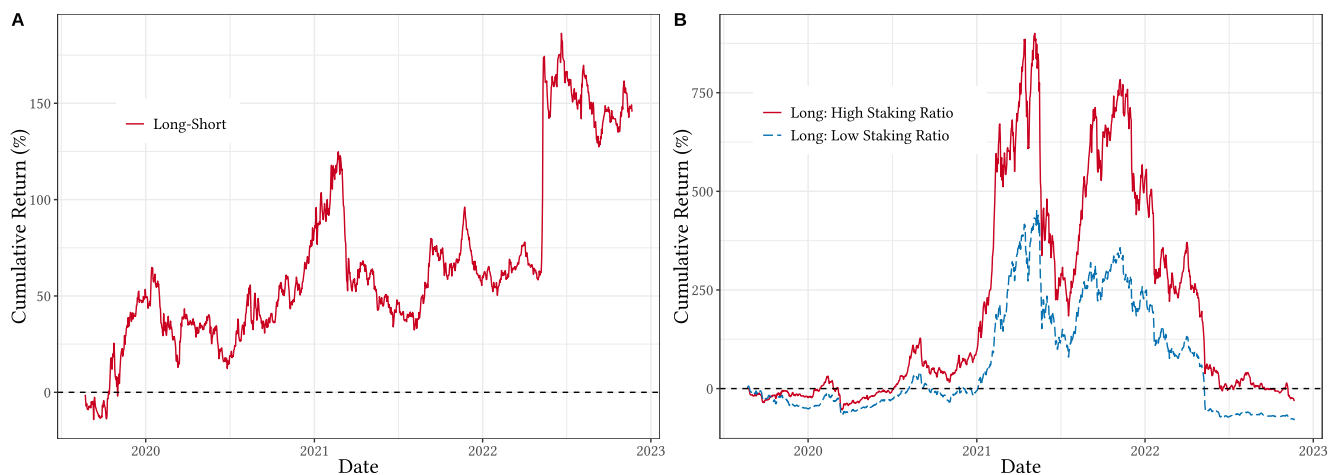


Figure OA.4: Cumulative returns of staking ratio sorted portfolios.

This figure corresponds to Hypothesis. Panel A shows the long-short portfolio cumulative return. Panel B shows the long-only strategies. The portfolios are constructed as Section 6.2 describes.

OA3.9 Additional discussion on UIP and Crypto Carry

UIP with in-sample tokens as local currencies. Table OA.3 repeats the specification of Table 5, implying that the UIP is generally violated within the token market, rather than only comparing with mainstream cryptocurrencies or fiat moneys.

Summary statics of crypto carry. Table OA.4 summarizes the annualized carry and excess return of all tokens in our sample. Sample means and standard deviations are reported. We also include the US Dollar as one of the assets for which the carry and excess return are, by definition, equal to zero.

Crypto carry trade: cumulative returns. We visualize the cumulative returns of mentioned strategies in Figure OA3.9. Panel (a) shows the long-short strategies. The red curve in Figure plots the cumulative return of such a carry trade strategy. It shows an overall increase and large cumulative returns. Especially, in the cryptocurrency market where price volatility is huge, such a strategy performs a relatively smooth growth, implying the carry premia always exists. The gray line shows the performance of the same carry portfolio, but without staking. That is, for long tokens, we do not stake them, and for short assets, we also do not compensate for the staking reward

⁶¹We also use Bitcoin as base asset

⁶²We repeat this test using bitcoin denomination to cancel out the crypto market trend, the main results in Panel A remains robust.

Table OA.2: Sorted Portfolio performance by staking ratio.

This table reports the statistics of portfolio performance. The upper panel reports the results of the long-short carry strategy, including long top 50% high staking tokens and short bottom 50% across the full sample, i.e., corresponding to Figure OA.4, and same strategies but within top 50% large-cap and small-cap groups, respectively. The lower panel reports equal-weighted long strategies, including the full-sample benchmark, long top 50% high staking ratio tokens, and long bottom 50%. The portfolios are rebalanced each week. For each strategy, the annualized mean, standard deviations, skewness, kurtosis, maximum drawdown (MDD) and Sharpe ratio are reported.

Strategy	Mean (Annual, %)	St.dev. (Annual, %)	Skewness	Kurtosis	MDD (%)	Sharpe Ratio (Annual)
<i>Long-short Strategy ():</i>						
Full Sample	36.081	41.731	2.273	27.582	41.135	0.865
Within Large-Cap Group	18.575	56.857	5.881	104.942	70.057	0.327
Within Small-Cap Group	40.052	62.720	0.588	5.177	40.065	0.639
<i>Long Strategy:</i>						
EW All assets	15.577	78.244	-1.576	7.672	92.934	0.199
EW High-Staking Ratio	22.873	80.737	-1.161	5.042	93.013	0.283
EW Low-Staking Ratio	-13.207	79.823	-1.724	9.547	96.115	-0.165

rate. The strategy also exhibits increasing cumulative returns, which implies that the carry strategy earns excess returns not only from carry (staking reward) but also from price appreciation. Moreover, the blue line reports the performance of the same carry portfolio, but is rebalanced every month. It exhibits fewer returns than 1W-carry trade. There are two potential explanations. To compare with the benchmark of the equal weighted long strategy, also consider the potential short-selling restrictions, we test the performance of the long-only strategies as Panel (b) shows. Since the market fluctuations are not hedged, all the strategies are volatile and move in co-trends. However, the strategy that go long top 50% tokens with high carry still provide a relatively better performance with a larger Sharpe ratio as Table 6 reports in the main text.

References for Online Appendices

- ACHDOU, YVES, JIEQUN HAN, JEAN-MICHEL LASRY, PIERRE-LOUIS LIONS, AND BENJAMIN MOLL (2022): “Income and wealth distribution in macroeconomics: A continuous-time approach,” *The review of economic studies*, 89 (1), 45–86.
- AUGUSTIN, PATRICK, ROY CHEN-ZHANG, AND DONGHWA SHIN (2022): “Yield Farming,” Available at SSRN 4063228.
- BERTUCCI, CHARLES (2021): “Monotone solutions for mean field games master equations: continuous state space and common noise,” *arXiv preprint arXiv:2107.09531*.
- BILAL, ADRIEN (2023): “Solving heterogeneous agent models with the master equation,” Tech. rep., National Bureau of Economic Research.
- BRUNNERMEIER, MARKUS K AND YULIY SANNIKOV (2016): “On the optimal inflation rate,” *American Economic Review*, 106 (5), 484–89.
- CARDALIAGUET, PIERRE (2010): “Notes on mean field games,” Tech. rep., Technical report.
- CARDALIAGUET, PIERRE, FRANÇOIS DELARUE, JEAN-MICHEL LASRY, AND PIERRE-LOUIS LIONS (2019): “The master equation and the convergence problem in mean field games,” in *The Master Equation and the Convergence Problem in Mean Field Games*, Princeton University Press.
- CARDALIAGUET, PIERRE AND CHARLES-ALBERT LEHALLE (2018): “Mean field game of controls and an application to trade crowding,” *Mathematics and Financial Economics*, 12 (3), 335–363.
- CARDALIAGUET, PIERRE AND PANAGIOTIS SOUGANIDIS (2020): “On first order mean field game systems with a common noise,” *arXiv preprint arXiv:2009.12134*.
- (2021): “Weak solutions of the master equation for Mean Field Games with no idiosyncratic noise,” *arXiv preprint arXiv:2109.14911*.

Table OA.3: UIP violation: in-sample local currencies.

This table tests (H3a), i.e., the panel regression results of UIP test. In each row, we use a different asset as local currency and report the estimated coefficients of β with different data horizons. Estimated coefficients of β and the corresponding robust standard errors clustered by tokens are reported.

Local Currency	Horizon: 7-day			Horizon: 30-day			Local Currency	Horizon: 7-day			Horizon: 30-day		
	Coef., β	Std. Err.	R^2	Coef., β	Std. Err.	R^2		Coef., β	Std. Err.	R^2	Coef., β	Std. Err.	R^2
<i>Currency & mainstream cryptocurrencies.</i>													
US Dollar	-1.02	(0.044)	0.33	-1.12	(0.176)	0.11	Ethereum	-1.04	(0.033)	0.37	-1.09	(0.126)	0.12
Bitcoin	-1.02	(0.034)	0.37	-1.08	(0.134)	0.11							
<i>In-sample Tokens.</i>													
1inch	-0.92	(0.039)	0.54	-0.72	(0.159)	0.22	kyber	-1.03	(0.024)	0.25	-1.01	(0.086)	0.14
aave	-1.03	(0.029)	0.32	-1.14	(0.119)	0.13	livepeer	-0.92	(0.013)	0.51	-0.52	(0.053)	0.24
aion	-0.90	(0.102)	0.43	-0.24	(0.604)	0.22	lto	-0.95	(0.129)	0.44	-0.16	(0.331)	0.25
algorand	-1.00	(0.014)	0.50	-1.12	(0.132)	0.13	matic	-1.06	(0.021)	0.37	-1.12	(0.086)	0.14
ark	-1.00	(0.053)	0.52	-0.90	(0.196)	0.30	mina	-1.06	(0.026)	0.30	-0.39	(0.224)	0.10
avalanche	-1.13	(0.049)	0.31	-1.34	(0.195)	0.13	mirror	-0.99	(0.008)	0.67	-0.88	(0.034)	0.32
band	-1.01	(0.031)	0.32	-1.05	(0.128)	0.11	near	-1.10	(0.033)	0.32	-1.42	(0.161)	0.14
bifi	-1.01	(0.067)	0.34	-0.80	(0.308)	0.16	nem	-1.07	(0.039)	0.58	-1.29	(0.330)	0.34
binance-sc	-0.99	(0.019)	0.36	-1.00	(0.081)	0.12	neo	-0.86	(0.053)	0.53	-0.47	(0.289)	0.26
bitbay	-0.83	(0.068)	0.17	-0.40	(0.790)	0.07	nuls	-0.98	(0.077)	0.49	-1.30	(0.602)	0.17
cardano	-1.01	(0.027)	0.33	-1.02	(0.134)	0.10	oasis	-1.04	(0.034)	0.29	-1.12	(0.135)	0.12
cosmos	-1.06	(0.035)	0.37	-1.17	(0.139)	0.13	olympus	-1.00	(0.010)	0.83	-1.12	(0.034)	0.49
cronos	-1.03	(0.040)	0.29	-1.07	(0.172)	0.22	osmosis	-0.91	(0.028)	0.41	-0.48	(0.106)	0.25
curve	-1.05	(0.028)	0.33	-1.15	(0.120)	0.13	pancakeswap	-1.13	(0.018)	0.74	-1.44	(0.070)	0.51
dash	-0.88	(0.096)	0.42	-0.56	(0.343)	0.24	peakdefi	-1.02	(0.027)	0.54	-1.03	(0.102)	0.25
decred	-1.03	(0.034)	0.37	-1.05	(0.123)	0.11	polkadot	-1.05	(0.031)	0.35	-1.69	(0.275)	0.08
dfinity	-0.98	(0.019)	0.29	-0.84	(0.120)	0.17	qtum	-0.87	(0.036)	0.57	-0.56	(0.156)	0.30
dodo	-0.91	(0.027)	0.33	-0.57	(0.149)	0.14	secret	-1.13	(0.030)	0.32	-1.68	(0.180)	0.14
dydx	-0.91	(0.050)	0.27	-0.77	(0.122)	0.29	smartcash	-0.90	(0.070)	0.45	-0.51	(0.403)	0.25
elrond	-1.06	(0.028)	0.33	-1.19	(0.126)	0.14	snx	-1.05	(0.018)	0.61	-1.20	(0.086)	0.31
eos	-1.10	(0.033)	0.50	-1.36	(0.142)	0.23	solana	-1.09	(0.052)	0.32	-1.17	(0.182)	0.12
eth2.0	-1.04	(0.014)	0.42	-1.25	(0.059)	0.17	stafi	-1.01	(0.030)	0.31	-1.10	(0.158)	0.12
fantom	-0.89	(0.013)	0.47	-0.48	(0.065)	0.10	stake-dao	-0.40	(0.087)	0.30	2.15	(0.323)	0.25
flow	-1.04	(0.027)	0.27	-1.03	(0.102)	0.12	sushi	-1.15	(0.085)	0.44	-1.16	(0.117)	0.15
harmony	-1.07	(0.032)	0.30	-1.31	(0.134)	0.12	terra	-2.10	(0.423)	0.05	-4.52	(1.686)	0.05
icon	-0.91	(0.071)	0.47	-0.70	(0.491)	0.22	tezos	-1.00	(0.028)	0.36	-0.93	(0.122)	0.11
idex	-1.11	(0.047)	0.28	-1.21	(0.121)	0.12	tron	-1.02	(0.033)	0.36	-1.05	(0.134)	0.11
injective	-1.06	(0.034)	0.27	-1.14	(0.157)	0.12	wanchain	-0.93	(0.073)	0.49	-0.61	(0.415)	0.27
iotex	-0.91	(0.029)	0.46	-0.63	(0.229)	0.22	waves	-1.01	(0.033)	0.31	-0.80	(0.148)	0.09
irisnet	-1.04	(0.046)	0.43	-0.97	(0.179)	0.18	wax	-1.02	(0.028)	0.26	-1.09	(0.114)	0.09
kava	-1.11	(0.018)	0.50	-1.41	(0.072)	0.24	yearn	-1.06	(0.021)	0.52	-1.14	(0.075)	0.18
kusama	-1.03	(0.031)	0.31	-1.10	(0.144)	0.12	zcoin	-0.87	(0.055)	0.57	-0.77	(0.316)	0.31

CARMONA, RENE (2020): “Applications of mean field games in financial engineering and economic theory,” [arXiv preprint arXiv:2012.05237](#).

CONG, LIN WILLIAM AND ZHIGUO HE (2019): “Blockchain disruption and smart contracts,” [Review of Financial Studies](#), 32 (5), 1754–1797.

CONG, LIN WILLIAM, ZHIGUO HE, AND JIASUN LI (2021a): “Decentralized mining in centralized pools,” [Review of Financial Studies](#), 34 (3), 1191–1235.

CONG, LIN WILLIAM, YE LI, AND NENG WANG (2021b): “Tokenomics: Dynamic adoption and valuation,” [Review of Financial Studies](#), 34 (3), 1105–1155.

HARVEY, CAMPBELL R, ASHWIN RAMACHANDRAN, AND JOEY SANTORO (2021): [DeFi and the Future of Finance](#), John Wiley & Sons.

IRRESBERGER, FELIX, KOSE JOHN, PETER MUELLER, AND FAHAD SALEH (2021): “The public blockchain ecosystem: An empirical analysis,” [NYU Stern School of Business](#).

JOHN, KOSE, THOMAS J RIVERA, AND FAHAD SALEH (2020): “Economic implications of scaling blockchains: Why the consensus protocol matters,” [Available at SSRN 3750467](#).

KRUSELL, PER AND ANTHONY A SMITH, JR (1998): “Income and wealth heterogeneity in the macroeconomy,” [Journal of political Economy](#), 106 (5), 867–896.

LASRY, JEAN-MICHEL AND PIERRE-LOUIS LIONS (2007): “Mean field games,” [Japanese journal of mathematics](#), 2 (1),

Table OA.4: Excess return and carry.

Token	Excess Return (%, Annual)		Carry (%, Annual)		Token	Excess Return (%, Annual)		Carry (%, Annual)	
	Mean	Std.dev.	Mean	Std.dev.		Mean	Std.dev.	Mean	Std.dev.
0x	0.42	0.30	6.75	20.62	kusama	12.97	1.93	16.61	25.75
1inch	2.94	6.49	1.46	17.05	kyber	1.32	3.53	1.88	17.67
aave	3.83	0.98	6.21	21.56	livepeer	62.04	29.54	63.61	49.84
aion	6.25	3.01	8.86	18.61	lto	6.70	1.01	12.19	17.18
algorand	7.20	11.72	7.81	19.22	matic	17.78	14.01	25.23	40.64
ark	8.09	0.52	9.52	17.02	mina	10.32	2.81	9.60	20.97
avalanche	8.43	2.74	13.31	35.40	mirror	39.15	37.41	34.85	42.27
band	10.88	3.10	13.62	27.93	near	10.13	2.85	13.30	23.35
bifi	7.95	3.43	11.76	26.02	nem	-1.35	0.51	-1.59	14.28
binance-sc	8.02	6.38	9.05	15.10	neo	0.92	0.97	2.71	14.94
bitbay	1.13	0.98	10.62	63.06	nuls	8.31	0.56	10.67	16.96
cardano	4.39	2.77	6.52	17.95	oasis	11.80	4.55	12.95	26.77
celo	6.08	0.13	6.07	4.95	olympus	49.79	41.90	37.95	48.49
cosmos	9.82	2.35	11.97	18.55	osmosis	35.90	17.56	30.03	20.48
cronos	10.15	2.67	6.25	13.11	pancakeswap	74.76	26.66	78.13	51.65
curve	1.12	2.83	1.45	19.34	peakdefi	43.88	16.92	43.26	32.91
dash	5.20	0.73	7.28	26.50	polkadot	11.56	1.68	13.14	17.63
decred	5.58	1.71	6.66	14.32	qtum	4.73	1.31	6.30	14.07
dfinity	7.68	4.78	3.87	15.34	secret	24.47	3.95	27.70	28.47
dodo	56.63	10.73	50.54	22.66	smartcash	1.63	0.36	3.64	15.35
dydx	10.66	2.76	8.53	19.03	snx	21.96	23.54	26.42	37.33
elrond	14.24	7.45	19.18	32.93	solana	5.94	3.82	8.94	24.75
eos	10.69	12.06	11.02	18.81	stafi	18.76	4.02	19.91	27.21
eth2.0	8.61	10.82	11.45	18.44	stake-dao	22.23	8.32	21.49	19.43
fantom	27.83	23.95	37.98	47.03	sushi	10.51	10.12	8.85	20.06
flow	6.95	2.05	3.29	16.56	terra	8.26	3.71	14.26	35.66
harmony	8.58	2.89	12.42	27.40	tezos	4.56	2.11	5.52	16.99
icon	16.42	2.80	19.99	23.99	tron	2.81	1.94	4.36	13.99
idex	8.05	8.85	15.12	78.53	wanchain	7.39	0.26	9.44	16.86
injective	3.87	0.58	2.16	13.91	waves	3.84	1.62	6.21	22.75
iotex	8.86	3.14	11.27	21.23	wax	1.56	2.64	3.34	19.81
irisnet	9.67	0.38	14.77	22.07	yearn	14.51	16.78	16.86	30.14
kava	19.55	16.44	22.29	26.61	zcoin	15.02	3.77	18.35	16.90
US Dollar	0.00	0.00	0.00	0.00					

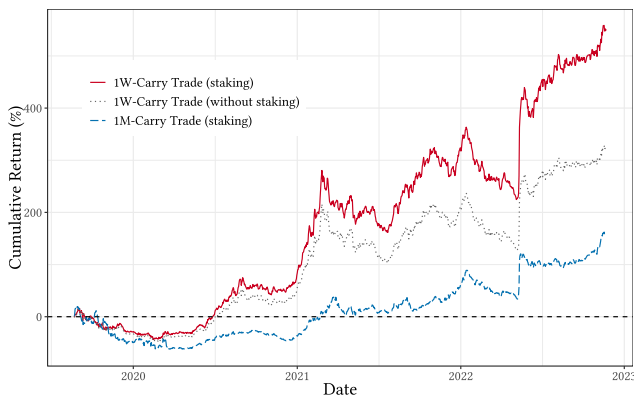
229–260.

LI, ZONGXI, A MAX REPPEN, AND RONNIE SIRCAR (2019): “A mean field games model for cryptocurrency mining,” arXiv preprint arXiv:1912.01952.

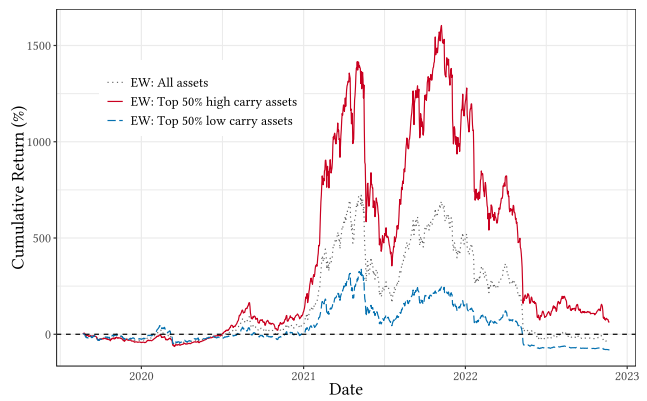
LIONS, PIERRE-LOUIS (2011): “Courses at the Collège de France.”

LUNDE, ASGER AND ALLAN TIMMERMANN (2004): “Duration dependence in stock prices: An analysis of bull and bear markets,” *Journal of Business & Economic Statistics*, 22 (3), 253–273.

SALEH, FAHAD (2021): “Blockchain without waste: Proof-of-stake,” Review of Financial Studies, 34 (3), 1156–1190.



(a) Long-short strategies.



(b) Long strategies.

Figure OA.5: Cumulative returns of carry strategies.

This figure corresponds to Hypothesis (H3b) and shows the cumulative returns of the carry-trade strategies. Panel (a) shows the long-short strategies. The red curve shows the cumulative return of main long-short carry strategies. The construction of the strategy is described in Section 6.3 and $X = 50$. The choice of X does not affect the main qualitative properties. As comparisons, the gray curve corresponds to the strategy without earning or compensating staking rewards, and the blue curve shows the strategy that rebalanced every month. Panel (b) shows the long-only strategies. The gray curve corresponds to the equal-weighted benchmark, i.e., borrow US dollar and long all the tokens with equal weight. The red curve shows the result of the top 50% EW strategy, that is, borrow US dollar and go long top 50% high carry tokens with equal weight. The blue curve shows the result of the lowest 50% EW strategy, i.e., borrow US dollar and go long the 50% tokens with the lowest carry with equal weight. The order of the tokens is evaluated every week.